# A review of remote sensing methods for the study of large wildland fires

*(Megafires project ENV-CT96-0256)*

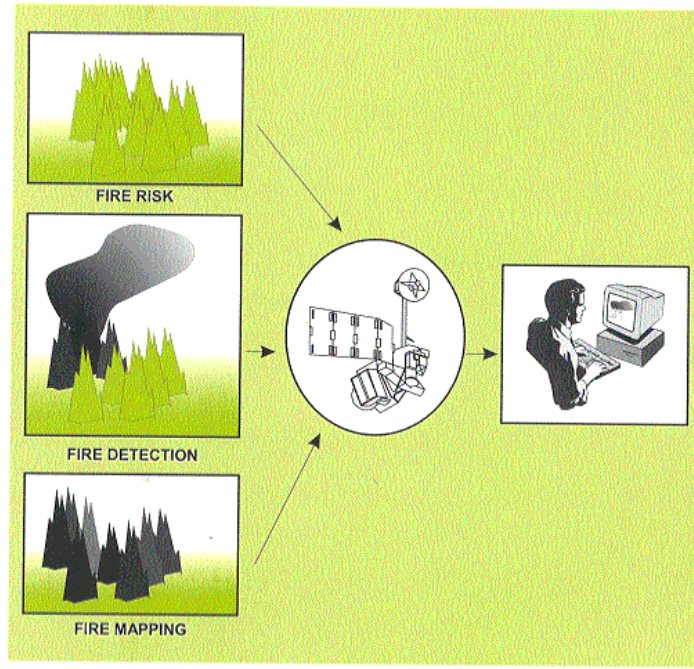


*Emilio Chuvieco (Editor)*

**(Megafires project** ENV-CT96-0256)

# A review of remote sensing methods for the study of large wildland fires

Emilio Chuvieco (Editor)
Universidad de Alcalá

Alcalá de Henares (Spain)
August, 1997

Departamento de Geografía, Universidad de Alcalá, Colegios 2, 28801 Alcalá de Henares (Spain).
Impreso en España - Printed in Spain.

ISBN: 84-8498-578-4
Depósito legal: M-30375-1997

# CONTENTS

# FOREWORD

Wildland fires are becoming a major concern for several Environmental Sciences. Assessment on fire effects at local scale is increasingly considered a critical aspect of ecosystem functioning, since fire plays a crucial role in vegetation composition, biodiversity, soil erosion and the hydrological cycle. At global scale, fire is the most generalised mean to transform tropical forest in agricultural areas, and it has severe impacts on global atmospheric chemistry.

Fire is a natural factor in many climates, such as the Mediterranean, with high levels of vegetation stress during the summer. However, changes in traditional land use patterns have recently modified the incidence of fire in these territories. Rural abandonment in the European Mediterranean basin has implied an unusual accumulation of forest fuels, which notably increases fire risk and fire severity. On the other hand, the increasing use of forest as a recreational resource involves a higher incidence of human induced fires, either by carelessness or arson.

In spite of the great incidence of fires in Southern Europe, a significant amount of information is still required to better understand fire risk factors and fire effects. Most of the National forest services do not provide a cartographic representation of burned areas. Therefore, there is a lack of understanding about the spatial factors related to fire incidence and the spatial consequences of fires. For instance, in many occasions only a general estimation of burned area is provided, but the fire perimeter is not available, and thus the fire fighting manager does not clearly known the spatial pattern of fire behaviour nor the areas more

severely affected by the fire. In the case of fire risk estimation, most of the current danger indices are based on a network of weather stations, which is frequently sparse and located far from the forested areas. Consequently, only general information about the spatial distribution of risk is available, and fire pre-suppression resources might not be optimally allocated.

Remote sensing from space is especially suitable for forest fire research. The wide area coverage and repetitivity provided by satellite sensors, as well as their information on non visible spectral regions, makes them a very valuable tool for prevention, detection and mapping of wildland fires. During the last decade, the range of applications has significantly increased, making satellite remote sensing a solid ally in many forest fire strategic plans. Within this context, the general goal of the Megafires proposal was to establish an integrated framework to analyse satellite remote sensing images for operational management of large wildland fires in Mediterranean countries. The three stages of fire management: pre-fire planning (fire risk), fire suppression (detection and fighting) and post-fire evaluation (fire effects) were considered in the project. The project was approved in the first call for proposals of the Fourth Framework programme of the DG-XII of the European Commission under the chapter named "Technologies to forecast, prevent and reduce natural risk: Forest Fires".

Several European projects have used satellite remote sensing as input for modelling fire behaviour or fire risk, but there is not yet available a comprehensive review of the possibilities offered by remote sensing techniques to forest fire management. This is the main goal of this book, which brings together the experience of the partners involved in Megafires, as well as methods developed by other colleagues in the field. Each chapter covers part or the whole of a Megafires workpackage, from the estimation of fire risk, both considering a short-term and a long-term temporal scale, to fire detection methods and fire effects assessment. A special effort has been dedicated to review global-scope

studies, since the Megafires project has a strong Euro-Mediterranean approach. Consequently, the applications of NOAA-AVHRR data are commented with special detail. However, local-high resolution studies are reviewed as well. The analysis of meteorological danger indices is also included, because they provide a necessary input to any operational fire risk system

Only review material is included in this book, since new advances from the Megafires project are still in progress and will be reported in the near future. We hope this book will help remote sensing specialists to gain a more comprehensive view of the potential applications of satellite data to forest fire research.

As the coordinator of the Megafires project, I should acknowledge the financial contribution of the DG-XII of the European Union, which has been crucial for the development of the project. The assistance of Dr. P. Balabanis has always been very helpful. Finally, I should also appreciate the great enthusiasm of the partners involved in Megafires in order to achieve our ambitious goals. I desire the reader will find our labour valuable.

Emilio Chuvieco
Universidad de Alcalá

# NOAA-AVHRR SATELLITE DATA PROCESSING: STATE OF THE ART AND CHOICES IN MEGAFIRES

*A. Vidal [(a')], N. Desbois [(a)], J.M. Pereira [(b)], J. Garcia [(c)] and E. Chuvieco [(d)]*

[(a)] Laboratoire Commun de Télédétection Cemagref-ENGREF, France.

[(a')] Irrigation Division, Cemagref, France.

[(b)] Instituto Superior de Agronomia, Portugal.

[(c)] INFOCARTO, S.A., Spain.

[(d)] Departamento de Geografía, Universidad de Alcalá, Spain.

The important use of NOAA-AVHRR images within the MEGAFiReS project implies to define a pre-processing and processing chain which would be applied for all these images to have homogeneous data from one country to another and from year to another. NOAA-AVHRR images are used to assess short-term fire risk, to detect fires and to monitor their growth and to map burned areas at global scale.

The main interest of such data is to provide, on a regular basis and on large areas, an exhaustive spatially distributed information on vegetation. The principal advantages of NOAA-AVHRR data are 1) its temporal resolution (two images per day) and 2) its good spectral information (visible, near, middle and thermal infrared). The first two channels (red, 0.58 to 0.68 µm, and near infrared, 0.72 to 1.10 µm) permit the computation of vegetation indices which are correlated with green biomass, photosynthetic activity (Tucker and

Sellers, 1986) and moisture content (Paltridge and Barber, 1988). The channel 3 (middle infrared, 3.75 µm), sensitive to the presence of liquid water in vegetation, could be useful for vegetation stress and burned area analysis. The two thermal infrared channels (band 4, 10.3 to 11.3 µm, and band 5, 11.5 to 12.5 µm) allow the computation of a Surface Temperature corrected from the atmospheric and emissivity effects (Gu *et al.*, 1994). Moreover, its medium spatial resolution (1.1 km at nadir) gives an integration of local variations and provides an average response well adapted to global scale (López *et al.*, 1991).

The pre-processing consists of the following steps: 1) calibrating each channel, 2) correcting, when it is possible, channels for the atmospheric and emissivity effects 3) correcting the images for the geometrical distortions and georeferencing them. Then the processing resides in computing vegetation indices adapted to MEGAFiReS purposes and to temporally compose the images derived from channels 1 and 2, in order to reduce the atmospheric effects.

Tasks described in this section are carried out automatically, to change NOAA-AVHRR data from 1b format type into ERDAS / IMAGINE format.

## 1. PRE-PROCESSING OF NOAA-AVHRR IMAGES.

### 1.1. Pre-processing of visible and near infrared bands (Channels 1 and 2)

Calibration of NOAA/AVHRR channels 1 (visible) and 2 (NIR) data consists of converting the raw digital counts recorded by the sensor into a reflectance measure, which may refer to the surface, if gaseous absorption and scattering due to aerosols and gases are taken into account, or to the top of the atmosphere otherwise. Since a consensus concerning adequate methodologies for correcting the effects of water vapour absorption and aerosol scattering has not yet reached (Townshend et al., 1994), no atmospheric corrections will be

implemented on the visible and near infrared data pre-processed under the scope of MEGAFIReS. This decision is additionally justified by the fact that visible and NIR data will be used primarily under the form of spectral vegetation indices, which partially but significantly reduce atmospheric effects, due to the normalization inherent in their calculation (Vermote and Roger, 1996). Further minimization of atmospheric effects is possible through the use of temporal compositing procedures (Holben, 1986) and atmospherically insensitive vegetation indices (Pinty and Verstraete, 1992; Kaufman and Remer, 1994; Leprieur et al., 1996). Therefore, the visible and near infrared AVHRR data pre-processed within the scope of MEGAFIReS will be calibrated to apparent (or top-of-the-atmosphere, TOA) reflectance ($\rho^*$).

Unlike the middle infrared and thermal channels of NOAA/AVHRR, the visible and near infrared channels lack on-board calibration, and the performance of the radiometers is known to deteriorate considerably during and after launch (Rao and Chen, 1994, 1995; Teillet and Holben, 1994). Consequently, the use of pre-launching calibration coefficients is inappropriate, especially when analysing long time series of data (D'Souza, 1996). This is known to have happened with the NOAA-14 instrument, which is the source of the data to be calibrated under MEGAFIReS, according to the reports Amendments to NOAA Technical Memorandum 107, Appendix-B for NOAA-J/14, dated November 22, 1994 and July 31, 1995.

A number of studies have been conducted in order to estimate the temporal drift of the calibration coefficients for the NOAA/AVHRR instruments. They have tried to calculate more suitable coefficients as a function of time since satellite launch (Abel et al., 1993; Kaufman and Holben, 1993; Teillet and Holben, 1994; Rao and Chen, 1994, 1995). These results

have been recently published for NOAA-14 by Rao and Chen (1996), of the NOAA/NESDIS Satellite Research Laboratory.

The calibration of the NOAA-14 AVHRR visible and near infrared channels to apparent reflectance is, then, accomplished in three steps: 1) calculation of calibration coefficients on day d after launch; 2) conversion of the raw digital counts into radiance; 3) conversion of radiance into apparent reflectance.

1.1.1. Calculation of the calibration coefficients on day d after launch

The intercept of the linear equation used to convert the raw digital counts into radiances has not suffered significant degradation since launch, and thus this step needs only be performed for the slope coefficient. The equations for calculating the slope for channels 1 and 2 are respectively (Rao and Chen, 1996):

$$S_1 = 0.000118 \cdot d + 0.557$$

and

$$S_2 = 0.000122 \cdot d + 0.423$$

where $S_i$ is the slope coefficient for channel i, and d is the number of days since satellite NOAA-14 launching (launch date is December 30, 1994, which should be counted as day 0).

1.1.2. Conversion of digital count (DN) into radiance (L)

The equation used to convert the raw digital counts (DN, scaled in 10 bits) into radiances ($L_i$, in $W.m^{-2}.sr^{-1}.\mu m^{-1}$) is:

$$L_i = S_i \, . \, (DN - 41)$$

The intercept coefficient is constant, and equal for both channels.

1.1.3. Conversion of radiance (L) into apparent reflectance (ρ*)

The radiance values obtained from the previous step are converted to apparent reflectances using the formula:

$\rho_i^* = (\pi \cdot L_i \cdot d^2) / (E_{0i} \cdot \cos\theta)$

where: d = Sun-Earth distance, in astronomical units (AU), $E_{0i}$ = exo-atmospheric solar irradiance in channel i ($W.m^{-2}.\mu m^{-1}$), and $\theta$ = solar zenith angle (°).

The values for $E_{0i}$ are (Kerdiles, 1996):

$E_{01} = 1605\ Wm^{-2}\mu m^{-1}$

$E_{02} = 1029\ Wm^{-2}\mu m^{-1}$

The Sun-Earth distance, in astronomical units, or under the form of an orbital eccentricity correction factor can be obtained from a variety of sources, namely Iqbal (1983).

### 1.2. Pre-processing of middle infrared band (Channel 3)

The AVHRR channel 3 (3.75μm) signal is a mixture of thermal emitted and solar reflected energy, the latter typically representing less than 10% of the total radiance for bare soil, and less than 3% for green vegetation (Holben and Shimabukuro, 1993). Since this spectral range overlaps with a water absorption band sensitive to the presence of liquid water in vegetation and soils, determination of the reflective component of this channel was considered useful for vegetation stress and burned area analysis.

The procedure for splitting the channel 3 total radiance into its emitted and reflected components is presented by Kaufman and Nakajima (1993) and Kaufman and Remer (1994):

The energy emitted at 3.75μm is calculated with Planck's function, using the brightness temperature in channel 4:

$$B_{3.75} = (3.74151 \times 10^{8}) / \lambda^{5} [\exp\{(1.43879 \times 10^{4})/\lambda T\} - 1]$$

where $B_{3.75}$ is in $Wm^{-2}\mu m^{-1}$, and $\lambda$ is in $\mu m$. In this case, $\lambda$ assumes the value of 3.75 $\mu m$, and T is the brightness temperature from channel 4. In order to obtain the desired units of spectral radiance ($W.m^{-2}\mu m^{-1}sr^{-1}$), the right hand-side of the equation above must be divided by $\pi$. Then, the reflective component of channel 3 is given by:

$$\rho_{3.75} = (L_{3.75} - B_{3.75}) / \{( E_{03} . \cos\theta) / \pi - B_{3.75})$$

where $L_{3.75}$ is the channel 3 total radiance ($Wm^{-2}\mu m^{-1}sr^{-1}$), $E_{03}$ is the in-band exoatmospheric irradiance of channel 3 (which has the value of 4.479 $Wm^{-2}$ for NOAA-14), and $\cos\theta$ is the cosine of the solar zenith angle, assuming a flat surface. Additional assumptions of this calculation are perfect atmospheric transmittance, and surface emissivity of 1 at all wavelengths concerned. Kaufman and Remer (1994) provide the justification for these assumptions.

### 1.3. Pre-processing of thermal infrared bands (Channels 4 and 5).

1.3.1. Conversion of digital count (DN) into radiance (L)

The equation used to convert the raw digital counts (DN, scaled in 10 bits) into radiances is:

$$L_i = - S_i \cdot DN + I_i \quad \text{in } mWm^{-2}sr^{-1}cm$$

where $L_i$ is the radiance measured by the sensor for the channel i, $S_i$ and $I_i$ are respectively the scaled slope and intercept values. These calibration coefficients can be derived from the standard 1b data specifications. Slope and intercept values must be scaled, by dividing the former by $2^{30}$ and the latter by $2^{22}$.

1.3.2. Conversion from radiance of channels 4 and 5 into surface temperature

1.3.2.1. Conversion from radiance (L) into brightness temperature (T*)

The conversion to brightness temperature from radiance is performed using an approximation of the inverse of Planck's radiation equation:

$$T^*(L) = \frac{c_2 n}{\ln(1 + c_1 n^3 / L_{sen,n})}$$

where : $T^*$ is brightness temperature in Kelvin, ν is the central wave length of each band ($cm^{-1}$), given in official NOAA documents, $c_1$ = 1,1910659·$10^{-5}$ $mWm^{-2}sr^{-1}cm^4$ , $c_2$ = 1,438833 cmK.

The use of thermal infrared data of NOAA-AVHRR within the MEGAFiReS project involves that atmospheric and surface emissivity effects are accounted for. The general trend of the scientific community during the 10 past years has allowed a better understanding of phenomena and a simplification of approaches. These approaches were initially based either on empirical relationships between raw satellite radiance values and ground-measured surface temperatures, or on a complex modelling of atmospheric radiative transfer (successive updates of the LOWTRAN code). Research results of these last years have produced simplified models that have been validated and shown as self-sufficient for most of operational uses of satellite data.

1.3.2.2. Thermal bands atmospheric and emissivity corrections.

The most common method used to correct thermal bands for atmospheric and emissivity effects is known as the ‘split-window’ method. According to this method, differential effects of atmosphere and surface emissivity in AVHRR thermal bands are used to derive a corrected surface temperature Ts from brightness temperatures obtained from bands 4 and 5 (respectively $T_4$ at

10.3-11.3 μm and $T_5$ at 11.25-12.5 μm), using the following general expression:

$$T_s = T_4 + A(T_4 - T_5) + B$$

where A and B are usually constants.

Several authors have published synthesis of previous literature on this method (Vidal, 1991; Gu et al., 1994), showing that it would be difficult to obtain a better precision than 1 to 1.5 K. Other authors however have tried to find a generic expression accounting for most cases of land surfaces, usually basing their work on field campaigns and improved radiative transfer models (Meliá *et al.*, 1991; Kerr *et al*., 1992; Valor and Caselles, 1996).

As these last authors based their work in a Mediterranean region, and as their methods have been used by others since they were published (e.g. Vidal et al., 1994), we decided to compare their methods before choosing one for MEGAFiReS.

The method developed by Meliá *et al*. (1991) suggests a common equation for all vegetated surfaces, such as crops, forests, shrublands, where A is a function of $T_4$-$T_5$, and mainly represents atmospheric effects, and B is a constant representing the surface mean emissivity:

$$A = 1.31 + 0.27(T_4 - T_5) \text{ and } B = 1.16 \pm 0.76K$$

The equation obtained by Kerr et al. (1992) is stated as more adapted to changes in vegetation cover (which commonly occur in Mediterranean forests and shrublands), and combines two split-window equations, one for bare soil (A = 2.1; B = 3.1) and one for full-covering vegetation (A = - 2.4; B = 2.6), using the NDVI as an estimator of the fractional vegetation cover $f_v$, with:

$$f_v = \frac{(NDVI - NDVI_{bs})}{(NDVI_v - NDVI_{bs})}$$

where *bs* and *v* subscripts correspond to bare soil and vegetation. The surface temperature is then obtained from corrected surface temperatures of bare soil and vegetation, using:

$$T_s = f_v \cdot T_v + (1 - f_v) \cdot T_{bs}$$

Valor and Caselles (1996) propose also a method adapted to areas with several types of soil and vegetation and where vegetation cover changes. This method consists, first, in applying a split-window equation to correct the atmospheric effects and, secondly, in correcting the surface temperature obtained of emissivity effects using the NDVI.

The three methods were tested on Les Maures Forest in France, along 4 transects oriented N-S. Les Maures Forest (888 km²) is located between Toulon and St-Raphaël in Southeast of France, and is mainly covered by cork oak (*Quercus suber*), in association with holm oak and pines (*Pinus halepensis, Pinus pinaster*) with large variations in vegetation cover, ranging from recently burned barren land ($NDVI_{bs}$ = 0.09) to full-covering forest vegetation ($NDVI_v$ = 0.66).

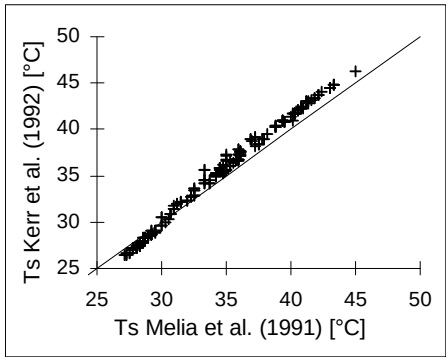


Figures 1, 2 and 3 presents the comparison between the corrected surface temperatures obtained with the three methods, on 26 June 1995.

*Figure 1: Comparison between Kerr et al. and Meliá et al. split-window equations*

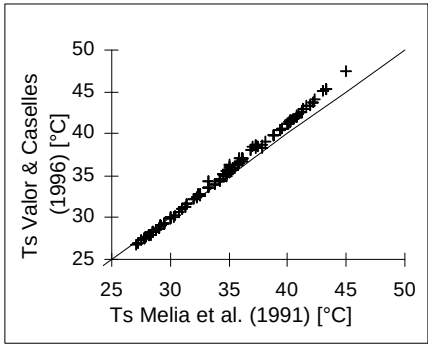


*Figure 2: Comparison between Meliá et al. and Valor and Caselles split-window equations.*

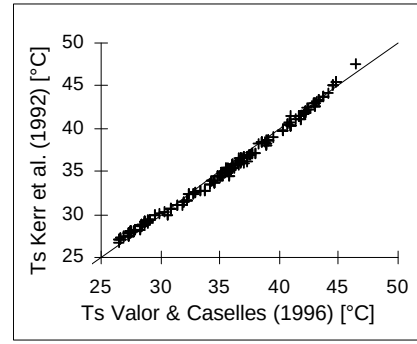


*Figure 3: Comparison between Valor and Caselles and Kerr et al. split-window equations.*

The RMSE between the corrected surface temperatures (1.15, 0.85 and 0.48°C) are lower than the RMSE of each method itself (around 1.50°C) when compared to ground measurements or radiative transfer models outputs. Moreover, the method proposed by Valor and Caselles gives the values which are the closest to those obtained by the other two methods (RMSE = 0.85°C and 0.48°C when compared respectively with Melia et al. and Kerr et al. methods). This method is also adapted to partial canopies common in the Mediterranean area and has been validated in France and Spain over flat to rough areas with an error of estimation of the emissivity of only 0.6 %. Consequently, the method proposed by Valor and Caselles (1996) will be adopted in MEGAFiReS. It is detailed below.

Nevertheless, it will be kept in mind, when deriving risk indices, that the precision on the corrected surface temperature, is of the order of 1.5 °C.

The atmospheric correction proposed by Coll and Caselles (1997) is:

$$T^*_s = T^*_4 + [1{,}34 + 0{,}39\,(T^*_4 - T^*_5)]\,(T^*_4 - T^*_5)$$

where $T^*_s$ is surface temperature; $T^*_4$ and $T^*_5$ are respectively brightness temperatures of channels 4 and 5.

And the emissivity correction is defined by (Valor and Caselles, 1996):

$$T_s = T^*_s + 0{,}51 + 40\,(1 - \varepsilon)$$

where ε is the emissivity, which is computed from:

$$\varepsilon = \varepsilon_v P_v + (1 - P_v)\varepsilon_s + 4d\varepsilon(1 - P_v)P_v$$

where the emissivity of green and soil can be generalised as 0.985 and 0.960 respectively, and the cavity effect dε in 0.015. Therefore:

$$\varepsilon = 0.985P_v + 0.960\,(1 - P_v) + 0.06(1 - P_v)P_v$$

and the percent of green cover is estimated as:

$$P_v = \frac{\left(1 - \left(NDVI / NDVI_{min}\right)\right)}{\left(1 - \left(NDVI / NDVI_{min}\right)\right) - k\left(1 - \left(NDVI / NDVI_{max}\right)\right)} * 100$$

where NDVI is the value of the NDVI for that pixel, and $NDVI_{min}$ and $_{max}$ are respectively the values of a bare soil and a fully vegetated pixel, and

$$k = \frac{r_{2v} - r_{1v}}{r_{2s} - r_{1s}}$$

with $\rho_1$ and $\rho_2$ respectively the visible and near infrared reflectances for full vegetation (v) or bare soil (s).

## 1.4. Geometrical corrections

1.4.1. Introduction

Data from remote sensors usually contain geometric errors. These can be systematic and non-systematic. They can be corrected using two methods:

- Using platform ephemerides and the knowledge of internal sensor distortion. The geometric distortions solved by this way include scan skew, mirror scan-velocity and perspective geometry.
- Adding a sufficient number of ground control points (GCP). A GCP is a point on the surface of the earth where both image coordinates (in rows and columns) and map coordinates (in degrees of latitude and longitude, feet or

meters) can be identified. The errors corrected by this method are roll, pitch, yaw and perspective geometry.

*Rectification* is the process by which the geometry of an image is made planimetric, but it may not remove distortion caused by topographic relief displacements in images. The process almost always involves relating GCP pixel and map coordinates.

A rectification comparing the image to correct with another image already rectified can also be done. This process is named *image registration*.

Rectification process includes:

- *Spatial interpolation*. It is the identification between the input pixel location and the associated map coordinates of this same point.
- *Intensity interpolation*. Determination of the pixel brightness values (BV). There is not a direct one to one relationship between the movement of input pixel values to output pixel locations. There are several methods of BV interpolation that can be applied including nearest-neighbour, bilinear interpolation and cubic convolution. The interpolation of bright values is also named *resampling*.

1.4.2. Characteristics of NOAA related to the geometrical corrections.

The orbital model is essential for the distortion corrections of NOAA images due to the geometry of the observation. There is no continuous data for the position and attitude of NOAA satellites, but a periodic revision of the mean orbital parameters have to be made. So that, it must be made a kleperian modelisation of the orbit.

The orbit is defined by six parameters:

- larger semiaxis (a)
- eccentricity (e)
- pitch (i)

- right ascension from the ascendant node (Ω)
- argument of the perigee (ω)
- time

Orbital parameters are available from several sources of remote sensed data and can easily be captured from Internet. The orbital trajectory is calculated from the Kepler equation for the orbital parameters given. It is essential to use some control points to complement the orbital information.

The orbital model used in MEGAFiReS to derive ground control points is the SGP4 orbital model. These positions are obtained using as input the time given for each image by the on-board G.P.S..

The spatial coverage of NOAA is very large because the swath system consists of a mirror that rotates 360º. Consequently, the observation angles on the extreme zones are very oblique. These distortions are very well described on the orbital model and, therefore, the images can be corrected effectively.

### 1.4.3. Corrections applied in Megafires

The distortions corrected on this study starts when the NOAA image is captured. The image header have some readable information including the name of the satellite, UTC time and date and the direction of the orbit (ascending or descending). The NOAA receiving station is connected to a GPS. This permits to have an accurate time to correct the satellite own time. This correction is recommendable because the satellite time normally suffers a deviation. If the satellite have an inverted orbit it is possible to change the image to the right position.

Orbital parameters, that provided the location of the satellite continuously, and the GPS time are used to locate a control point at a chosen interval of lines.

Panoramic distortion is corrected with the orbital model when the image is imported to ERDAS / Imagine format. The GCPs are also written at this time.

The last step is the georeferencing, which means to assign map coordinates to image data. The selection of the map projection is very important depending of the type of work. NOAA images of this study are georeferenced to Albers Equal area. The resampling is done with a nearest neighbour interpolation, transformation order of 1 and accepting an RMS error below 1.

1.4.4.Projection selected to this study.

NOAA-AVHRR images will be produced at the same projection currently used by the European Environmental Agency (EAE, 1996): the Albers Equal Area projection, in order to assure an easier connection with existing European geo-databases.

This projection is mathematically based on a cone which axe corresponds to the polar axe and that is secant to the earth in two standard parallels. The pole is represented by an arc of circle. This projection conserves the surfaces but not the shapes. However, the distortion of shape is minimized in the region between the standard parallels and those just beyond. It is widely used for maps at small scale and especially for land masses that extend more in the East to West direction than those lying North to South. The different countries, although deformed, conserve their relative surfaces which is useful for representing themes such as burnt areas, vegetation dryness, etc.

The parameters of the Albers Conical Equal area projection are the following:

Spheroid: WGS 72

Latitude of the 1st standard parallel: 35°

| | |
|---|---|
| Latitude of the 2st standard parallel: | 60° |
| Longitude of central meridian: | 5° |
| Latitude of origin of projection: | 45° |
| False easting at central meridian: | 0 |
| False northing at origin: | 0 |

## 2. PROCESSING OF NOAA-AVHRR IMAGES

### 2.1. Generation of vegetation indices.

Vegetation indices used in the MEGAFiReS project are detailed in the papers ″Short term fire risk mapping ″ and ″Burned areas mapping ″.

### 2.2. Temporal image compositing.

The temporal compositing of NOAA/AVHRR imagery is an active research, due to the problems that affect the most commonly used technique, i.e. NDVI maximum value compositing (MVC) (Cihlar et al., 1994a,b; Qi and Kerr, 1994; Townshend, 1994). This technique tends to favour pixels with off-nadir viewing angles in the forward scattering direction, introducing a directional bias and degrading the true spatial resolution of the composite image (D'Iorio et al., 1991; Qi and Kerr, 1994). In the case of MEGAFIReS, compositing on the basis of vegetation index criteria would create an additional problem for those tasks involving comparisons of the performance of various VI. The composited data would become biased by the index selected to guide the compositing procedure, and rendered inappropriate to assess the performance of other VI for tasks such as monitoring vegetation stress or detecting burned surfaces. It may be possible to avoid this specific problem by using other classifiers (Qi and Kerr, 1994), such as minimum channel 1, or maximum channel 4 compositing, which seem to produce results similar to

those of the NDVI MVC (Qi and Kerr, 1994). However, these techniques are less well known than maximum value compositing of vegetation indices, and may very well be affected by similar problems.

Another important consideration is that vegetation stress monitoring and burned area mapping require different, even contrasting compositing criteria. The aim of vegetation stress monitoring is to emphasize the vegetation signal, and therefore any of the techniques mentioned above would be acceptable. However, maximization of the vegetation signal in a given compositing period will obliterate any burned area signals generated during that same period, and alternative compositing techniques are required (Cahoon et al., 1994). This issue will be addressed in more detail on the position paper on burned area detection and mapping.

It appears inevitable that some research into the topic of temporal image compositing will have to be performed in the early stages of the MEGAFIReS project, in order to identify techniques that will satisfy the objectives of the various relevant project tasks. Regardless of the compositing technique(s) selected, a compositing period of about 8 days seems appropriate, since it approximates the minimum compositing period required for capturing the entire range of satellite view angles, and would yield a set of 15 images, for the period of June through September which will be the focus of MEGAFIReS activities.

## 3. CONCLUSION

Since vegetation stress indexes based on surface temperature can considerably vary from one day to another, it is of high importance to know their admissible error that result from the above pre-processings, as well as from the models used to transform radiative surface temperatures into vegetation water stress indexes.

Based on published errors on radiative surface temperatures resulting from high quality pre-processing methods that have been selected for this project (Vidal, 1991 ; Valor and Caselles, 1996), the following RMS errors can be expected for each pre-processing step :

| *Pre-processing Step* | *RMS Error (K)* | *Source and Comments* |
|---|---|---|
| Atmospheric correction | 1.5 | This paper |
| Emissivity correction | 0.6 | Valor and Caselles, 1996 |
| Geometric correction | 1.2 | Dataset used in 1.3.2.2. with a RMS position error of 1 AVHRR pixel |
| Total error | 2.0 | $de = \sqrt{\sum de_i^2}$ |

On the other hand, in the frame of the EU-funded feasibility study of the future MUST instrument, Vidal et al. (1997) have shown that, for assessing forest water stress on the basis of 5 stress classes, which correspond to the approach used in MEGAFIReS, the required precision on the surface temperature could be estimated as a function of climatic condition, i.e. global radiation, air temperature and moisture, as shown in *Figure 2*.

This figure shows that the Total RMS error appearing above is compatible in most cases of Mediterranean forest during fires periods, where climatic conditions allow a requested precision on air temperature around 2°K.

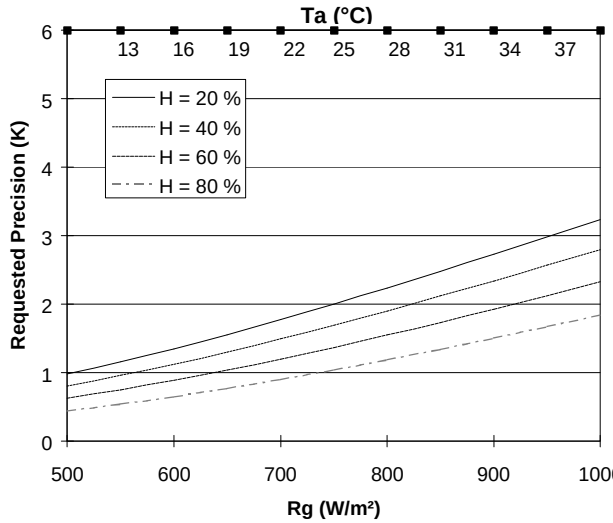


Figure 2: Requested precision for vegetation stress estimation on forest (ra =16 s/m) as a function of global radiation Rg, air temperature Ta and air moisture (from Vidal et al., 1997)

**REFERENCES**

ABEL, P., GUENTHER, B., GALIMORE, R.N. and COOPER, J.W. (1993) Calibration results for NOAA-11 AVHRR channels 1 and 2 congruent path aircraft observations. *Journal of Atmospheric and Oceanic Technology*, 10: 493-508.

CAHOON JR, D.R., STOCKS, B.J., LEVINE, J.S., COFER III, W.R., and PIERSON, J.M. (1994) Satellite analysis of the severe 1987 forest fires in northern China and South-eastern Siberia. *Journal of Geophysical Research* 99 (D9): 18627-18638.

CIHLAR, J., MANAK, D., and D'IORIO, M. (1994a). Evaluation of compositing algorithms for AVHRR data over land. *IEEE Transactions on*

*Geoscience and Remote Sensing*, 32: 427-437.

CIHLAR, J., MANAK, D. and VOISIN, N. (1994b). AVHRR bidirectional reflectance effects and compositing. *Remote Sensing of Environment* 48: 77-88.

COLL, C. and CASELLES, V. (1997). A global split-window algorithm for land surface temperature from AVHRR data: validation and algorithm comparison, *Journal of Geophysical Research* (in press).

D'IORIO, M.A., CIHLAR, J. and MORASSE, C.R. (1991). Effect of the calibration of AVHRR data on the normalized difference vegetation index and compositing. *Canadian Journal of Remote Sensing* 17: 251-262.

D'SOUZA, G. (1996). Basic radiometric calibration of NOAA-AVHRR data. In *Advances in the Use of NOAA AVHRR Data for Land Applications*, G. D'Souza, A.S. Belward and J.-P. Malingreau, Eds., pp.21-48. Dordrecht, NL: Kluwer Academic Publishers.

EUROPEAN ENVIRONMENTAL AGENCY (1996). Natural Resources, CD-ROM, Copenhagen, European Environmental Agency.

GU, X.F., SEGUIN, B., HANOCQ, J.F., GUINOT, J.P. (1994). Evaluation and comparison of atmospheric correction methods for thermal data measured by ERS1-ATSR, NOAA11-AVHRR, and Landsat5-TM sensors. *Proceedings of ISPRS 6$^{th}$ International Symposium " Physical Measurements and Signatures in Remote Sensing"*, Val d'Isère, France, 793-800.

HOLBEN, B.N. (1986). Characteristics of maximum-value composite images from temporal AVHRR data, *International Journal of Remote Sensing*, vol. 7, pp. 1417-1434.

HOLBEN, B.N. and SHIMABUKURO, Y.E. (1993). Linear mixing model applied to coarse spatial resolution data for multispectral sensors. *Int. J. Rem. Sensing* 14:2231-2240.

IQBAL, M. (1983). An Introduction to Solar Radiation. Academic Press, New York.

KAUFMAN, Y.J. and HOLBEN, B.N. (1993). Calibration of the AVHRR visible and near-IR bands by atmospheric scattering, ocean glint, and desert reflection. *International Journal of Remote Sensing*, 14: 21-52.

KAUFMAN, Y.J. and NAKAJIMA, T. (1993). Effect of Amazon smoke on cloud microphysics and albedo - analysis from satellite imagery. *J. Appl. Meteorology*, 32:729-744

KAUFMAN, Y. and REMER, L. (1994). Detection of forests using mid-IR reflectance: an application for aerosol studies. *IEEE Transactions on Geoscience and Remote Sensing*, 32: 672-683.

KERDILES, H., 1996. Software for processing AVHRR data for the Communities of Europe (SPACE).: algorithms used in SPACE version 2. MARS project, JRC.

KERR, Y.H., LAGOUARDE, J.P. and IMBERNON, J. (1992).. Accurate land surface temperature retrieval from AVHRR data with use of an improved split-window algorithm. *Remote Sens. Environ*., 41: 197-209.

LEPRIEUR, C., KERR, Y.H. and PICHON, J.M. (1996). Critical assessment of vegetation indices from AVHRR in a semi-arid environment. *International Journal of Remote Sensing*, 17: 2549-2563.

LÓPEZ, S., GONZÁLEZ, F., LLOP, R. and CUEVAS, M. (1991). An evaluation of the utility of NOAA-AVHRR images for monitoring forest fire risk in Spain. *International Journal of Remote Sensing*, 12: 1841-1851.

MELIA, J., LOPEZ-BAEZA, E., CASELLES, V., SEGARRA, D., SOBRINO, J.A., GILABERT, M.A., MORENO, J. and COLL, C. (1991). *EFEDA Annual Report*, EPOC - CT90 - 0030 (LNBE), University of Valencia.

PALTRIDGE, G.W. and BARBER, J. (1988). Monitoring Grassland Dryness and Fire Potential in Australia with NOAA-AVHRR Data. *Remote Sensing of Environnement*, 25:381-394.

PINTY, B. and VERSTRAETE. M.M. (1992). GEMI: a non-linear index to monitor global vegetation from satellites. *Vegetatio*, 101: 15-20.

QI, J. and KERR, Y. (1994). On current compositing algorithms. In *Proceedings of the International Symposium on Physical Measurements and Signatures in Remote Sensing*, ISPRS Commission VII, January 1994, Val d'Isère, France, pp. 135-142.

RAO, C.R.N. and CHEN, J. (1994). Post-launch calibration of the visible and near infrared channels of the Advanced Very High Resolution Radiometer on NOAA-7, -9, and -11 spacecraft. NOAA Technical Report NESDIS 78, Washington, DC.

RAO, C.R.N. and CHEN, J. (1995). Inter-satellite calibration linkages for the visible and near-infrared channels of the Advanced Very High Resolution Radiometer on NOAA-7, -9, and -11 spacecraft. *International Journal of Remote Sensing*, 16: 1931-1942.

RAO, C.R.N. and CHEN, J. (1996). Post-launch calibration of the visible and near infrared channels of the Advanced Very High Resolution Radiometer on the NOAA-14 spacecraft. *International Journal of Remote Sensing*, 17: 2743-2747.

SOBRINO, J.A., COLL, C. and CASSELLES, V. (1991). Atmospheric correction for land surface temperature using NOAA-11 AVHRR channels 4 and 5. *Remote Sensing of Environment*, 38: 19-34.

TEILLET, P.M. and HOLBEN, B.N. (1994). Towards operational radiometric calibration of NOAA AVHRR imagery in the visible and near-infrared channels. *Canadian Journal of Remote Sensing* 20: 1-10.

TOWNSHEND, J.G.R., JUSTICE, C.O., SKOLE, D., MALINGREAU, J.P., CIHLAR, J., TEILLET, P., SADOWSKI, F. and RUTTENBERG, S. (1994). The 1km resolution global data set: needs of the International Geosphere-Biosphere Programme. *Int. J. Rem. Sensing* 15:3417-3441.

TUCKER, C.J. and SELLERS, P.J. (1986). Satellite remote sensing of primary production. *International Journal of Remote Sensing, 7, 11: 1395-1416.*

VALOR, E. and CASELLES, V. (1996). Mapping land surface emissivity from NDVI: Application to European, African and South American Areas. *Remote Sensing of Environment*, 57:167-184.

VERMOTE, E. and ROGER, J.C. (1996). Radiative transfer modelling for calibration and atmospheric correction. In *Advances in the Use of NOAA AVHRR Data for Land Applications*, G. D'Souza, A.S. Belward and J.-P. Malingreau, Eds., pp.49-72. Dordrecht, NL: Kluwer Academic Publishers.

VIDAL, A. (1991). Atmospheric and emissivity corrections of land surface temperature measured from satellite using ground measurements or satellite data. *Int J. Rem. Sens*., 12: 2449-2460.

VIDAL, A., DUTHIL, P., CASELLES, V., MURTAGH, J. and STRANG, M. (1997). MUST Users Requirements - Step Report on Requirements of Users from Spain, UK, France and the JRC. Report EU - DG XII Contract ENV4-CT96-0331-DG12 EHKN, Cemagref Montpellier, 1997, 22 p.

VIDAL, A., PINGLO, F., DURAND, H., DEVAUX-ROS, C. and MAILLET, A. (1994). Evaluation of a temporal fire risk index in Mediterranean forests from NOAA thermal IR. *Remote Sens. Environ*., 49: 296-303.

# SHORT TERM FIRE RISK MAPPING USING REMOTE SENSING

*N. Desbois [(a)], J.M. Pereira [(b)], A. Beaudoin [(a)], E. Chuvieco[(c)] and A. Vidal[(a')]*

[(a)] Laboratoire Commun de Télédétection Cemagref-ENGREF, France

[(a')] Irrigation Division, Cemagref, France

[(b)] Instituto Superior de Agronomia, Portugal

[(c)] Departamento de Geografía, Universidad de Alcalá, Spain

The short term fire risk or fire danger, is closely associated with weather conditions, which have great influence on vegetation water status and consequently its susceptibility to fire (Chuvieco and Martín, 1994). Assessing the fire danger is the basis of an efficient prevention. The protection against forest fire can be reinforced in the areas labelled with high danger, where the vegetation is particularly dry and consequently where fire ignition and fire propagation are made easier.

The moisture status of the vegetation can change significantly over periods of a few days depending on the weather conditions and species physiology. This is why the assessment of fire danger needs a very regular monitoring to identify periods and areas of higher danger.

Currently, most of the fire danger indices are based on meteorological data such as air temperature, air humidity and wind speed (Drouet, 1982; Van Wagner, 1987; Sol, 1989; Carrega, 1991). But daily estimation of vegetation water status for large areas remains difficult. Direct measurements of fuel moisture require costly spatial sampling and cannot therefore be generalised to

all forested areas. Moreover, current fire danger indices, computed from meteorological station data, are not spatially distributed because of the sparse geographical dispersion of such stations.

Several authors have shown the interest of remote sensing data, especially NOAA-AVHRR data, to monitor vegetation water stress. The main interest of such data is to provide, on a regular basis and on large areas, an exhaustive spatially distributed information on vegetation status. From an operational point of view, NOAA-AVHRR presents several advantages. The main ones are its temporal resolution (two images per day) and its good spectral information (visible, near, medium and thermal infrared). The first two channels (red, 0.58 to 0.68 µm, and near infrared, 0.72 to 1.10 µm) permit the computation of vegetation indices which are correlated with green biomass, photosynthetic activity (Tucker and Sellers, 1986) and moisture content (Paltridge and Barber, 1988). The two thermal infrared channels (band 4, 10.3 to 11.3 µm, and band 5, 11.5 to 12.5 µm) allow the computation of a Surface Temperature corrected for atmospheric and emissivity effects (Vidal, 1991; Gu *et al.*, 1994; Meliá *et al.*, 1991; Kerr *et al.*, 1992). Moreover, its spatial resolution (1.1 km at nadir) gives an integration of local variations and provides an average response well adapted to global scale (López *et al.*, 1991).

## 1. CURRENT METHODS FOR FIRE DANGER ESTIMATION USING REMOTE SENSING

Several studies have shown the interest of remote sensing to monitor vegetation water status for agricultural canopies (Malingreau and Belward, 1989; Jackson *et al.*, 1983; Vidal and Perrier, 1990; Lagouarde and Brunet, 1991; Seguin *et al.*, 1991, etc.). Among them, few concern the estimation of Mediterranean forest water stress (López *et al.*, 1991; Vidal *et al.*, 1994;

Chuvieco and Martin, 1994; Prosper-Laget *et al.*, 1995; Illera *et al.*, 1996, Vidal and Devaux-Ros, 1995).

Four different types of methods can be distinguished. Most of them are based on the study of multitemporal series of vegetation indices, especially the NDVI (Paltridge and Barber, 1988; López *et al.*, 1991; Gouyet *et al.*, 1991), or indices derived from them (Burgan and Hartford., 1993; Alonso *et al.*, 1996).

A second category is based on the thermal dynamism of the vegetation as an indicator of its water stress. Thermal infrared data are then combined with meteorological data -especially air temperature- to estimate the vegetation evapotranspiration (Seguin, 1990; Vidal *et al.*, 1994, Desbois et Vidal, 1996).

A third category of research is oriented on the combination of vegetation indices and thermal data (Nemani and Running, 1989; Prosper-Laget et al, 1995; Illera *et al.*, 1996, Vidal and Devaux-Ros, 1995).

Finally, radar data, which are sensitive to water content, could be an interesting mean for assessing the fuel moisture.

### 1.1. Methods using vegetation indices.

The spectral characterisation of plant water stress has been attempted by several authors (Tucker, 1980; Jensen, 1983; Rock et al., 1986; Westman and Price, 1988; Hunt and Rock, 1989; Cohen, 1991a; Cibula *et al*., 1992). These studies conclude that the medium infrared band is the most sensitive to changes in moisture content, since water is the main factor of absorption in this channel. The effect of water stress is only observed in visible and near infrared bands when clear leaf deterioration is shown as a result of moisture loss. For instance, it has been observed in field studies that reflectance in TM band 4 (0.76 - 0.90 μm) of a drying plant decreases only when the plant has lost more than 40 % of its initial moisture. The reflectance in near infrared decreases significantly, as a result of a decrease in volume of cells. The red and medium

infrared bands, on the contrary, increase their reflectance while the plant is losing water (Westman and Price, 1988). In laboratory studies, a good correlation has been measured between plant water content of herbaceous species and most TM channels, the higher values being for the medium infrared channels (bands 5 and 7) (Cibula *et al*., 1992). Same authors also found good correlation between moisture content and two synthetic bands in the border between the near and medium infrared (Cibula *et al*., 1992). After these conclusions, traditional vegetation indices for moisture content estimation should be used with cautious. Several authors have found that indices combining medium infrared and near infrared bands are more sensitive to water content than conventional near infrared to red ratios (Westman and Price, 1988; Hunt and Rock, 1989). Following these ideas some authors have defined the "Moisture Stress Index":

$$MSI = \frac{r_{1,65mm}}{r_{1,26mm}}$$

as a ratio of the reflectance in two medium infrared bands (Rock et al., 1986). A similar index using TM bands 5 and 4 has been observed to be highly and positively correlated with plant water stress of coniferous species (Westman and Price, 1988). The Normalized Difference Infrared Index (NDII) has also been suggested as a good predictor of water content (Hunt and Rock, 1989):

$$NDII = \frac{r_{NIR} - r_{MIR}}{r_{NIR} + r_{MIR}}$$

where $\rho_{NIR}$ and $\rho_{MIR}$ are near infrared and medium infrared reflectances, respectively. A similar trend has also been observed with the Wetness component of the Tasseled Cap transformation (Crist and Cicone, 1984), with the advantage in this case of having a greater spectral variability (Cohen, 1991b).

The main difficulty in using these moisture indices is the lack of available data with appropriate temporal resolution. AVHRR data provides daily information to compute conventional vegetation indices, but its medium infrared channel which is mostly influenced by the target temperature, is not suitable for direct use in moisture indices. However a method allows to split channel 3 into its emissive and reflective components (see the paper NOAA-AVHRR Satellite Data Processing: State of the Art and Choices in MEGAFiReS) and to retain only the emissive component to compute vegetation indices using medium infrared.

However, most studies on fuel moisture determination have been based on vegetation indices, particularly the normalised difference vegetation index (NDVI: Rouse *et al.*, 1974). This index slightly reduces atmospheric and viewing effects, while it is clearly correlated to chlorophyll content and amount of radiation absorbed by the plant (Sellers, 1987). Some studies have also tested the use of this index to estimate leaf water stress of cultures (Tucker, 1980; Ajai *et al.*, 1983) and fuel moisture content (FMC) of grasslands (Paltridge and Barber, 1988; Chladil and Nunez, 1995). According to previous paragraphs the observed good correlation between NDVI and FMC may be caused by the leaf deterioration as a result of water stress, and it has been observed after a long period (10 - 15 days) of water deficit (Cibula *et al.*, 1992). Considering fire risk in Mediterranean conditions, this period should not be an obstacle to use vegetation indices in water stress determination, although NDII indices and others based on thermal channels (see below) will also be included in the MEGAFiReS project.

Other vegetation indices, such as the following ones, could be used within this project to estimate vegetation vigour:

- The soil adjusted vegetation index, SAVI (Huete, 1988):

$$SAVI = \frac{r_{NIR} - r_R}{r_{NIR} + r_R + L}(1+L)$$

where $\rho_{NIR}$ and $\rho_{NIR}$ are respectively the reflectances in near infrared and red wavebands, and L is an unitless constant assumed to be 0.5 for a wide majority of LAI values.

- The Global Environmental Monitoring Index, GEMI (Pinty and Verstraete, 1991)

$$GEMI = eta \times (1 - 0.25 \times eta) - \frac{r_R - 0.125}{1 - r_R}$$

where $eta = \frac{2 \times (r_{NIR}{}^2 - r_R{}^2) + 1.5 r_{NIR} + 0.5 r_R}{r_{NIR} + r_R + 0.5}$

Other vegetation indices adapted to vegetation water stress estimation could also be created and tested.

Three methods using vegetation indices are presented below.

1.1.1. Multitemporal series of vegetation indices.

Vegetation dryness can be detected through decrements in the vegetation index computed during spring and summer (López *et al.*, 1991; Gouyet *et al.*, 1991). Strong decrements are related to high temperatures and low precipitation (López *et al.*, 1991). Paltridge and Barber (1988) and Chladil and Nunez (1995) have shown very good correlation between NDVI and FMC for grasslands in Australia. The latter authors suggest to include meteorological indices to refine the estimation of FMC using multiple variable regressions. Adjustments of 71 % have been measured in Tasmania (Chladil and Nunez, 1995). However, results on grasslands are extended with difficulty to shrub and forest lands. Indeed, NDVI measured over grassland is directly related to LAI and chlorophyll production whereas, on shrubs or forests, the existence of dryer components may veil the spectral signature link to growth or changes in

moisture content (Eidenshink *et al*. 1990). This is why these authors propose to use relative variations of NDVI instead of absolute ones, by computing greenness indices.

1.1.2. Greenness indices.

Greenness indices proposed by Eidenshink *et al*. 1990, are the following:

$GRN_{rel} = 100\ (ND_0 - ND_{min}) / (ND_{max} - ND_{min})$

where $GRN_{rel}$ is relative percent green, $ND_0$ observed NDVI for a pixel, $ND_{max}$ and $ND_{min}$ the maximum and the minimum NDVI for that pixel during the whole study period.

$GRN_{abs} = 100\ (ND_0 - NR_{min}) / NR_{max}$

where $GRN_{abs}$ is absolute percent green, $ND_{max}$ the maximum NDVI observed on historical series of images (0.66) and $ND_{min}$ the minimum NDVI observed on dry grass (0.05).

$SM = 250\ (GRN_{rel} + GRN_{abs})/2$

where SM is the site moisture.

These indices indicate how green a pixel is in relation to historical range of NDVI observations or to NDVI observed for extreme covers (dry grassland and very thick forest).

Burgan and Hartford, 1993 have used in the United States the $GRN_{rel}$, that they called Relative Greenness Index (*RGI*), to follow the vegetation susceptibility to fire. Such greenness maps have been successfully tested in the field and appear to be useful to assess fire potential across large areas (Burgan, 1995).

Moreover, Alonso *et al. (*1996) found correlation coefficients higher than 0.8 between shrubs moisture content and Relative Greenness Index (Figure )

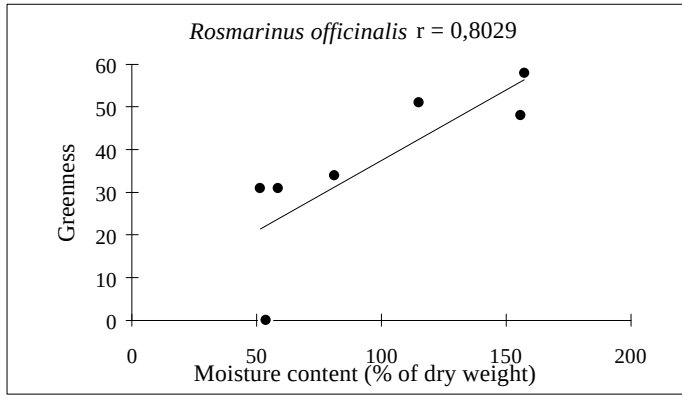


*Figure 1: Correlation between Rosmarinus officinalis moisture content and Relative Greenness Index (after Alonso et al., 1996).*

1.1.3. Cumulated decrements of vegetation indices.

At last, a method consists of computing cumulated decrements of NDVI from Spring to the end of Summer. Such indices have been applied in Spain by López et al. (1991) and Illera et al. (1996). The formulation proposed by López et al. (1991) is the following:

$$ARND = \sum_{h=d_1}^{d_t} \frac{NDVI(id_{h+1}) - NDVI(id_h)}{NDVI(id_h)}$$

where ARND is the cumulated relative NDVI decrement, $id_h$ is the image of the date h, $d_1$,$d_2$ ... are the dates of available NDVI images. The greater the ARND is, the greater the susceptibility of forest to fire may be. In the maps of ARND produced for Spain, the area that was burnt some days after, appeared with very high values (López *et al.*, 1991).

## 1.2. Methods using thermal infrared (surface temperature) and meteorological data.

An alternative to the use of vegetation index series is to follow the thermal dynamism of the vegetation cover. Several studies on crop moisture might be quite useful for fire danger estimation (Chuvieco and Martín, 1994).

The use of NOAA-AVHRR thermal infrared has been successful for estimating the daily evapotranspiration of agricultural canopies which is closely related to the water stress (Seguin et al., 1989; Vidal and Perrier, 1990; Kerdiles et al., 1991). According to Seguin (1990), this method could be applied to vegetation moisture estimation in forested areas.

The ratio of actual/potential evapotranspiration (*LE/LEp*) appears to be a good indicator of canopy water status. Canopy instantaneous actual evapotranspiration can be related to its instantaneous measured surface temperature (which can be derived from satellite data) through the surface energy balance:

$Rn = G + H + LE \quad (1)$

$LE = (Rn-G) - H \quad (2)$

$LE = (Rn-G) - (Ts-Ta)\rho\, Cp/ra \quad (3)$

where: *Rn* is net radiation, *G* soil heat flux, *H* sensible heat flux, *LE* latent heat flux or actual evapotranspiration, *Ts* and *Ta* respectively surface and air temperature, $\rho Cp$ volumetric heat capacity of air, *ra* aerodynamic resistance.

The *net radiation, Rn,* can be obtained from the expression of the surface radiative budget :

$$Rn = (1-a)Rg + Ra - e\,s\,Ts^4 \quad (4)$$

where : *a* is the surface albedo, ($a \approx 0.15$, Lagouarde and Brunet, 1991),

*e* is the surface emissivity, ($\varepsilon \approx 0.98$, Lagouarde and Brunet, 1991),

*s* is the Stefan-Boltzmann constant ($\sigma = 5.67 \times 10^{-8}$ W m$^{-2}$ K$^{-4}$).

Ts is the surface temperature (K)

Rg is the shortwave incoming solar radiation, measured by ground meteorological stations ($Wm^{-2}$)

*Ra* is the longwave incoming (atmospheric) radiation, which can be estimated for clear-sky conditions using the relation (Brutsaert, 1975):

$$Ra = 1.24(e_a / Ta)^{1/7} s Ta^4 \quad (5)$$

where $e_a$ is the vapor pressure (mb) and *Ta* is the air temperature (K), and

$$e_a = H.P \quad (6)$$

where *H* is the air humidity and *P* is the saturated vapor pressure ($Pa.K^{-1}$), computed as follows:

P= (6984.505294+Ta.(-188.903931+Ta.(2.133357675+Ta.(-0.01288580973 +Ta.(0.00004393587233+Ta.(-0.0000000802392308 +Ta.(6.136820929E-11)))))) *(7)*

Seguin *et al.* (1991) have measured, over long term periods at regional scale, correlation coefficients of r = 0.99 between *åLE - Rn* and *å(Ts-Ta).* This last parameter is the accumulated difference, over 5 and 10-day periods, between the mid-afternoon surface temperature from satellite and the maximum air temperature obtained from the meteorological ground network). These authors propose *å(Ts-Ta) / Rn* as an index of regional water stress.

Another vegetation water Stress Index, called the ***Stress Index (SI)*** has been successfully applied to fuel moisture estimation in the French Mediterranean region (Vidal *et al.*, 1994; Desbois et Vidal, 1996). Its formulation is the following:

*SI = 1 - LE/LEp,*

*LE* is estimated from satellite derived surface temperature and synoptic meteorological data and *LEp* only from synoptic meteorological data (Vidal *et al.*, 1994).

The *computation of LE* is based on the expression of the surface energy budget (Equations (1) and (2)):

$$LE = (Rn\text{-}G) - H$$

The *net radiation, Rn,* is computed with Equation *(4), t*he *soil heat flux, G,* can usually be neglected for vegetation cover and the *sensible heat flux, H* can be expressed as follows:

$$H = \frac{rCp}{r_a + r_o}(Ts - Ta)$$

where: $rCp$ is the volumetric heat capacity of air (≈ 1200 J m-3 K-1),

$r_a$ is the aerodynamic resistance (s/m)

$r_o$ is the structural resistance due to stratification of the leaves in the canopy (s/m) (Perrier, 1975). This parameter is here considered as an adjustment factor to maintain the *LE/LEp* ratio between 0 to 1. For *Les Maures* forest, it has been estimated at 16 s/m (Vidal *et al.*, 1994)

Due to the high roughness of the forest canopy, $r_a$ is usually low (Lagouarde and Brunet, 1989) compared to $r_o$, and a simple expression based on stable conditions can be used (Perrier, 1975):

$$r_a = \frac{1}{0.16u}\left(\ln\frac{z_{ref} - D}{z_o}\right)\left(\ln\frac{z_{ref} - D}{z_h - D}\right)$$

where : $u$ is the wind-speed at satellite overpass time (m/s)

$z_{ref}$ *is* the reference height, where meteorological measurements are made (=2m)

$z_h$ is the canopy height (m),

$z_o$ is the canopy roughness length (m): $z_o = z_h e^{-LAI/2}(1-e^{-LAI/2})$ , and

*D* is the displacement height given by Perrier (1982),

$D = z_h\left[1-\frac{2}{LAI}(1-e^{-LAI/2})\right]$ where LAI is the leaf area index

The computation of LEp is performed with a classical expression given by many authors (for example Jackson et al., 1981):

$$LEp = \frac{P' Rn + gEa}{P' + g(1 + r_0 / r_a)}$$

where: P' is the derivative of the saturated vapor pressure function P (Pa $K^{-1}$) (Eq. (7)),

$\gamma$ is the psychometric constant = 0.66 Pa $K^{-1}$

Ea is the evaporative potential of air given by Ea = $18(P-e_a)/r_a$ (W $m^{-2}$).

Higher values of Stress Index correspond with larger burnt areas and lower shrub ignition delay, which is highly correlated with relative water content (r = - 0.90 to - 0.96 measured by Valette *et al*., 1994) (Figure 2).

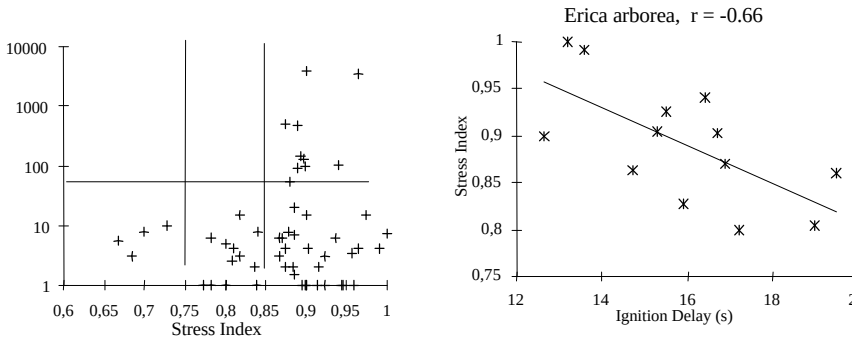


*Figure 2: Correlation between Stress Index and: Daily burnt surface (left), Ignition Delay of Erica arborea (right) (From Desbois et Vidal,1996).*

This SI index requires meteorological data such as air temperature and humidity, wind speed and global radiation which are only measured in some

observation points (meteorological ground stations). The spatially distributed remote sensing data and the locally recorded meteorological data can be combined using two ways:

- The first one consists in computing an averaged Stress Index for each homogeneous area (concerning climatic and vegetation criteria) using an averaged Ts and meteorological parameters measured at the nearest ground station.

- The second one consists in generating maps of meteorological parameters, which will be combined with NOAA-AVHRR surface temperature images to provide a Stress Index map at 1 km of resolution. However, the production of maps of meteorological parameters is very difficult, especially for wind speed and air humidity. But as these two parameters have low influence on the stress index, they are considered as constant on a given homogeneous area, whereas air temperature is spatialized. To produce Ta maps, several methods are currently available (see the position paper concerning Long-term Fire Risk Mapping) but the most promising for our purpose could be the use of multiple regressions with auxiliary variables (such as elevation, exposition, topographic shape ...).

### 1.3. Methods combining vegetation indices and thermal infrared data.

Regional estimates of vegetation water status have been developed using the slope of Ts versus NDVI relationship (Nemani and Running, 1989; Nemani *et al.*, 1993). The ratio NDVI / Ts has been tested as an indicator of fire risk in Spain (Illera *et al.*, 1996; Alonso *et al.*, 1996). Comparison with ground data (burned areas, fuel moisture content) show that a decrease in this ratio indicates an increase of fire danger. A correlation higher than 0.8 was observed between shrub moisture content and the NDVI / Ts ratio (Alonso *et al.*, 1996) (Figure 3).

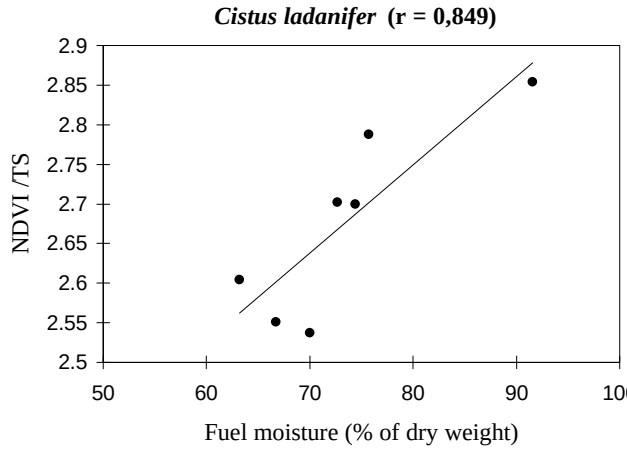


*Figure 3: Correlation between Cistus Ladanifer moisture content and the ratio of NDVI and Ts (after Alonso et al., 1996).*

Another study, carried out in French Mediterranean region, has shown that fire risk classes can be determined using the inverse relation between NDVI and Ts derived from NOAA-AVHRR satellite (Prosper-Laget *et al.*, 1995). These classes are obtained by dividing the bidimensional histogram, NDVI=f(Ts), into equipopulation classes (Figure 4). The combination of high surface temperature and low NDVI values corresponds to high fire risk. Whereas low Ts associated to high NDVI corresponds to low fire risk. Areas with higher fire risk were associated with the larger burnt areas.

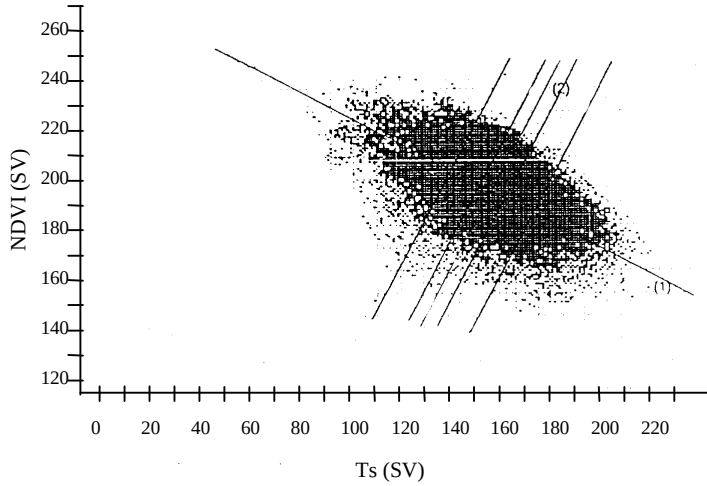


*Figure 4: Five classes of forest fire departure risk in Summer. The scatter plot is computed with all pixels of 10 scenes from April to September 1990 for 21 areas in South Eastern France (each pixel is defined by its NDVI and Ts scaled values SV). From Prosper-Laget et al., 1995.*

An other index, the ***Water Deficit Index (WDI),*** proposed by Moran *et al*. (1994), is based on the combination of a vegetation index and the difference surface minus air temperature obtained from Landsat TM images and meteorological data. This graphic method aims at better estimating the water stress of partial canopies.

According to Moran et al. (1994) the actual evapotranspiration versus potential evapotranspiration ratio can be estimated as follows:

$$\frac{LE}{LEp} = \frac{(Ts - Ta) - (Ts - Ta)_{dry}}{(Ts - Ta)_{wet} - (Ts - Ta)_{dry}} = \frac{BC}{AB} = 1 - WDI \qquad (8)$$

where A, B and C are reported on Figure 5. WDI is then computed from the position of a given pixel in the diagram representing fractional vegetation cover vs. surface minus air temperature difference. Its position is theoretically comprised within a trapezoidal pattern (Figure 5).

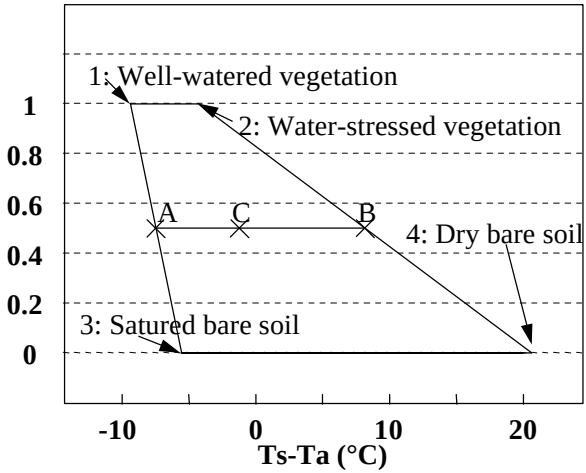


*Figure 5: The theoretical trapezoidal shape showing the different biomass vs. water stress conditions of a canopy-soil continuum (from Moran et al., 1994). The WDI (water deficit index) of point C is given by AC/AB as shown in Equation 8.*

Fractional Vegetation Cover can be estimated using spectral vegetation indices (Huete, 1988; Huete and Jackson, 1988) such as NDVI or SAVI.

The four points of the trapezoid can be defined using an image-derived NDVI vs. Ts-Ta bi-dimensional scattergram (figure 6), according to the following rules (numbers refer to Figure 5) :

•points 1 and 3 both correspond to the minimal value of *Ts-Ta* (left limit of the scattergram) inside the whole image: theoretical and observed values of wet soil and vegetation values of *Ts-Ta* suggest a similar value for soil and vegetation (Moran et al., 1994 ; Carlson et al., 1994) ;

•points 1 and 2 both correspond to the maximum value of *NDVI* (upper limit of the scattergram) inside the whole image ;

•the line joining vertices 2 and 4 follows the right limit of the scattergram ;

•the line joining vertices 3 and 4 corresponds to the maximum value of *NDVI* for bare soil in the area (NDVI = 0.09 for the example presented in figure 6).

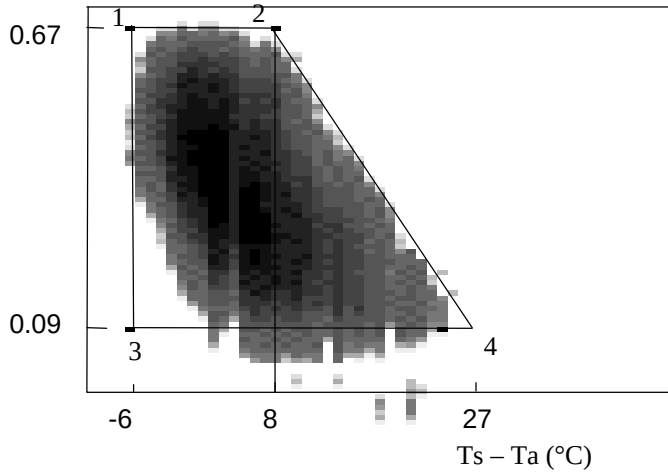


*Figure 6: NDVI vs. Ts-Ta scattergram from Landsat TM images on Les Maures 90/08/09. Trapezoid vertices were estimated from scattergram using rules given above (From Vidal and Devaux-Ros, 1995).*

Such a scattergram is created for each date of acquisition of a clear Landsat image.

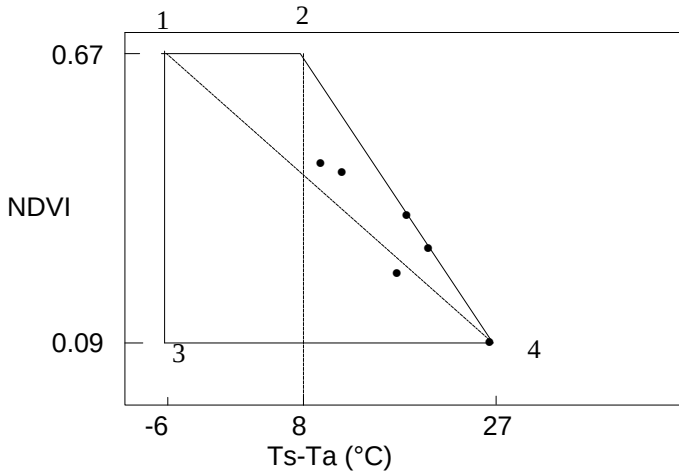


*Figure 7: Location of the couples of values (Ts-Ta, NDVI) of the areas where the 6 fires of more than 1 ha started during Summer 1990 in Les Maures (From Vidal and Devaux-Ros, 1995)*

Vidal and Devaux-Ros (1995) have successfully tested this method on a French forested area. It has been shown that areas where WDI ≥ 0.6 concern 100% of fire events of more than 1 ha occurring after Landsat overpass and only 19% of the forested area. The area of critical risk corresponds to the right part of the scattergram. Vidal and Devaux-Ros (1995) have shown that significant fire events mainly occurred in areas whose couples of values (*Ts-Ta*, *NDVI*) are above the line joining points 1 and 4 (Figure7).

The main interest of this approach is the possibility of estimating both *Ts-Ta* and Fractional Vegetation Cover from remote sensing measurements.

This method using Landsat TM data gives a local scale estimation of vegetation water status about twice a month that could be very useful to have a precise water stress mapping of some areas.

To have access to greater repeatitivity, NOAA-AVHRR images can be used instead of Landsat TM ones, but the dynamic range of NDVI and Ts-Ta is reduced, and the derived index may have a lower sensitivity. Nevertheless, the scattergram could be computed using several NOAA images corresponding to the temporal compositing period retained for vegetation indices, in order to increase the range of variation.

### *1.4. Interest of radar data to assess fuel moisture.*

1.4.1. Short state of the art.

Active radar sensors using SAR (synthetic aperture radar) techniques transmit their own microwave pulses towards the earth surface (using a given frequency, incidence angle and polarisation), where they interact with natural targets. A part of the energy is scattered back (backscattered) to the sensor, allowing to measure and create, through SAR data processing, an image of the surface backscattering coefficient, which characterises the target properties and can be of interest for various applications. The main advantages of SAR imagery are the following: 1) it provides images in all weather conditions, 2) it penetrates in the observed media (ground, vegetation, snow...) depending on the SAR configuration, and 3) it gives information linked to the water status and the geometry of this media. However, SAR also involves some difficulties as the speckle noise due to the coherent nature of the SAR illuminating random natural media, and the strong radiometric and geometric distortions. Both problems need to be solved to obtain significant information from radar images.

The fuel moisture content to be taken into account in fire risk assessment can be potentially monitored using SAR data (Westman and Paris, 1987; Gates, 1991). However, the radar is also sensitive to the amount of vegetation (woody and foliar parts) and its structure, and possibly to the underneath soil moisture and roughness if the forest cover is sparse and/or fragmented. Therefore, monitoring the vegetation water content using multi-temporal SAR images requires being careful with possible changes of the cover biomass and structure, and perturbations due to soil moisture. Fortunately, for Mediterranean forests mainly made of evergreen species, the main changing parameter is the water content during the summer drought. In particular, a recent study showed that multi-temporal ERS-1 SAR images (C-band, VV polarisation and 23° incidence angle) could be useful for fuel moisture content monitoring in the Mediterranean region (Beaudoin et al., 1995a). The backscatter temporal behaviour of a forest in South France (the *Massif des Maures*, mainly composed of oaks and pine trees), was found indicative of the change in water content of the foliar mass. The lowest backscatter was found to correspond with the minimal water content in August and a backscatter change ranging between 1 and 2.5 dB.

Other studies have shown relations between vegetation water content and radar backscatter (Ahern et al., 1993; McDonald et al., 1992; Weber and Ustin, 1991; Westman and Paris, 1987; Wismann et al., 1995) but none of them addressed the case of Mediterranean forest ecosystems. Therefore, quantitative work must be pursued to link in a robust way the radar backscatter to the water content and to take into account possible perturbations. These perturbations are mainly due to forest cover structure, heterogeneity and coverage, to possible ground backscatter mixed with the vegetation backscatter and to distortions due to topography that must be removed using appropriate tools.

## 2. VALIDATION METHODS

Validation of fire danger indices is difficult because fire danger depends on many factors, and especially, anthropic pressure. Three methods are classically used. They consist of relating fire danger indices with 1) fire events 2) meteorological data, and 3) fuel moisture content. For each method, two general approaches are possible: either comparing temporal profiles of both fire danger indices and field data, either establishing correlation between those two types of variables.

### 2.1. Correlation with forest fire statistics

This method is the simplest to be applied, considering that each partner country produces statistics on fire events which can be easily browsed. Fire statistics and fire danger indices will be computed and integrated over homogeneous areas (concerning climate and fuel type) near a meteorological station. But fire events (number and burnt areas) are indirect indicators of vegetation susceptibility to fire. Indeed, many factors influence fire ignition and extension such as wind, topography, human pressure, fire fighting conditions, etc. Nevertheless, the burnt areas, could be considered as a better indicator of the ability of the vegetation to spread fire. However, in order to define which parameters are the most pertinent for the validation of fire danger indices our teams will take into account the opinion of users (foresters, fire-fighters).

### 2.2. Correlation with meteorological data

The second method consists in assessing the sensibility of remote sensing fire danger indices to meteorological conditions (air temperature and humidity, wind, rain) and to see if these indices evolve logically in comparison with

them. For that purpose, temporal profiles of meteorological data and fire danger indices could be compared.

But meteorological data are equally indirect indicators of vegetation drought.

### 2.3. Correlation with fuel moisture content

The two previous types of assessment are therefore insufficient and must be complemented by correlation with direct measurement of vegetation moisture content. This is the reason why campaigns of fuel moisture content measurements have been conducted for summers 1995 and 1996, on study areas in Spain, France and Greece. Such a validation is costly in time and personal but provides direct indicators of vegetation drought that fire danger indices are supposed to estimate. However, the main problem is the difference of spatial resolution between field measurements, which concern several square meters, and remote sensing variables, which integrate data over 1 km² (NOAA) or more than 1 ha (Landsat TM). For that reason, field sampling has been done on areas as homogeneous as possible in order to have measurements representative of larger areas.

For low resolution data, sites of 2 x 2 km (4 NOAA-AVHRR pixels) were chosen whereas for high resolution sensors smaller sites have been defined (360 x 360 m for Landsat-TM and 250 x 250 m for ERS-2). Average satellite derived fire risk indices are computed for each site and compared with the corresponding fuel moisture content.

Samplings are made on shrubs and grass on the most representative species of each area. For instance, in *Les Maures* forest, two shrub species, very common there, have been selected: Strawberry tree (*Arbutus unedo*) and Heather (*Erica arborea*). On several individuals per site, only the shoots of the

year (leaves and branch) are collected, in order to eliminate the variability due to the age and the place of the shoots in the plant.

Samples are immediately weighted with a field balance to obtain the moist matter. Their are then placed 48h in a heater at 60°C and weighted to obtain the dry matter.

Measurements are done every 8 days for correlation with NOAA-AVHRR and every 16 days for Landsat-TM. For the specific case of *Les Maures* in France, the measurements were performed twice a week by the *Institut National de la Recherche Agronomique* (INRA). Moreover, since summer 1996, a network of fuel moisture measurements, managed by the *Office National des Forêts,* have been organised in the Mediterranean French region. The protocol used is the one developed by INRA and applied by MEGAFiReS partners. Some of these data could also be integrated to validate remote sensing derived water stress indices.

For the accuracy assessment using fuel moisture measures, fire danger indices derived from NOAA-AVHRR are computed on areas of 2 by 2 pixels around each sampling site and then correlated with the fuel moisture content measured the same day (for indices daily computed) or measured at the end of the 8-days period (for indices computed with temporal composite values) (Cf § 3.1.). For correlation using Landsat TM derived water stress index, the area for which the indices are computed represents 3 by 3 thermal pixels (360x360 m).

## 3. CONCLUSIONS

First and foremost, the delimitation of homogeneous fuel areas on which each index will be computed, is an imperative preliminary to multitemporal monitoring. Such fuel maps could be equally derived from NOAA-AVHRR images but this requires a complete study that can not be managed in

MEGAFiReS project. This is the reason why the fuel map would be rather generated from a reclassification of the CORINE Land-Cover.

We have seen that some indices require meteorological data (air temperature and humidity, wind speed and global radiation). The main difficulty is then to map them with a resolution compatible with that of NOAA. This question will be treated in MEGAFiReS in order to provide spatially distributed meteorological fire danger indices.

Remote sensing should provide basic data for fuel water status mapping but meteorological fire danger indices and topographic and human factors to allow for a complete short-term estimation of fire danger should complement such information.

Research concluded in MEGAFiReS is oriented to the elaboration of operational methods for forest fire management. Consequently, in order to make operational use of space technology for forest fire danger estimation the following aspects have to be taken into account:

- Fire danger requires a short term estimation to help the organisation (size and location) of surveillance and fighting means.
- Fire danger maps should be accurate and thus validated.
- Fire danger maps should be simple enough to be produced on large areas and to be used by services in charge of fire prevention and fire fighting. Fuel maps should allow a computation of indices for each fuel unit.

**REFERENCES**

AHERN, F. J., LECKIE, D.G. and DRIEMAN, J. A (1993). Seasonal changes in relative C-band backscatter of Northern forest cover types, *IEEE Trans. on Geoscience and Remote sensing*, Vol 31, No.3, May 1993, pp. 668-680.

AJAI, D., KAMAT, G.S., CHATURVEDI, A.K., SINGH, and SINHA, S.K. (1983). Spectral assessment of leaf area index, chlorophyll content and biomass of chickpea. *Photogrammetric Engineering and Remote Sensing*, 49:1721-1727.

ALONSO, M., CAMARASA, A., CHUVIECO, E., KYUN, I.A., MARTIN, M.P. and SALAS, F. J. (1996). Estimating Temporal Dynamics Of Fuel Moisture Content of Mediterranean Species from NOAA-AVHRR data, *EARSeL Advances in Remote Sensing,* 4-4: 9-21.

BEAUDOIN, A., VIDAL, A., DESBOIS, N. and DEVAUX-ROS, C. (1995a). Monitoring the water status of Mediterranean forests using ERS-1, to support fire risk prevention. *Proc. of IGARSS'95 Symposium,* Florence, Italy, 10-14 July 1995.

BEAUDOIN, A., STUSSI, N., TROUFLEAU, D., DESBOIS, N., PIET, L. and DESHAYES, M. (1995b), On the use of ERS-1 SAR data over hilly terrain: necessity of radiometric corrections for thematic applications, *Proc. of IGARSS'95 Symposium,* Florence, Italy, 10-14 July 1995.

BRUTSAERT, W.H. (1975). On a derivable formula for long-wave radiation from clear skies. Water Resources Res., 11, 742-744.

BURGAN, R. E. (1995). Use of remotely sensed data for fire danger estimation. *Proc. of EARSeL Int. Workshop on Remote Sensing an d GIS Applications to Forest Fire Management*, Alcalá de Henares, Spain, 87-95.

BURGAN, R. E. and HATFORD, R. A. (1993). Monitoring vegetation greenness with satellite data, USDA Forest Service, INT-297, Ogden.

CARLSON, T.N., GILLIES, R.R. and PERRY, E.M. (1994). A method to make use of thermal infrared temperature and NDVI measurements to infer surface soil water content and fractional vegetation cover. Remote Sensing Reviews, 9, 161-173.

CARREGA, P. (1991). A meteorological index of forest fire hazard in Mediterranean France. Int. J. Wildland Fire, 1 (2), 79-86.

CHLADIL, M.A. and NUNEZ, M. (1995). Assessing grassland moisture and biomass in Tasmania. The application of remote sensing and empirical models for a cloudy environment. *International Journal of Wildland Fire*, 5:165-171.

CHUVIECO, E. and MARTIN P. M. (1994). Global Fire mapping and Fire Danger Estimation Using AVHRR Images. *Photogrammetric Engineering and Remote Sensing*, 60: 563-570.

CIBULA, W.G., ZETKA, E.F. and RICKMAN, D.L. (1992), Response of Thematic Mapper bands to plant water stress. *International Journal of Remote Sensing*, 13:1869-1880.

COHEN, W.B. (1991a): Response of vegetation indices to changes in three measures of leaf water stress, *Photogrammetric Engineering and Remote Sensing*, vol. 57, pp. 195-202.

COHEN, W.B. (1991b): Chaparral vegetation reflectance and its potential utility for assessment of fire hazard, *Photogrammetric Engineering and Remote Sensing*, vol. 57, pp. 203-207.

CRIST, E.P. and CICONE, R.C. (1984). A physically-based transformation of Thematic Mapper data. The TM Tasseled Cap, *IEEE Transactions on Geoscience and Remote Sensing*, 22: 256-263.

DESBOIS, N. and VIDAL, A. (1996). Real Time monitoring of vegetation flammability using NOAA-AVHRR thermal infrared data. *EARSeL Journal Advance in Remote sensing*, 4-4: 25-32.

DROUET, D. (1982). Un moyen de prévoir les risques d'éclosion et de propagation des feux de forêts. Revue Forêt Méditerranéenne, II (2).

EIDENSHINK, J.C, BURGAN, R.E. and HAAS, R.H. (1990). Monitoring fire fuels condition by using time series composites of Advanced

Very High Resolution Radiometer (AVHRR) data, *Proc. Resource Technology 90*, ASPRS, Washington, D.C., 68-82.

GATES, D.M. (1991). Water relations of forest trees, *IEEE Transactions on Geoscience and Remote Sensing*, vol. 29 No 6, pp. 836-842.

GOUYET, J.F., KING, C., LE GLEAU, H., MALON, J.F., PHULPIN, T. and VALETTE, J.C. (1991). Apport des données satellitaires NOAA-AVHRR dans le suivi de la végétation forestière. *Proc. 5th Int. Coll. - Physical Measurements and Signatures in Remote Sensing*, Courchevel, France, 14-18 January 1991. ESA SP-319, May 1991. 625-630.

GU, X.F., SEGUIN, B., HANOCQ, J.F. and GUINOT, J.P. (1994). Evaluation and comparison of atmospheric correction methods for thermal data measured by ERS1-ATSR, NOAA11-AVHRR, and Landsat5-TM sensors. *Proceedings of ISPRS 6th International Symposium " Physical Measurements and Signatures in Remote Sensing "*, Val d'Isère, France, 17-21 Janv. 1994, 793-800.

HUETE, A.R. (1988). A soil-adjusted vegetation index (SAVI). *Remote Sensing of Environment*, 27: 47-57.

HUETE, A.R. and JACKSON, R.D., (1988). Soil and atmosphere influences on the spectra of partial canopies. *Remote Sensing of Environment*, 25, 89-105.

HUNT, E.R. and ROCK, B.N. (1989): Detection of changes in leaf water content using near-and medium -infrared reflectances, *Remote Sensing of Environment*, vol. 30, pp. 43-54.

ILLERA, P., FERNANDEZ, A., CALLE, A., CASANOVA, J.L. (1996). Evaluation of fire danger in Spain by means of NOAA AVHRR images. *EARSeL Journal Advance in Remote sensing*, 4-4: 33-43.

JACKSON, R.D., IDSO, S.B., REGINATO, R.J. and PINTER, P.J. JR. (1981). Canopy temperature as a crop water stress indicator. *Water Resour. Res*., 17, 1133-1138.

JACKSON, R.D., HATFIELD, J.L., REGINATO, R.J., IDSO, S.B., and PINTER, P.J. JR. (1983). Estimation of daily evapotranspiration from one time-of-day measurements. Agri. Water Management, 7, 351-362.

JENSEN, J.R. (1983). Biophysical remote sensing, *Annals of the Association of American Geographers*, vol. 73, pp. 111-132.

KERDILES, H., LOUAHALA, S., VIDAL, A. and SEGUIN, B. (1991). Analyse multidate de scènes NOAA-AVHRR sur la France: relation avec les caractéristiques agroclimatiques. *Proc. 5th Int. Coll. - Physical Measurements and Signatures in Remote Sensing*, Courchevel, France, 14-18 January 1991. ESA SP-319, May 1991. 631-634.

KERR, Y.H., LAGOUARDE, J.P. and IMBERNON, J. (1992). Accurate land surface temperature retrieval from AVHRR data with use of an improved split-window algorithm. *Remote Sens. Environ*., 41: 197-209.

LAGOUARDE, J.P. and BRUNET, Y. (1991). Suivi de l'évapotranspiration journalière à partir des données NOAA-AVHRR lors de la campagne HAPEX-MOBILHY. *Proc. 5th Int. Coll. - Physical Measurements and Signatures in Remote Sensing*, Courchevel, France, 14-18 January 1991. ESA SP-319, May 1991, 569-572.

LAGOUARDE, J.P. and BRUNET, Y. (1989). Spatial integration of surface latent heat flux and evaporation mapping. Adv. Space Res., 9 (7), 259-264.

LÓPEZ, S., GONZÁLEZ, F., LLOP, R. and CUEVAS, M. (1991). An evaluation of the utility of NOAA-AVHRR images for monitoring forest fire risk in Spain. *International Journal of Remote Sensing*, 12: 1841-1851.

MALINGREAU, J.P and BELWARD, A.S. (1989). Vegetation monitoring using AVHRR data at different resolutions. Proc. of the 4th NOAA-AVHRR data users meeting ...

McDONALD, K.C., ZIMMERMANN, R., WAY, J. and OREN, R. (1992). An investigation of the relationship between trees water potential and dielectric constant. *Proc. of the 1992 Int. Geoscience and Rem. Sens. Symposium.* Clear Lake (TX). 523-*525.*

MELIA, J., LOPEZ-BAEZA, E., CASELLES, V., SEGARRA, D., SOBRINO, J.A., GILABERT, M.A., MORENO, J. and COLL, C. (1991). *EFEDA Annual Report*, EPOC - CT90 - 0030 (LNBE), University of Valencia.

MORAN, M.S., CLARKE, T.R., INOUE, Y. and VIDAL, A. (1994). Estimating crop water deficit using the relation between surface-air temperature and spectral vegetation index. *Remote Sens. Environ*., 49 (3), 246-263.

NEMANI, R.R. and RUNNING, S.W. (1989). Estimation of regional surface resistance to evapotranspiration from NDVI and thermal IR AVHRR data. *J. Appl. Meteorol*, 28 (4): 276-274.

NEMANI, R.R., PIERCE, L., RUNNING, S.W. and GOWARD, S. (1993). Developing satellite-derived estimates of surface moisture status. *J. Appl. Meteorol*., 32 (3): 548-557.

PALTRIDGE, G. W. and BARBER, J. (1988). Monitoring Grassland dryness and fire potential in Australia with NOAA - AVHRR data. *Remote Sens. Environ*., 25: 381-394.

PERRIER, A. (1975). Etude physique de l'évapotranspiration dans les conditions naturelles. I. Evaporation et bilan d'énergie des surfaces naturelles. Ann. Agron., 16(1), 1-18. III. Evapotranspiration réelle et potentielle des couverts végétaux. Ann. Agron., 26 (3), 229-243.

PERRIER, A. (1982). Land surface processes: Vegetation. In "Land surfaces processes in atmosphere general circulation models". Ed. P.S. Eagleson, Cambridge University Press, 1982, 395-448.

PINTY, B. and VERSTRAETE, M.M. (1992). GEMI: a non-linear index to monitor global vegetation from satellites. *Vegetatio*, 101: 15-20.

PROSPER-LAGET, V., DOUGUEDROIT, A. and GUINOT, J.P. (1995). Mapping the risk of forest fire occurrence using NOAA satellite information. *EARSeL Advances in Remote Sensing* 4 (3-XII) 30-38.

ROCK, B.N., VOGELMANN, J.E., WILLIAMS, D.L., VOGELMANN, A.F. and HOSHIZAKI, T. (1986). Remote detection of forest damage, *Bioscience*, vol.36, pp. 439-445.

ROUSE, J.W., HAAS, R.H., SCHELL, J.A. and DEERING, D.W. (1974). Monitoring vegetation systems in the Great Plains with ERTS. Proc., Third ERTS-1 Symposium, Goddard Space Flight Center, NASA SP-51, Science and Technical Information Office, Washington D.C., 309-317.

SEGUIN, B. (1990). La température de surface d'un couvert végétal et son état hydrique. Possibilités d'application à la surveillance des forêts par satellite. *Revue Forestière Française*, XLII, 106-111.

SEGUIN, B., ASSAD, E., FRETEAUD, J.P., IMBERNON, J., KERR, Y. and LAGOUARDE, J.P. (1989). Use of meteorological satellites for water balance monitoring in Sahelian regions. *International Journal of Remote Sensing*, 10: 1101-1118.

SEGUIN, B., LAGOUARDE, J.P. and SAVANE, M. (1991). The assessment of regional crop water conditions from meteorological satellite thermal infrared data. *Remote Sens. Environ*., 35: 141-148.

SELLERS, P.J. (1987). Canopy reflectance, photosynthesis and transpiration, II. The role of biophysics in the linearity of their interdependence, *Remote Sensing of Environment.* 21:143-183.

SOL, B. (1989). Risque numérique météorologique d'incendies de forêt en zone méditerranéenne: dépouillement du test de l'été 1988 et propositions d'améliorations. Note de travail du Service Météorologique Interrégional Sud-Est (SMIRSE) n°1 - mai, 49 p.

TUCKER, C.J. (1980). Remote sensing of leaf water content in the near infrared. *Remote Sensing of Environment*, 10, 23-32.

TUCKER, C.J. and SELLERS, P.J. (1986) Satellite remote sensing of primary production. *International Journal of Remote Sensing, 7, 11: 1395-1416.*

VALETTE, J.C., SOL, B. and MORO, C. (1994). Flammability parameters and soil water reserve to improve the forecast of the meteorological forest fire danger index. *Proc. 2sd Int. Conf. Forest Fire Research*. Vol II. C.08, pp 611-624, Coimbra, Nov. 1994.

VAN WAGNER, C.E. (1987). Development and structure of the Canadian Forest Fire Weather Index system, Canada Forest Service, Ottawa.

VIDAL, A. (1991). Atmospheric and emissivity corrections of land surface temperature measured from satellite using ground measurements or satellite data. Int. J. Rem. Sens., 12 (12) 2449-2460.

VIDAL, A. and DEVAUX-ROS, C. (1995). Evaluating forest fire hazard with a Landsat TM derived water stress index . *Agr. and Forest Meteo*., 77: 207-224.

VIDAL, A. and PERRIER, A. (1990). Irrigation monitoring by following the water balance from NOAA-AVHRR thermal IR data. *IEEE Transactions on Geoscience and Remote Sensing*, 28: 949-954.

VIDAL, A., PINGLO, F., DURAND, H., DEVAUX-ROS, C., and MAILLET, A. (1994). Evaluation of a temporal fire risk index in Mediterranean forests from NOAA thermal IR. *Remote Sensing of Environment*, 49: 296-303.

WEBER, J.A. and USTIN, S.L. (1991). Diurnal water relations of walnut trees: implications for remote sensing, *IEEE Transactions on Geoscience and Remote Sensing*, vol. 29 No 6, pp. 864-874.

WESTMAN, W.E. and PARIS, J.F. (1987). Detecting forest structure and biomass with C-band multipolarisation radar: Physical model and field tests. *Rem. Sens. of Env.*, 22: 249-269.

WESTMAN, W.E. and PRICE, C.V. (1988). Spectral changes in conifers subjected to air pollution and water stress : experimental studies, *IEEE Transactions on Geoscience and Remote Sensing*, vol. 26, pp. 11-20.

WISMANN, V.R., BOEHNKE, K. and SCHMULLIUS, C. (1995). Monitoring ecological dynamics in Africa with ERS-1 scatterometer. *Proc. of IGARSS'95 Symposium*, Florence, Italy, 10-14 July 1995, 1246-1248.

# PROTOCOL FOR FUEL MOISTURE CONTENT MEASUREMENTS

*N. Desbois, M. Deshayes and A. Beaudoin*

*Laboratoire Commun de Télédétection Cemagref-ENGREF, Montpellier, France*

## 1. OBJECTIVE

The objective is to assess fire danger indices derived from satellite data, by establishing correlation between them and the fuel moisture content. Vegetation moisture content will be related to :

1. indices derived from optical and thermal infrared satellite data (NOAA-AVHRR and Landsat TM) to estimate short-term and long-term fire danger at global and local scale.
2. the backscattering radar coefficient of ERS-2 that is, theoretically, directly linked with the vegetation moisture content (long-term- fire danger at local scale).

## 2. STUDY AREAS AND SAMPLING SITES

### *2.1. Study areas*

Three study areas, characteristic of the Mediterranean vegetation, have been chosen in Spain, France and Greece (figure 1).


Figure 1 : General location of the study areas

- **France : *Les Maures forest***

This large forest of almost 90.000 ha, is located in the *Var département* (Southern France), between Toulon and Saint-Raphaël (Figure 2). Well individualised and rather homogeneous, this area is mainly covered by cork oak (*Quercus suber*), in association with holm oak (*Quercus ilex*) and pines (*Pinus halepensis*, *Pinus pinaster*) and various types of shrubs, especially heather (*Erica arborea*) and *Arbutus unedo*. This vegetation grows on acid soils. Elevation ranges from 0 to 780 m and the topography is rough. Fire danger is closely associated with a N-NW wind, the *Mistral*, violent, sudden and dry.

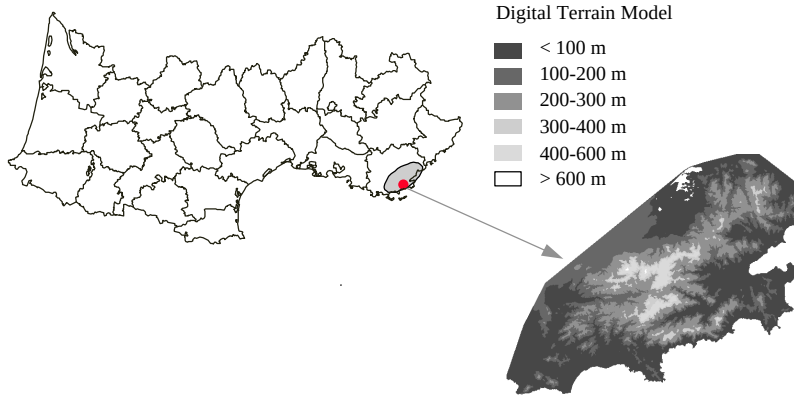


Figure 2 : Map of the French study area : Les Maures Forest.

- ***Spain : Cabañeros***

This area is a national park of 40000 ha located in central Spain, in the autonomous community of Castilla-la Mancha (Figure3). It is composed of three main units of vegetation: forest of *Quercus suber* and *Quercus rotundifolia*, shrublands with *Arbutus unedo, Phillyrea angustifolia, Pistacia terebinthus, Erica and Cistus* and grasslands. Elevation ranges from 500 to 1043 m as presented in Figure3.

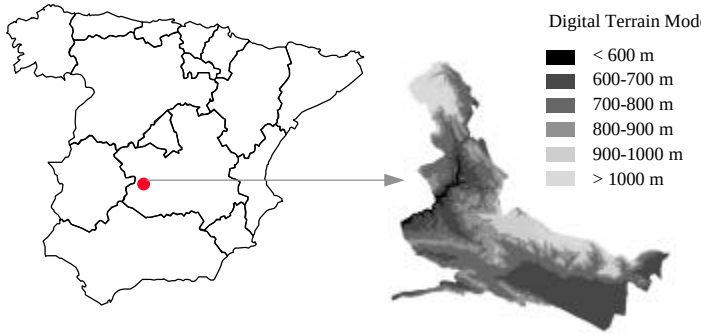


Figure 3: Map of the Spanish study area: Cabañeros.

***Greece : Halkidiki***

This area is located in Northern Greece, in Macedonia (Figure4). It is composed of diverse Mediterranean plant communities, such as *Oleo-ceratonion, Quercion ilicis, Ostryo carpinion, Quercion confertae, Fagion moesiacae* which are highly representative of the vegetation all over Greece. The topography of the area is rough. This area has been enduring an on-going history of forest fires. The average forest and grassland area burnt during the period 1971-1986 was 19 and 33 ha/year respectively.


Figure 4: Map of the Greek study area : Halkidiki.

**2.2. Choice of the location of the sampling sites**

Inside each study area, several sampling sites are selected. The main constraint to choose them is the spatial resolution of the satellites. Indeed, these sites must be homogeneous as possible concerning the type of vegetation and the topography.

Sites have been chosen mainly in shrublands and grasslands, which are easier to sample. But, in *Les Maures*, some sites have been selected in forest for correlation with ERS data.

The general constraints for site selection are the following :

- The vegetation should be thick enough (covering > 70 %) to prevent the soil from having too much influence on signal.
- The topography should be as homogeneous as possible, to avoid including influence of the variability in exposition.
- The distance between the sites and the number of sites should be adjusted so that the tour could be done between 11:00 and 16:00 LST (local solar time).

In a first step, the identification of the areas responding to these constraints can be done by combining a vegetation map and a digital terrain model (aspect and slope) or using a high resolution satellite image to identify homogeneous areas. Then, a field trip is necessary to check and to adjust the location of the sampling sites.

For each type of satellite data used, the following recommendations can be made:

- For NOAA-AVHRR :

It is recommended to extract the useful satellite parameters (surface temperature, vegetation indices) within a window of 2 x 2 pixels. This size allows to compensate the inaccuracy in the navigation of NOAA-AVHRR images (position known at 500 m) and is not too large, so that it could correspond to a relatively homogeneous area concerning vegetation type and topography.

However, considering the wide variability of environment in the European Mediterranean region, the homogeneity could not be sufficient within areas of 4 square kilometres. That is why the optimum would be to sample vegetation in several sampling spots within this window (Figure 5).

Then, the NOAA-AVHRR derived data will be compared with an average of the measurements.

- For Landsat TM:

The NOAA-AVHRR sampling spots have been used too for Landsat TM. The measurements in each sampling spot (Figure 5) are then correlated with the indices computed within a window of 12 x 12 pixels of 30 m for TM1 to TM5, which is equivalent to a window of 3 x 3 thermal pixels (120 m-resolution for TM6).

- For ERS:

The spatial resolution is 12.5 m. However to limit speckle noise effect, the signal must be averaged on a minimum of 200 pixels. Consequently, the ERS sampling sites should have a minimal size of 250 by 250 m.

The main limiting condition to choose these sites is the radar local incidence angle ($\theta_{loc}$) (Figure 6): the areas were $\theta_{loc}$ is normal to the terrain (< 15°) are not suitable, because of the degradation of the spatial resolution and of the perturbing ground radar echo in the backscatter. Consequently, it is important to choose areas where $\theta_{loc} \in [18°,45°]$. $\theta_{loc}$ is computed with equation (E), using a digital elevation model. Moreover these sites should be covered by homogeneous and thick vegetation.

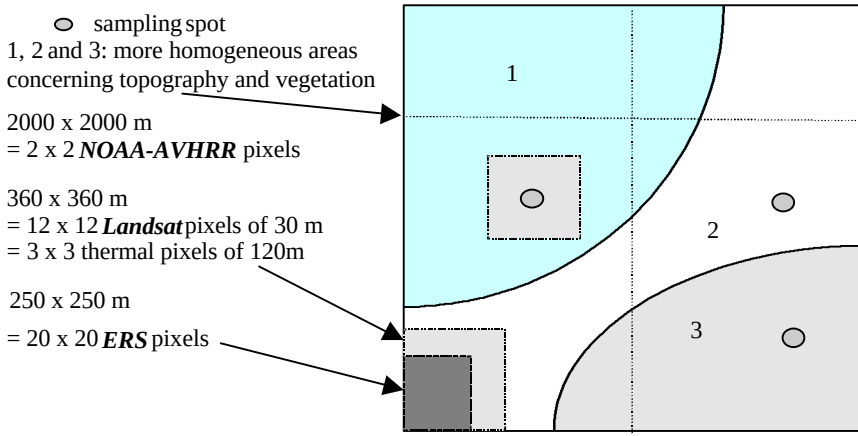


Figure 5: NOAA-AVHRR, Landsat TM and ERS sampling sites

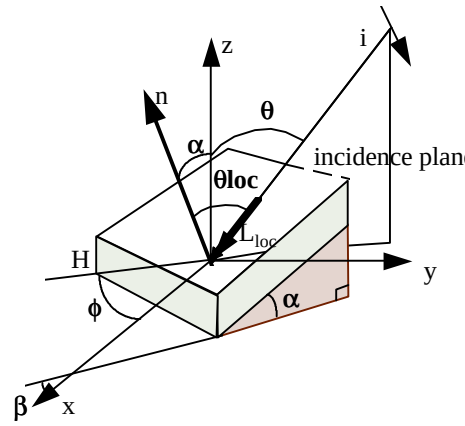


Figure 6: Scattering geometry over hilly terrain

E) $\theta_{loc} = \arccos [\cos\alpha \cos\theta - \sin\alpha \sin\theta \cos(\beta-\phi)]$

where : $\alpha$ = slope

$\beta$ = aspect

$\theta$ = SAR incidence angle = 23 °

$\phi$ = azimuthal viewing angle = 284 ° for descending pass and 77 ° for ascending pass

## 3. LENGTH OF THE CAMPAIGN AND PERIODICITY OF THE MEASUREMENTS.

### *3.1. Length of the campaign*

The campaign of measurements should run from April or May to the end of September in order to have a wide range of fuel moisture contents. But, depending of the countries, the drought period is not the same. For example, in Spain it can start early June, whereas in France it is rarely before early July. The moisture measurements should thus start after Spring rains, in order to have the highest rate of moisture content, and continue until the beginning of Autumn rains, to have the complete evolution of the vegetation water status.

Fuel moisture measurements are performed from end April to end of September and between 11:00 and 16:00 Local Solar Time, when air temperature is highest and most steady. This period of the day is also when vegetation is most affected by water stress and when the number of fire ignitions is likely to be more important. No measurement is done when it is raining or when the foliage is wet. This period coincides as well with NOAA-AVHRR and ERS data acquisition (respectively about 13:00 LST and 11:00 LST).

Measurements should not be done when it rains or when the foliage is wet (after rainfalls).

### 3.2. Periodicity of the measurements

As the periodicity of Landsat TM images is 16 days, measurements are to be done at each Landsat acquisition (every 16 days) and one more time between two Landsat acquisition (every 8 days) for correlation with NOAA-AVHRR. For the same reason, the beginning of the sampling period should correspond to an overpass of Landsat-TM.

For the specific case of *Les Maures* forest, the measurements will be done with a higher periodicity (twice a week ) by INRA (*Institut National de Recherche Agronomique*), as this has been done every summer in one sampling site since 1989, and since 1993 in several sampling sites distributed in the whole study area of *Les Maures* (Rochas, 1994). The INRA has agreed to transfer to Cemagref the measurements done in 1996 and 1997 in order to make correlations with satellite derived indices.

The measurements done for correlation with radar data, are made in Les Maures at each ERS overpass, from early June to the end of October.

The protocol for sampling and measuring the moisture content is derived from the one proposed by INRA and applied in Les Maures Forest (Valette et Moro, 1990 ; Rochas, 1994).

## 4. VEGETATION SAMPLES

### *4.1. Species*

For Landsat-TM and NOAA-AVHRR sites the measurements are limited to shrub and herbaceous species, the sites having being chosen in shrublands and grasslands (only for the Spanish study area) for commodity of sampling. However, for the study with ERS data, sites have been chosen in *Les Maures* in forest (cork and holm oaks) and shrublands.

The species sampled must be the most representative of the study area. For instance, in *Les Maures* forest, two shrub species, very common there, have been selected by INRA : *Arbutus unedo* and *Erica arborea.*

**4.2. Sampling**

The sampling spots are of about 50 x 50 m within the sampling site, in order to take into account the local variability of the vegetation water status.

The sampling protocol as the plant level had to take into account different variabilities within the crown, for example related to age or to position in the crown. As it was not possible to sample according to every possible source of variability, the solution taken has been to devise a simple, reproducible and coherent sampling, based on terminal shoots. Only these shoots (leaves and branch) are collected on individuals taken at random (at least 5 individuals per sampling spot and at least 10 shoots on each individual). On shrubs, the shoots of the year are well identifiable and, as the branch is not yet woody, they do not present a great difference of moisture content with the leaves. The fact to take only terminal shoots eliminates the variability due to the age and the place of the shoots in the plant (for shrubs). Thus, the measurements will be comparable from one day to an other and from one site to an other. It is however clear that the measured changes will be larger than what should be expected at the whole plant level.

These samples (between 100 g and 200 g) are immediately put in an hermetic box or in a plastic bag in order to conserve water content. They can equally be weighted in the field, with a balance of at least 0.1g- precision.

## 5. MEASUREMENTS

### 5.1. Case 1: without any field balance

- Before leaving for the field, each empty box is weighed and identified → Tare (T)

- Back to the laboratory, full, closed boxes are weighed → Tare + Wet matter (WM)

- Boxes are placed 48 h in a heater at 60°C (at this temperature, no carbonisation is observed, only the water and the very volatile elements are eliminated)

- Then, the sample is weighed in the box to avoid loosing some fine elements→ T+ Dry matter (DM)

### 5.2. Case 2: with a field balance

- The samples are placed in well identified boxes or bags, that can resist to high temperatures, and are weighted in the field as soon as they are collected → T + WM

- Back to the laboratory, they are placed 48 h in a heater at 60°C and then weighted → T+ DM

The moisture content (MC) can be then expressed either in percent of dry matter or in percent of wet matter :

$$MC(\%WM) = \frac{WM - DM}{WM} \times 100$$

**REFERENCES**

ROCHAS L., 1994. Inflammabilité et indice de siccité de la bruyère arborescente et de l'arbousier. Campagne 1994. INRA, Laboratoire de recherches forestières méditerranéennes, Avignon. Document PIF9425 - 43 p.

VALETTE J.C and C. MORO, 1990. Inflammabilités des espèces forestières en région méditerranéenne française. Document interne INRA, Centre de Recherche d'Avignon, Station de Sylviculture.

# METEOROLOGICAL INDICES FOR LARGE FIRES DANGER RATING

*Giovanni Bovio and Andrea Camia*

Dipartimento di Agronomia Selvicoltura e Gestione del Territorio (AGROSELVITER) Università di Torino, Italy

Meteorological factors play a key role in affecting wildfire occurrence and behaviour. Weather variables are often combined in specific meteorological fire danger indices that provide estimations of fire danger level at a given time.

A number of indices have been developed so far, and many of them are currently applied in operational conditions. Some indices are more suited to rate the probability of fire occurrence, while others are also related to the conditions for fire spreading; It should be reminded that the fire danger concept refers to both fire occurrence probability and expected fire severity (FAO, 1986).

In the European funded projects Minerve I and II (Bovio *et al.*, 1994; Viegas *et al.*, 1996), extensive studies were made comparing fire danger rating capabilities of different meteorological danger indices tested in the Mediterranean countries of the European Union.

The specific problem that is faced in the meteorological fire danger task of MEGAFiReS project, is the rating, from ground weather measurements, of the probability of large fires occurrence at a given time, where large fires are defined as wildfires with burned area of more than 500 hectares.

The entire European Mediterranean basin is concerned in the study.

It is therefore required to identify weather conditions under which larger fires are more likely to occur, trying to define severe fire weather conditions, through the analysis of the situations during past largest fires in Europe.

Another way of reformulating the problem could be the following (Brotak and Reifsnyder 1977): given a certain number of wildfires active in an area, some of them can become large fires, how can we estimate when they are more likely to occur? It is felt that both the probability and behaviour aspects of fire danger should be considered, but with a major emphasis on the latter.

## 1. EXTREME FIRE DANGER STUDIES

Large fires occur under extreme fire danger conditions. Meteorological variables are certainly not enough to determine large fire behaviour, as major fires are usually the results of many concurrent danger factors. Many efforts have been made in recent years to study extreme fire behaviour. Although a crown fire behaviour prediction model has not been developed so far, some results have already been provided that give interesting indications both on the conditions related to the start of crown fires (Van Wagner, 1977; Xanthopoulos and Wakimoto, 1991) and on the behaviour of most severe fires (Anderson, 1983; Rothermel, 1991a, 1991b; Van Wagner, 1974).

Putting together some concepts illustrated in the referenced papers, the favourable conditions for extreme fire behaviour can be summarised as follows:

- Dry fuels
- Low humidity and high temperatures
- Strong surface winds
- Unstable atmosphere

- Typical wind profile and low level jets
- Heavy accumulations of fuels
- Steep slope
- Height and bulk density of the forestry canopy

The variables synthetically indicated give an idea of the complexity of the phenomenon and the number of factors that are involved. Some of the key issues will be discussed in the sequel, referring to the most interesting results for our study.

According to Van Wagner (1967) moisture content of living foliage is an important factor for crown fires, and its variation according to the author's measurements both in conifers and broadleaves trees, seems to follow pretty much a seasonal trend, while very little year to year variation can be observed due to weather differences. Similar results were found by Chrosciewicz (1986) and by other authors cited in the mentioned papers.

The seasonal trend that was found by Van Wagner in Canada is different according to the age of leaves. In the case of old foliage (most conifer species but also broadleaves and many shrubs) the highest foliar moisture content is reached in late July-early August (120%), and the minimum in May-June (90%) before the new growth flushes. In the case of new foliage the highest level is in May-June (300%) decreasing gradually in July (200%), August (150%) and September (130%)

If the seasonal variation of foliar moisture content is taken into account, Van Wagner (1974) affirms that the upper range of the Initial Spread Index (ISI), one of the subindices of the Canadian Fire Weather Index (FWI) (Van Wagner, 1987) can be taken as a measure of crown fire spread.

According to Haines et al. (1976) "*moisture content of living vegetation is partially determined by the availability of moisture to root systems, while the*

*water content of large surface fuels responds to the same environmental stimuli as does soil water*". This statement, which is somehow in contrast with Van Wagner's results, is partially confirmed by a study of Olson (1981), that could correlate the foliar moisture content of four perennial brush species, with the Keetch-Byram (K-B) Drought Index (Keetch and Byram, 1968-1988), developed to evaluate the effects of long-term drying on litter and duff and thus on fire activities (Melton, 1989). Using the K-B index Burgan (1976) found a linear relationship with living fuel moisture.

Contradictory results in the literature about the relationship between living fuel moisture and soil moisture or long-term moisture balance models were mentioned also by Simard et al. (1989) that developed a live fuel damping model for North America, integrating both season trend and drought (long-term moisture) conditions.

With special emphasis on meteorological factors, several studies have addressed the problem of forecasting extreme fires occurrence, often from the analysis of weather conditions preceding and during past major fires.

An assessment of some drought indexes analysing the conditions before 26 critical fire periods was made by Haines et al., (1976). The drought indices considered were the Keetch-Byram Drought Index (K-B), the Palmer Drought Severity Index (PDSI) and the Build Up Index (BUI) of the 1964 National Fire Danger Rating System (NFDRS). Stating that large fires occur during long-term moisture deficiency periods, the authors wanted to see which index would have been more suitable to represent such conditions. The indices were chosen because of their capability of representing different moisture regimes with different response time to weather changes, thus providing estimates of the moisture content of various fuel types. In addition, the different moisture regimes considered were those found at different soil depth, and considering all of them had the important meaning of accounting for the eventually

correlated moisture content of different fuel layers (duff, litter, large surface fuels, living fuels).

In fact the BUI was designed to represent drying in the top 5-8 cm of soil, the K-B Drought Index is applicable to a layer from surface to deeper soil, having a moderately fast response to weather changes, while the PDSI has a slow response, again applicable to a layer from surface to deeper soil.

Haines et al. (1976) could not find a precise threshold value of any drought index for large fires, but some typical ranges were defined.

In addition, as the importance of moisture to fire potential changes with season, they observed a different behaviour in spring and autumn; in spring large fires occur when ground vegetation is in the cured stage and this is often the decisive factor. Also moisture loss in lower soil layers may be negligible, but evaporation from the upper levels may be high. Thus in spring what is important is moisture at surface and extreme upper layer.

In summer living vegetation gradually draws moisture from upper and lower level and a number of other phenomena cause water loss from all soil layers.

Thus, a good system that work throughout the seasons should not depend upon a fixed depth of soil horizon to indicate fire danger. A system employing a multilayer soil model is desirable but very complex. A possible alternative proposed by the authors is the use of a litter-duff index with rapid response feature in spring, and an index with slower response feature (long-term moisture deficiency) for late summer-autumn fires, that consider a greater depth of soil and also, in case, could be used in combination with a litter-duff model. In fact in summer the best should be a measure of long-term progressive drying focused on both the upper and the lower layers as a source of moisture.

In this way the best approach seems then to be a two-layer system to estimate long-term moisture deficiency, although further investigation should focus on the actual integrated response of the total fuel complex to drought.

Brotak and Reifsnyder (1977) analysed meteorological conditions associated with 52 fires of more than 2000 Hectares.

The extreme meteorological conditions identified were the following:

- Strong surface wind
- Typical wind profile (surface wind always more than 24 km/h, and generally greater than 32 km/h, while wind at 3000 m high was always more than 64 km/h)
- Presence of low-level jets (at 3000 m high)
- Atmospheric instability, especially with reference to the 950-850 mb lapse rate (i.e. the temperature difference between about 600 and 1500 m high). This was considered high enough to avoid the variability of surface temperature and the occurrence of surface based inversions, but it is still greatly influenced by day solar heating, and is probably a local rather than a macroscale parameter. The vast majority of large fires occurred when the lapse rate between these two levels was more than the standard atmosphere value (i.e. 6°C). Lapse rates between 850-700 mb (1500-3000 m) and 850-500 mb (1500-5500 m) indicate macroscale instability and were somehow still linked but less strictly.
- Location of low and high pressure areas, cold fronts and warm sectors in a weather map, according to some rule of thumb given by the authors, can help the prediction of large fires occurrence.

Aronovitch (1989), derived from two Byram's energy-criterion equations (1959) some expressions that could help in forecasting wildfire "blow-up", considering the wind profile and the existence of low-level jet (negative wind profile).

Stressing the importance of considering atmospheric stability to predict major wildfires, Haines (1988) proposes a Lower Atmosphere Severity Index (LASI) for identifying extreme wildfire conditions, based on temperature and dew point measurements at different layers of the lower atmosphere.

In practice the LASI is computed from the lapse rate values between two lower atmosphere layers and the moisture of one of them. The layers can be 950- to 850-mb or 850- to 700 mb or 700- to 500-mb according to the elevation of the area, resulting in a low-elevation, mid-elevation or high-elevation index respectively.

Brotak (1991) studied conditions (temperature, moisture, wind patterns) preceding 72 major wildfires in the USA. His results were that the LASI developed by Haines (1988) had some drawbacks when computed at noon, mainly because of destabilisation of lapse rates due to solar heating. In addition low-level wind profiles had not a constant correlation with extreme fire behaviour, depending on the location considered. Namely in the climatological situations where the driest period occurs in conjunction with strong synoptic winds, big chances of large fires are encountered because of these two factors. On the contrary, where the lowest fuel moistures occur in the period when strong synoptic winds are rare, large fires are more likely to be controlled by local or topographically induced winds.

According to Sol (1990), the “catastrophic days” can be predicted more easily than normal risk days, as extreme conditions, especially for the wind, are expected. But the forecasting of a severe fire day in a given area is quite complex because of the number of factors involved.

Some Authors (Flannigan and Harrington, 1987; McCutchan and Main, 1989) have found good correlation between meteorological variables or drought indices and fire severity, extending the period to which the prediction is related, i.e. referring severity conditions to months instead of days.

The Palmer Drought Severity Index (PDSI) is a measure of long-term moisture change, computed weekly for all the climatic districts of the United States of America to monitor the level of fire severity during the fire season (Haines et al., 1976; Heddinghaus, 1985; Karl, 1986). The PDSI is a highly complex system that measures a departure from normal drought conditions for a given period. It is based on a large number of coefficients that have been determined from a 30 years climatic period in the USA, the minimum and maximum air temperature (weekly or monthly means) and precipitation (weekly or monthly means). Normally it should be computed monthly, but to be operational it can be computed weekly.

Saying with Haines et al., (1976), "*most critical fires are caused by a combination of factors that occur in conjunction with drought conditions*". Drought conditions determine the amount of available fuel for a given site, but long-term moisture deficiency alone cannot be used to predict critical fire situations. Wind and atmospheric stability play also a very important role, especially in conjunction with drought conditions.

Simard et al., (1987) addressed the development of a Extreme Fire Potential Index (EFPI) to discriminate the days with extreme fire potential from the other days for decision making purposes.

The modelling work was concentrated only on the "*most extreme portion of the fire environment*" and was performed trying to identify that combination of indices and fuel characteristics the best discriminate days above or below a critical, extreme, fire potential threshold.

Their studies brought to the development of an information system for wildland fire severity called METAFIRES (Simard and Eenigenburg, 1991a; Simard and Eenigenburg, 1991b; Simard et al., 1989; Simard and Main, 1991), which has been reported as being quite reliable in North America.

The fire Severity Index is made up by six weather components: spread, upper air, short-term, mid-term and long-term moisture, season. Each component is based on a single index, selected among a number of existing ones, as best "large fires discriminator". The authors incorporate in this way in a single index all the different aspects and factors affecting large fires occurrence.

## 2. CHOICES IN MEGAFiReS

From what has been illustrated so far, it seems quite reasonable for the purposes of MegaFiReS, to follow an approach similar to Simard et al. (1987), namely to consider a number of different existing indices, representing different components of fire danger, selecting the ones with the best performances for discriminating extreme danger conditions in the European environment, and combine them in a unique, comprehensive fire severity index.

This approach will allow to account for the many different aspects of extreme fire danger conditions, trying to integrate them in a unique system.

Although many of the fire danger indices currently used in Europe have been designed to estimate surface fire danger conditions, part of them could also be useful to estimate specific conditions, eventually introducing some critical thresholds.

An empirical approach will be followed. Past large fires in Europe in the period from 1991 to 1995 will be considered and the meteorological conditions previous and during their occurrence will be analysed. A number of indices will be computed, namely the indices listed below.

Short-term moisture content (fine dead fuels):

- McArthur's 1967 fuel moisture model (part of the Australian Forest Fire Danger Meter) (McArthur, 1967)
- Simard's Equilibrium Moisture Content equations (Simard, 1968)
- American NFDRS 1-Hour Timelag Fuel Moisture (Deeming et al., 1977)
- Canadian Fine Fuel Moisture Code (FFMC) (Van Wagner, 1987)
- BEHAVE fine fuel moisture model (Rothermel et al., 1986)

Mid-term and Long-term moisture (mid size dead fuels, large dead fuels and live fuels):

- NFDRS 10-Hour and 100-Hour Timelag Fuel Moisture (Bradshaw et al., 1983)
- Fosberg's et Al. 1000-Hour Timelag Fuel Moisture (Fosberg et al., 1981)
- Keetch-Byram Drought Index (Keetch and Byram, 1968 - revision 1988)
- Canadian Drought Moisture Code (DMC) (Van Wagner, 1987)
- Canadian Duff Code (DC) (Van Wagner, 1987)

Live fuel moisture will also be considered accounting for the seasonal variations, stratifying the sample according to the time periods.

Some simple indices will be used to account for fire spread potential:

- Canadian Initial Spread Index (ISI) (Van Wagner, 1987)
- McArthur's Fire Danger Meters (Noble et al., 1980)
- Italian Fire Danger Index (Palmieri et al., 1993)

Other indices will be analysed, also to assess their performances in discriminating extreme fire danger days:

- Canadian Fire Weather Index (FWI) (Van Wagner, 1987)
- Canadian Build Up Index (BUI) (Van Wagner, 1987)
- Orieux Index (Orieux, 1979)
- Carrega '87 Index (Carrega, 1990)
- Sol Numerical Risk (Sol, 1990)
- ICONA Method (ICONA, 1993)
- Portuguese Index (Gonçalves and Lourenço, 1990)
- IREPI index (Bovio et al., 1994)

Although the introduction of an atmosphere instability component or some wind profile parameter could be convenient, at present time it is not planned, because no upper air data will be available for the research.

Meteorological data from ground weather stations of the JRC-MARS database will be used. As these data come from point sources, a spatial interpolation is required, and the knowledge-based procedure developed by Van Der Voet et al. (1994), which is regularly applied on the database, has proved to be suitable to the purposes of MEGAFiReS. Thus the meteorological data will be referred to a grid of 50x50 $km^2$ cells which also fits the requirements for the prediction of large fires in Europe.

As also site characteristics are involved in large fire danger, even if the study is in principle limited to weather factors, also some site issues will be considered. A climatic classification will be applied to the European Mediterranean countries, to account for both environmental modifications due to climate, and to different follow up of the fire seasons.

In the same perspective, a pre-stratification of the territory according to land use should also be convenient, but at present time it has not been planned in the context of MEGAFiReS.

**REFERENCES**

ANDERSON, H.E., 1983 - Predicting Wind-Driven Wild Land Fire Size and Shape. USDA For. Serv., Interm. For. And Range Exp. St., Research Paper INT-305, Odgen, UT, p. 26.

ARONOVITCH, B.B., 1989 - Forecasting wildfire “Blow up”. - Proceedings Tenth Conference on Fire and Forest Meteorology, April 17-21 1989, Ottawa, Canada.

BOVIO, G., QUAGLINO, A. and NOSENZO, A. 1984 - Individuazione di un indice di previsione per il pericolo di incendi boschivi. Monti e Boschi. 35, 4: 39-44.

BOVIO, G., SOL, B. and VIEGAS, D.X., 1994 - Synthese des Travaux sur l’intercomparison des indices de danger meteorologique d’incendie. In: Environment Programme, Minerve 1 Project, Final Report, 22-38.

BRADSHAW, L.S., DEEMING, J.E., BURGAN, R. E. and COHEN, J.D., 1983 - The National Fire Danger Rating System: Technical Documentation. USDA General. Technical Report INT-169, p. 41.

BROTAK, E.A., 1991 - Low-level temperature, moisture, and wind profiles preceding major wildland fires. - Proceedings Eleventh Conference on Fire and Forest Meteorology April, 16-19, 1991 Missoula, Montana.

BROTAK, E.A. and REIFSNYDER, W.E., 1977 - Predicting major wildland fire occurrence. - Fire Management Notes, Spring 1977.

BURGAN, R.E., 1976 - Correlation of plant moisture in Hawaii with the Keetch-Byram Drought Index. USDA For. Serv. Res. Note PSW-307. Cited in: Simard A.J., Eenigenburg J.E., Main W.A. 1989 - A weather-based fire season

model. - Proceedings Tenth Conference on Fire and Forest Meteorology, April 17-21, 1989 Ottawa, Canada.

BURGAN, R.E., 1989 - National fire danger rating system revisions. - Proceedings Tenth Conference on Fire and Forest Meteorology, April 17-21 1989, Ottawa, Canada.

BYRAM, G.M., 1959 - The Fire System Model In: Forest Fires Control and Use, K.P. Davis ed., McGraw-Hill Book Co.

CARREGA, P., 1990 - Climatology and index of forest fire hazard in Mediterranean France. Proceedings of the International Conference on Forest Fire Research, Coimbra. B.05-1/11.

CHROSCIEWICZ, Z., 1986 - Foliar moisture content variations in coniferous tree species of central Alberta. - Can. J. For. Res. 16, 157-162.

DEEMING, J. E., BURGAN, R. E. and COHEN, J. D., 1977 - The National Fire Danger Rating System-1978. USDA Forest Service. General Technical Report INT-39 p. 63.

FAO, 1986 - Wildland Fire Management Terminology. Forestry Paper 70, p. 257.

FLANNIGAN, M.D. and HARRINGTON, J.B., 1987 - A study of the relationship of meteorological variables to monthly provincial area burned by wildfire in Canada 1953-80. - Proceedings Ninth Conference on Fire and Forest Meteorology April 1987, San Diego, California.

FOSBERG, M. A., ROTHERMEL, R. C. and ANDREWS, P. L., 1981 - Moisture content calculations for 1000-Hour Timelag Fuels. Forest Sci. 27(1): 19-26.

GONÇALVES, Z.J. and LOURENÇO, L., 1990 - Meteorological index of forest fire risk in the portuguese mainland territory. Proceedings of the International Conference on Forest Fire Research, Coimbra. B.07-1/14.

HAINES, D.A., 1988 - A lower atmosphere severity index for wildlife fires. - National Weather Digest, 13(2): 23-27.

HAINES, D.A., JOHNSON, V.J. and MAIN, W.A., 1976 - An assessment of three measures of long-term moisture deficiency before critical fire periods. Res. Pap. NC-131 St. Paul MN North Central For. and Range Exp. St. USDA FS, 13 p.

HEDDINGHAUS, T.R., 1985 - The Palmer drought index and its availability as an indicator of forest fire watch areas. - Proceedings of Eight National conference on Fire and Forest Meteorology, Detroit, Michigan.

ICONA, 1993 - Manual de operaciones contra incendios forestales. Madrid. 5.1/65

KARL, T.R., 1986 - The sensitivity of the Palmer Drought Severity Index and Palmer's Z-Index to their Calibration Coefficients Including Potential Evapotranspiration. - Journ. of Climate and Appl. Meteor., 25,1, 77-86.

KEETCH, J.J. and BYRAM, G.M., 1968 (revision 1988) - A drought index for forest fire control. USDA Forest Service Research Paper SE-38.

LEE, B.S. and JEFFREY, A., 1994 - The Canadian forest fire severity information system. - Proceedings Second Int. Conf. on Forest Fire Research Vol. II, C.04, p.569, Coimbra, Nov. 1994.

McARTHUR, A.G., - 1967 - Fire behaviour in eucalypt forests. Commonwealth of Australian Forest and Timber Bureau, Leaflet Number 107, Canberra, Australian Capital Territory. 25 pages. In: Viney N.R. 1991 - A Review of Fine Fuel Moisture Modelling. The International Journal of Wildland Fire 1(4):215-234.

McCUTCHAN, M.H. and MAIN, W.A., 1989 - The relationship between mean monthly fire potential indices and monthly fire severity. -

Proceedings Tenth Conference on Fire and Forest Meteorology, April 17-21, 1989 Ottawa, Canada.

MELTON, M., 1989 - The Keetch-Byram drought index: a guide to fire conditions and suppression problems. - Fire Management Notes 50, 4, 30-34.

NOBLE, I.R., BARY, G.A.V. and GILL, A.M., 1980 - McArthur's fire-danger meters expressed as equations. Australian Journal of Ecology, 5, 201-203.

OLSON, C.M., 1980 - An evaluation of the Keetch-Byram drought index as a predictor of foliar moisture content in a chaparral community. - Proceedings of Sixth National conference on Fire and Forest Meteorology, April 22-24 1980, Society of American Foresters.

ORIEUX, A., 1979 - Conditions météorologiques et incendies di forêts en région mèditerranéenne. Ministère des Transports, Direction de la Météorologie, Note Technique du Service Météorologie Métropolitain.

PALMIERI, S., INGHILESI, R. and SIANI, A.M., 1993 - Un indice meteorologico di rischio per incendi boschivi. Proceedings from "Seminar on fighting forest fires" 26-28 April 1993 Tessaloniki.

ROTHERMEL, R. C., WILSON, R.A., MORRIS, G.A. and SACKETT, S.S., 1986 - Modelling moisture content of fine dead wildland fuels: input to BEHAVE fire prediction system. USDA For. Ser. Res. Pap. INT-359. Interm. Res. St., Odgen, Utah. p. 61. In: Viney N.R. 1991 - A Review of Fine Fuel Moisture Modelling. The International Journal of Wildland Fire 1(4):215-234.

ROTHERMEL, R.C., 1991a - Crown fire analysis and interpretation. - Proceedings Eleventh Conference on Fire and Forest Meteorology April, 16-19, 1991 Missoula, Montana.

ROTHERMEL, R.C., 1991b - Predicting Behaviour and Size of Crown Fires in the Northern Rocky Mountains. USDA For. Serv., Interm. For. And Range Exp. St., Research Paper INT-438, Odgen, UT, p. 46.

SIMARD, A.J., 1968 - The moisture content of forest fuels - A review of the basic concepts. Forest Fire Research Institute. Ottawa, Ontario. Information report FF-X-14, p. 47.

SIMARD, A.J. and EENIGENBURG, J.E., 1991a - Forecasting fire severity. - Proceedings Eleventh Conference on Fire and Forest Meteorology April, 16-19, 1991 Missoula, Montana.

SIMARD, A.J. and EENIGENBURG, J.E., 1991b - Metafire User's guide. - USDA Forest Service north Central Forest Experiment Station, Unpublished paper, p.39.

SIMARD, A.J., EENIGENBURG, J.E. and HOBRLA, S.L., 1987 - Predicting extreme fire potential. - Proceedings Ninth Conference on Fire and Forest Meteorology April 1987, San Diego, California

SIMARD, A.J., EENIGENBURG, J.E. and MAIN, W.A., 1989 - A weather-based fire season model. - Proceedings Tenth Conference on Fire and Forest Meteorology, April 17-21, 1989 Ottawa, Canada.

SIMARD, A.J. and MAIN, W.A., 1991 - A fire load index for the Western United States. - USDA Forest Service north Central Forest Experiment Station.

SOL, B., 1990 - Estimation du risque meteorologique d'incendies de forêts dans le Sud-est de la France. - Revue Forestière Française, Nancy. n° spécial, 263-271.

TAPPER, N.J., GARDEN, G. and FERNON, J., 1991 - Climatological and meteorological aspects of high fire danger in the Northern Territory, Australia. Proceedings Eleventh Conference on Fire and Forest Meteorology April, 16-19, 1991 Missoula, Montana.

VAN DER VOET, P., VAN DIEPEN, C.A. and VOSHAAR, J.O., 1994 - Spatial interpolation of daily meteorological data. A knowledge-based

procedure for the region of the European Communities. Report 53.3, DLO Winand Staring Centre, Wageningen (The Netherlands) p. 105.

VAN WAGNER, C.E., 1967 - Seasonal variation in moisture content of Eastern Canadian tree foliage and the possible effect on crown fires. - Forestry Branch, Departmental Publ. n° 1204.

VAN WAGNER, C.E., 1974 - A spread index for crown fires in spring. Petawawa Forest Experiment Station, Information Report PS-X-55, Chalk River, Ontario, p. 8.

VAN WAGNER, C.E., 1977 - Conditions for the start and spread of crown fire. Canadian Journal of Forest Research. 7(1): 23-34.

VAN WAGNER, C.E., 1987 - Development and Structure of the Canadian Forest Fire Weather Index System. Canadian Forestry Service. Forestry Technical Report 35, Ottawa. 37 p.

VIEGAS, D. X., BOVIO, G., CAMIA, A., FERREIRA, A. and SOL, B., 1996 - Testing Meteorological Fire Danger Methods in Southern Europe, In: Proceeding 13th Conference on Fire and Forest Meteorology, Australia.

XANTHOPOULOS, G. and WAKIMOTO, R.H, 1991 - Development of a wildland crown fire initiation model. - Proceedings Eleventh Conference on Fire and Forest Meteorology April, 16-19, 1991 Missoula, Montana.

# REMOTE SENSING AND G.I.S. FOR LONG-TERM FIRE RISK MAPPING

*Emilio Chuvieco, Francisco Javier Salas and Cristina Vega*

Departamento de Geografía, Universidad de Alcalá, Spain

## 1. TEMPORAL SCALE IN THE CONSIDERATION OF FIRE RISK

The risk of forest fire occurrence can be considered at different spatial and temporal resolutions. Accordingly, different approaches to fire risk may be taken into account. If we focus on the spatial dimension of fire risk, we could distinguish between local and global studies. Both assessments of danger would address the diverse factors associated to fire ignition risk and fire behaviour hazard, but with different levels of spatial and thematic resolution. They would mainly be directed towards the pre-suppression phase of fire management. Local, national or international authorities would, therefore, use maps of fire risk to establish guidelines for the allocation of fire resources or to plan fuel management activities.

In a similar way, two temporal scales related to fire risk assessment may be distinguished: (i) a short-term estimation, which is required to take update decisions on fire pre-suppression and suppression activities, and (ii) a long-term, which is directed to the general, more permanent, planning of fire fighting resources. The former should ideally provide daily estimations of fire risk and it is typically based on weather data. The potential application of satellite imagery to this level of temporal resolution is discussed in Desbois et al. (1997).

Long-term fire risk refers to those permanent factors associated to fire ignition or fire propagation, such as topography, vegetation structure, human activities or weather patterns. These factors do not change daily but in a long-term basis, and at least can be considered stable during a whole fire season. This temporal scale is very useful to better understand spatial patterns of fire risk and to improve fire prevention management. The most critical variables related to long-term fire hazard are vegetation structure (height to surface ratio, flammability) and human activities (land use types, recreational practices), but they do not need to be updated frequently. Two to five year updates are accurate enough for fire management. Long-term fire risk maps are quite relevant for prevention and suppression purposes. They can help to design regional fire defence plans, which include fuel management practices and vigilance controls, such as fire-break design, dispatch, prescribed burning, look-out tower location, etc.

Since fire risk implies to consider several variables that offer great spatial variation, the use of geographic information systems (GIS) is quite necessary for this application. Integration and spatial analysis capabilities of GIS make them suitable tools for fire risk modelling. Moreover, fire-risk oriented GIS can also be used for other purposes, such as training hotshot crews when they are not familiar with the fire area. Obviously, this information may also be used for other applications unrelated with forest fires, such as wildlife or recreational management planning.

## 2. THE USE OF GIS IN FIRE RISK ASSESSMENT

A comprehensive consideration for fire risk implies to take into account a wide range of variables. A well-established terminology distinguishes between the concepts of risk associated to the beginning of a fire (fire ignition risk or flammability) and to the spreading of an active fire (fire behaviour risk or fire

hazard) (Vasconcelos, 1995). In each case, different variables and different risk weights should be considered. However, both approaches require being capable of integrating different spatial variables. GIS provide tools to create, transform and combine geo-referenced variables. Every analysis of geographical data with a GIS preserve the spatial dimension of variables being processed, because all transformations are performed cartographically. Therefore, GIS oriented towards fire risk mapping may portray the geographical location of those areas where risk factors are most severe and fire protection programs may be spatially and temporally oriented to the areas labelled as having high risk.

Traditionally, fire risk rating is based on sample areas and therefore the spatial distribution of fire risk was coarsely approached. Several GIS applications have been developed in the last decade to improve management of fire risk. Different authors have proven the capacity of GIS to improve the spatial representation and the analysis of risk indices that are used by forest protection agencies for prevention and pre-suppression planning. A GIS can spatially integrate several hazard variables, such as vegetation, topography, climatology and fire history, which can cover the whole study area. This spatially-comprehensive capacity of GIS have been extensively used in forest fire management to map fire risk (Cosentino et al., 1981; Brass et al., 1983; Burgan and Shasby, 1984; Gum, 1985; Yool et al., 1985; Root et al., 1986; van Wyngarden and Dixon, 1989; Lowell and Astroch, 1989; Chuvieco and Congalton, 1989; Lu et al., 1990; Chou, 1992; Woods and Gossete, 1992; De Vliegher, 1992; Vasconcelos and Guertin, 1992; De Vliegher et al., 1993; Vega et al., 1993; Dagorne et al., 1994; Salas and Chuvieco, 1994; Vasconcelos et al., 1994; Chuvieco and Salas, 1996). Most of these applications have been developed at the local level and therefore they cover a small area at high resolution (typically from 50 to 100 meter grid size). However, there are also some experiences with

global, low resolution, fire danger maps (Werth et al., 1985; McKinley et al., 1985).

For an in-depth analysis on the application of this technology to fire risk mapping, we will first consider the generation of the different risk and hazard variables, and then discuss the different schemes for their integration in a simple model of fire danger.

### *2.1. Description of geographical variables of fire risk*

The applications of GIS to fire risk modelling have considered a wide range of hazard variables, depending on the specific characteristics of fire events in the different test sites. From the projects previously quoted, we may summarise the following list of variables:

- Topography (elevation, slope, aspect and insolation)
- Vegetation (fuel types, flammability of species)
- Weather patterns (temperature, relative humidity, wind, and precipitation)
- Accessibility to roads and camping sites
- Land property type
- Distance to cities
- Soils
- Fire history
- Water availability

From all these variables, the most complex to generate is the vegetation map. Traditional vegetation maps are focused on the spatial delimitation of vegetation species following different taxons. From a fire management point of view, vegetation species are not necessarily relevant for risk determination, since

the same species may present completely different risk levels according to their morphological (height, density) or physiological (moisture status) characteristics. Fire behaviour strongly depends on plant size, vertical and horizontal continuity, plant moisture, compactness, ratio of dead to live elements, oil contents and density (Valette et al., 1979; Rothermel, 1983; Burgan and Rothermel, 1984; Hernando, 1989).

In modelling fire behaviour, the great variety of vegetation characteristics related to the spreading or the fire has been summarised by the definition of different fuel types (Deeming et al., 1978; Andrews, 1986). A fuel type may be defined as a classification of vegetation species according to their properties for combustion (fuel loading, density, vertical continuity, compactness, area to volume ratio; Anderson, 1982). Most fuel models have been developed considering that surface fires are the rule rather than the exception, and therefore they mostly consider the understorey component of forested areas. This is the case with the models developed for the Behave fire simulation program (Andrews, 1986), which is extensively used in fire propagation modelling. The importance of the understorey component severely difficult the discrimination of fuel types from remotely sensed data. Remote sensors only obtain information from the upper canopy layer, with very little penetration capability. On the other hand, the average height and density of plants define some of these fuel types (for instance, Behave models 4, 5 and 6 are shrubs of different heights and densities), which are very difficult to discriminate from the spectral information gathered by remote sensors.

In spite of these difficulties, several papers have explored the use of satellite remote sensing to generate these fuel models through digital image processing. Most attempts are local-scale oriented and have worked with Landsat-MSS or TM images (Rabii, 1979; Shasby et al., 1981; Salazar, 1982; Dixon et al., 1984; Agee and Pickford, 1985; van Wingarden and Dixon, 1989; Burgan, 1995; Salas

and Chuvieco, 1995; Castro and Chuvieco, 1996). However, there are also interesting experiences of global fuel type mapping using low resolution sensors like the NOAA-AVHRR (Miller and Johnston, 1985; Sadowski and Westover, 1986; Zhu and Evans, 1994). The accuracy measured by these studies ranges widely according to the different fuel types considered. Globally, estimated accuracies of 65 to 80 % have been obtained for Behave fuel types. Discrimination was particularly difficult between models 4 (high density and tall shrub, around 2 meters of height), 6 (shrub between 0,6 and 1,2 meters) and 7 (similar shrub to model 6 but mixed with tree species) of the Behave program. They are spectrally very similar and usually require auxiliary information to achieve significant levels of accuracy. Topographic variables and texture bands have been commonly added to the original bands for digital classification of these fuel types (Salas and Chuvieco, 1995). Radar data could also provide complementary information for fuel mapping, particularly at local scale, since radar is very sensitive to temporal and spatial variation of the canopy biomass (Beaudoin et al., 1994).

The human component of fire risk is critical in most Mediterranean countries, since human beings are the main agents of fire ignition, either by carelessness or arson. The spatial analysis of human risk is quite complex to model, since human activities related to fire are very diverse and difficult to be spatially represented (Vega et al., 1993). Therefore, to simplify the process two approaches may be considered: (i) deductive and (ii) inductive. In the first alternative, human risk maps are created by overlaying several variables related to fire ignition. Some of these activities are spatially concrete, such as recreation and dry grass burning, which tend to be associated to particular areas. However, some others do not have a clear spatial pattern, such as arson, which is the main cause of fire ignition in some areas. Therefore, to map all the human factors that may cause fire ignition is very complex.

The second approach for human risk modelling is more inductive, and tries to map human risk by looking at the spatial distribution of fire occurrence. As most national fire statistics provide information on fire starts, a frequency map of fire origins could be computed. This map would serve as a basis to create a human risk map, by relating fire occurrence to spatial corridors, for instance roads, camping sites, cities, urban-forest interface, etc. (Chuvieco and Congalton, 1989; Vega et al., 1993; Chuvieco and Salas, 1996; Castro and Chuvieco, 1996). In the case of having access to fire perimeters of past events, they could be used to weight the different variables related to human activity by means of local adjustments, which are frequently based on multiple regression (Chou, 1992).

As far as climatological variables is concerned, the main problem to solve is the accurate spatial interpolation of single point observations to create grid layers. For instance, temperature or air humidity data are usually obtained from meteorological weather stations and therefore do not cover the whole territory. To obtain temperature or air humidity maps spatial interpolation techniques must be applied (Delfiner and Delhomne, 1975; Muñoz, 1979-80; Taylor and Waite, 1980; Fernández and Moreno, 1981; Polo et al., 1981; Fujioka, 1983; Kindschy, 1984; Boyer, 1985; Hungerford et al., 1989; Justicia and Domínguez, 1992) . The most frequently used techniques for the spatial interpolation of climate data are:

- Thiessen polygons
- Weighted distance averaging
- Kriging
- Multiple regressions with auxiliary variables, such as elevation

The first three procedures are based on distance, while the fourth assumes a clear relationship between the meteorological variable to be interpolated and the auxiliary variable (commonly elevation). In our experience, this last choice is best for temperature, specially in those areas with sharp contrasts in altitude. Extrapolation criteria might be used for the spatial distribution of air relative

humidity, if some assumptions are held and a temperature map is previously generated (Chuvieco and Salas, 1996). Wind data, on the contrary, is very difficult to interpolate, since wind flows are very difficult to model in complex terrain (Ryan, 1983; Fosberg and Sestak, 1986; McCutchan and Fox, 1986; Ross et al., 1988).

### *2.2. Criteria to integrate forest fire danger variables*

After creating the different risk and hazard layers to be included in the model, the most critical problem is to establish a coherent criterion to properly combine those variables. Since the goal is to obtain a single index of fire risk, the component variables (vegetation, topographic, weather, etc.) should first be classified in a numerical scale of risk and then combined in a single index. In some cases, the creation of risk levels from the original variables implies changing the nominal-categorical scale to an ordinal scale. For instance, the different vegetation categories or topographic aspects should be assigned a numeric value associated with a specific hazard level. On the other hand, the integration of these layers in a single risk index requires that a weight be applied to each variable according to its importance on the fire occurrence (i.e., how much riskier is the vegetation than the slope?).

Both questions may be approached in a qualitative-subjective way or using a quantitative-objective scheme. The former results from the expert knowledge that assigns risk levels and weights according to the experience of fire managers. The simplest way to develop this procedure is to create risk tables, where the combinations of two variables are assigned specific danger values (Brass et al., 1983; Yool et al., 1985). Tables 1 and 2 include examples of such combinations.

Table 1: Fire risk model proposed by Brass et al., 1983 (study area in Nevada)

| Slope \ Vegetation | I | II | III | IV | V |
|---|---|---|---|---|---|
| 0-9 | Low | Low | Moderate | Moderate | Moderate |
| 10-19 | Low | Moderate | High | High | Very High |
| 20-29 | Moderate | High | High | Very High | Extreme |
| 30-39 | High | High | Very High | Extreme | Extreme |
| 40 and more | High | Very High | Extreme | Extreme | Extreme |

(I) Agriculture, riparian, lush, grass

(II) Sparse brush, sparse sage, sparse grass, hardwood, aspen

(III) Jeffrey pine, pinyon/juniper < 30 % of crown closure, cured grass, manzanita, medium density sage, mountain mahogany

(IV) Jeffrey pine, pinyon/juniper 30-50 % crown closure, dense sage.

(V) Jeffrey pine, pine > 50 % of crown closure.

Table 2: Fire risk index proposed by Salas and Chuvieco (1994) (study area in Central Spain)

| | Behavior Risk | | | |
|---|---|---|---|---|
| Ignition Risk | Very High | High | Moderate | Low |
| Very High | Very High | Very High | Moderate | Moderate |
| High | Very High | High | Moderate | Moderate |
| Moderate | High | High | Moderate | Low |
| Low | Moderate | Moderate | Low | Low |

The human risk, vegetation, illumination and elevation maps defined ignition risk, while Behaviour risk was defined by vegetation, slope, aspect, elevation and fire breaks maps.

The main problem of this approach lies on its subjectivity and local-orientation. Experts make the decisions, but even assuming their good knowledge of fire events in the study area, the method does not offer a clear rationale for extending the defined criteria to other areas. On the other hand, qualitative categories do not provide a clear image about gradients of risk presented in the field.

The quantitative approach to integrate fire-related variables can be achieved in different ways. First, it could be based on the selective weighting of danger variables to create single danger indices (Chuvieco and Congalton, 1989; Vliegher, 1992; Salas and Chuvieco, 1994). Commonly these weights are based in the knowledge of the authors, as with the qualitative criterion, but this procedure does offer a gradient of risk levels, which can eventually be classified in different risk categories or used as they are produced. Some examples of such indices are (Salas and Chuvieco, 1994):

(1) Ignition Risk: $IR = 4 * H + 3 * V + 2 * I - E$

where H represents human risk factor, V represents vegetation, I represents illumination factor, and E represents the elevation factor.

(2) Behaviour Risk: $BR = 5 * V + 4 * S + 3 * A - E - FB$

where V represents fuel models factor, S slope factor, A aspect factor, E elevation factor and FB, the presence of fire-breaks.

These indices require establishing previously quantitative risk levels for each variable. For instance, vegetation or fuel type categories should be ranked according to their ignition or behaviour risk. They are more objective than the qualitative criteria previously discussed, but they should be interpreted in a relative and not absolute way. In other words, they define higher and lower levels of fire risk, but they can not be used to infer probabilities of fire ignition or rates of fire spread. Multicriteria evaluation techniques (Barredo, 1996) may be a good alternative to reduce the subjectivity of this assigning process.

This problem may be overcome by using weights based on multiple regression. In this case, the different risk variables are related to the fire occurrence of the study area, which is obtained from fire perimeters or fire statistics. Fire occurrence is the dependent variable, while fire risk variables are the independent ones. Models proposed in the literature for obtaining these functions range from simple multiple linear regressions (Castro and Chuvieco, 1996), to log-linear models (Chou, 1992; Vega, 1995) and neural networks (Vega, 1996). Since these models are produced by statistical fitting procedures, the accuracy can be estimated quantitatively (that is the percentage of original variance explained by the model) and therefore, a better understanding of the importance of each variable in fire occurrence can be obtained. However, they can not be applied outside the period and study area where they were produced, and therefore have only a limited value as general procedures for the integration of risk variables.

Finally, the variables can be combined using standard danger indices, such as national-based systems, like the US National Fire Danger Rating System (Agee and Pickford, 1985), or the ICONA's Spanish method (Chuvieco and Salas, 1996). Fire Modelling programs, like BEHAVE (Burgan and Rothermel, 1984) can also be used to obtain quantitative weights of each of the risk variables (Van Wyngaarden and Dixon, 1989; Vasconcelos and Guertin, 1992; Woods and Gossette, 1992). Using this approach, the risk maps produced may be consistent in across management. However, these national-based methods may offer poorer adjustments to local conditions than multiple regressions.

**REFERENCES**

AGEE, J.K. and PICKFORD, S.G., 1985, Vegetation and fuel mapping of North Cascades National Park. Final Report, College of Forest Resources. Seattle.

ANDERSON, H.E., 1982, Aids to determining fuel models for estimating fire behavior, USDA Forest Service.

ANDREWS, P.L., 1986, BEHAVE. Fire behavior prediction and fuel modelling system. Burn subsystem, USDA Forest Service. Ogden, UT.

BARREDO, J.I., 1996, Sistemas de Información Geográfica y Evaluación Multiciterio en la ordenación del territorio, Madrid, RA-MA.

BEAUDOIN, A., DESHAYES, M., PIET, L., STUSSI, N. and LE TOAN, T., 1994a. Retrieval and analysis of forest backscatter signatures from multitemporal ERS-1 data acquired over hilly terrain, Proceedings of the first ERS-1 Pilot Project Workshop, Toledo, Spain (ESA SP-365).

BOYER, D.G., 1985, Estimation of daily temperature means using elevation and latitude in mountainous terrain, Water Resources Bulletin, 20 (4): 583-588

BRASS, J., LIKENS, W.C. and THORNHILL, R.R., 1983, Wildland Inventory for Douglas and Carson City Counties, Nevada, Using Landsat and Digital Terrain Data, NASA Technical Paper 2137. Moffet Field.

BURGAN, R.E., 1995, Use of remotely sensed data for fire danger estimation, Int. Workshop on Remote Sensing and GIS applications to forest fire management, EARSeL, University of Alcalá de Henares: 87-97.

BURGAN, R.E. and ROTHERMEL, R.C., 1984, BEHAVE: Fire Behavior Prediction and Fuel Modelling System. Fuel Subsystem, USDA Forest Service. Ogden, Utah.

BURGAN, R.E. and SHASBY, M.B., 1984, Mapping broad-area fire potential from digital fuel, terrain, and weather data. Journal of Forestry, 82, 228-31.

CASTRO, R. and CHUVIECO, E., 1996, Modeling forest fire danger from geographic information systems, *Geocarto International* (in press).

CHOU, Y.H. 1992. Management of wildfires with a Geographical Information System. International Journal of Geographic Information Systems, 6, 123-40.

CHUVIECO, E. and CONGALTON, R.G., 1989, Application of remote sensing and Geographic Information Systems to forest fire hazard mapping. Remote Sensing of Environment, 29, 147-59

CHUVIECO, E. and SALAS, J., 1996, Mapping the spatial distribution of forest fire danger using GIS, Int. J. Geographical Information Systems, vol. 10 (3), 333-345

COSENTINO, M.J., WOODCOCK, C.E. and FRANKLIN, J., 1981, Scene analysis for wildland fire-fuel characteristics in a Mediterranean climate. Proc. 15th International Symposium on Remote Sensing of Environment, Ann Arbor, 635-46.

DAGORNE, A., DUCHÉ, Y., CASTEX, J.M., and OTTAVI, J.Y., 1994, Protection des forêts contre l'incendie and système d'information géographique. Application à la commune d'Auribeau-sur-Siagne (Alpes-Maritimes), Forêt Méditerraneénne, XV (4), 409-420.

DEEMING, J.E., BURGAN, R.E. and COHEN, J.D., 1978, The National Fire-Danger Rating System, U.S. Department of Agriculture, Forest Service, Ogden.

DELFINER, P. and DELHOMME, J.P., 1975, Optimum interpolation by Kriging, in Display and analysis of spatial data., J.C. Davis and M.J. McCullagh Eds.

DESBOIS, N, PEREIRA, J.M.C and CHUVIECO, E., 1997**,** Short Term Fire Risk Mapping Using Remote Sensing, Megafires project, Interim report.

DIXON, R., SHIPLEY, W. and BRIGGS, A., 1984, LANDSAT - A tool for mapping fuel types in the Boreal Forest of Manitoba: a pilot study, Winnipeg,

Manitoba Remote Sensing Centre, Fire Management and Communications Section, Canada Centre for Remote Sensing.

FERNÁNDEZ, F. and MORENO, A., 1981, Elaboración automática del mapa de isoyetas en un área montañosa del centro peninsular, VII Coloquio de Geografía, Pamplona, Tomo I, 23-29.

FOSBERG, M.A. and SESTAK, M.L., 1986, KRISSY: user's guide to modeling three dimensional wind flow in complex terrain, Gen.Techn. Report PSW-92, Berkeley, Pacific Southwest Forest and Range Experiment Station

FUJIOKA, F., 1983, Weighted interpolation as an interpretive tool. Implications for meteorological network design, Seventh Conference on Fire and Forest Meteorology, Fort Collins (Colorado), 1-6.

GUM, P.W., 1985, Computerization of fire dispatch utilizing satellite imagery 'Okanogan Project'. Pecora X Symposium, Fort Collins, 315-25.

HERNANDO, C., 1989, Inflamabilidad y poder calorífico de especies del sotobosque (zona Centro, Levante y Andalucía), Doctoral dissertation, Escuela Superior de Ingenieros de Montes, Universidad Politécnica de Madrid.

HUNGERFORD, R.D., NEMANI, R.R., RUNNING, S.W. and COUGHLAN, J.C., 1989, MTCLIM: A Mountain Microclimate Simulation Model, Research Paper INT-414, U.S. Department of Agriculture, Forest Service, Ogden .

JUSTICIA, A. and DOMÍNGUEZ, R., 1992, Notas metodológicas para la cumplimentación de series climáticas y extrapolación de datos. Su aplicación al mapa de temperaturas de Andalucía, BAETICA. Estudios de Arte, Geografía e Historia, 14: 55-80.

KINDSCHY, R.R., 1984, A method for estimating precipitation amounts at remote field site, Northwest Science, 58 (4): 256-261.

LOWELL, K.E. and ASTROH, J.H., 1989, Vegetative succession and controlled fire in a glades ecosystem. International Journal of Geographic Information Systems, 3, 69-81

LU, J., BOMBA, P., and KIND, T., 1990, A microcomputer-based geographic information system for forest fire management, ACSM-ASPRS Annual Convention, Denver, vol. 3, 180-192.

McCUTCHAN, M.H. and FOX, D.G., 1986, Effect of Elevation and Aspect on Wind, Temperature and Humidity, Journal of Climate and Applied Meteorology, 25: 1996-2013.

McKINLEY, R.A., CHINE, E.P. and WERTH, L.F., 1985, Operational fire fuels mapping with NOAA-AVHRR data. Pecora X Symposium, Fort Collins, 295-304.

MERRIL, D.F. and ALEXANDER, M.E. 1987. Glossary of Forest Fire Management Terms, Ottawa, Ontario, National Research Council Canada, 4th Edition.

MILLER, W. and JOHNSTON, D., 1985, Comparison of fire fuel maps produced using MSS and AVHRR data, *Pecora X Symposium*, Fort Collins, pp. 305-314.

MUÑOZ, J., 1979-1980, Una aproximación al cálculo de las temperaturas en el valle del Lozoya, Geographica, XXI-XXII: 95-107.

POLO C., VILLARINO, M. and RODRÍGUEZ, R., 1981, El cálculo de la precipitación en una cuenca de montaña. Aplicación del método Thiessen, VII Coloquio de Geografía, Pamplona, Tomo I: 13-22.

RABII, H.A., 1979, An Investigation of the Utility of Landsat-2 MSS Data to the Fire-Danger Rating Area, and Forest Fuel Analysis within Crater Lake National Park, Oregon, Oregon State University. Ph.D. dissertation.

ROOT, R.R., STITT, S.C.F., NYQUIST, M.O., WAGGONER, G.S. and AGEE, J.K., 1986, Vegetation and fire fuel models mapping of North Cascades National Park. ACSM-ASPRS Annual Convention. Tech. Papers, 3, 78-85.

ROSS, D.G., SMITH, I.N., MANINS, P.C. and FOX, D.G., 1988, Diagnostic wind field modelling for complex terrain: Model development and testing, J. Appl. Met., 27: 785-796.

ROTHERMEL, R.C. 1983. How to predict the spread and intensity of forest and range fires, USDA Forest Service. Ogden, UT.

RYAN, B.C., 1983, WNDCOM: estimating surface winds in mountainous terrain, General Technical Report PSW-73, Berkeley, Pacific Southwest Forest and Range Experiment Station, USDA, Forest Service.

SADOWSKI, F.G. and WESTOVER, D.E., 1986, Monitoring the fire-danger hazard of Nebraska rangelands with AVHRR data. Proc. 10th Canadian Symposium on Remote Sensing, Edmonton, 355-63.

SALAS, F.J. and CHUVIECO, E., 1994. Geographic Information System for Wildland fire risk mapping. Wildfire, Vol. 3 (2), pp. 7-13.

SALAS, F.J. and CHUVIECO, E., 1995. Aplicación de imágenes Landsat-TM a la cartografía de modelos combustibles, Revista de Teledetección, 5, 18-28.

SALAZAR, L.A., 1982, Remote Sensing Techniques Aid in Preattack Planning for Fire Management, Pacific Southwest Forest and Range Experiment Station, Berkeley.

SHASBY, M.B., BURGAN, R.E. and JOHNSON, R.R., 1981, Broad area forest fuels and topography mapping using digital Landsat and terrain data. Proc. 7th International Symposium on Machine Processing of Remotely Sensed Data, West Lafayette, 529-537.

SHEPPARD, D. 1968, A two-dimensional interpolation function for computer mapping of irregulary spaced data, Harvard papers in theoretical Geography, Geography and the properties of surface series, núm. 5.

SHERMAN, C.A., 1978, A Mass-Consistent Model for Wind Fields over Complex Terrain, Journal of Applied Meteorology, 17: 312-319.

TAYLOR, B. and WAITE, W., 1980, Interpolating climatological data for rugged terrain: some analytical techniques, Sixth Conference on Fire and Forest Meteorology, Seattle (Washington), pp. 163-173.

VALETTE, J. CH., CLEMENT, A. and DELABRAZE, P., 1979, Inflammabilité d'especes mediterranéennes, Avignon, INRA.

VAN WYNGARDEN, R. and DIXON, R, 1989, Application of GIS to model forest fire rate of spread, Challenge for the 1990's GIS, Ottawa, 967-977.

VASCONCELOS, M., 1995, Integration of Remote Sensing and Geographic Information Systems for fire risk management, Int. Workshop on Remote Sensing and GIS applications to forest fire management, EARSeL, University of Alcalá de Henares, 129-147.

VASCONCELOS, M. and GUERTIN, D.P., 1992, FIREMAP. Simulation of fire growth with a Geographic Information System, International Journal of Wildland Fire, 2, 87-96.

VASCONCELOS, M.J.P., CAETANO, M.S., PEREIRA, J.M.C, and CORREIA, S., 1994, Spatially distributed estimation of forest fire ignition probabilities, 2nd International Conference on Forest Fire Research, Coimbra, 647-648.

VEGA, C., 1996, Predicción de incendios forestales de causalidad humana en Withecourt Forest, Alberta, Alcalá de Henares, Trabajo de investigación inédito.

VEGA-GARCÍA, C., WOODARD, P.M. and LEE, B., 1993, Geographic and temporal factors that seem to explain human-caused fire occurrence in Whitecourt forest, Alberta, GIS'93 Symposium, Vancouver, 115-119.

VLIEGHER, B.M. de, 1992, Risk assessment for environmental degradation caused by fires using remote sensing and GIS in a Mediterranean region (Souty Euboia, Central Greece), IGARSS'92, Houston, 44-47.

VLIEGHER, B.M. de, DAPPER, M. de, and BAZIGOS, P.S., 1993, Assessment of fire risk in forests and grazing lands using multisource data. An example for SW-Messina, Greece, Int. Symp. Operationalization of Remote Sensing, Enschede (The Netherlands), vol. 2, 75-85.

WERTH, L.F., McKINLEY, R.A. and CHINE, E.P., 1985, The use of wildland fire fuel maps produced with NOAA-AVHRR scanner data. Pecora X Symposium, Fort Collins, 326-331.

WOODS, J.A. and GOSSETTE, F., 1992, A Geographic Information System for brush fire hazard management, Proc. ACSM-ASPRS Symposium, Washington, 56-65.

YOOL, S.R., ECKHARDT, D.W., ESTES, J.E. and COSENTINO, M.J., 1985, Describing the brushfire hazard in southern California. Annals of the Association of American Geographers, 75, 417-430.

ZHU, Z. and EVANS, D.L, 1994, U.S. Forest types and predicted percent forest cover from AVHRR data, Photogrammetric Engineering and Remote Sensing, 60: 525-531.

# DETECTION OF FOREST BURNING SITES WITH NOAA-AVHRR. TRIAL OF A FORWARD METHOD.

*Javier García, Consuelo Sánchez, Julia Yagüe and José Chuvieco*

*INFOCARTO, S.A., Madrid, Spain.*

## 1. INTRODUCTION

Active forest fires can be detected with NOAA satellites, even though the initial mission goal of the NOAA series of satellites had an atmospheric monitoring nature. Furthermore, early fire detection is of key importance for effective combating. Various international EO based forest fire research units recall NOAA as the most practical and feasible mean for fire detection, prior fire risk assessment and after fire determination of macro changes occurred in vegetation status.

Focusing on hot spots detection with NOAA, applications and experiences are numerous and vast world wide, not only for forest fires but also for monitoring a wider range of temperature anomalies, such as:

- magmatic and tectonic interaction (Luxley et al, 1995).
- thermal anomalies prior to earthquakes, as proved by Tronin (1996) in Central Asia, Iran and Egypt through the analysis of 10000 NOAA thermal images.
- ground heat flux measurements and thermal inertia of different types of soils and rocks (Cracknell et al, 1996).

- monitoring of volcanic thermal features such as active lavas and pyroclastic flows (Harris et al, 1995 ; Ridley et al, 1995).
- thermal ranges derived from vegetation and soil water content variations (Bussieres, 1995).
- evapotranspiration determination from EO thermal data (Caselles, 1994) and irrigation control (Vidal et al, 1990).

The development of MEGAFiReS tasks relative to forest fire detection during the fire prone season over the Mediterranean Basin requires close considerations of the pre-processing methods to be applied to NOAA-AVHRR data. Images characteristics (radiometric and geometric parameters according to Kidwell, 1993 and Rao et al, 1993) will be taken into account together with the most common methods used, up to date, for routinely fire detection (Ceccato et al, 1995; Downey et al, 1995) in order to advance in the development of improved sub-pixel detection algorithms. A refined algorithm developed from temperature differences in channels 3 and 4 will be used for the expected project outcome: the possibility of obtaining automatic listing of georreferenced burning pixels matching fires smaller than a pixel.

## 2. BACKGROUND REVIEW IN RELATION TO THE MEGAFiReS DATA CHAIN.

Thermal measurements from satellite sensors have a long history, starting as far back as 1978, when the Heat Capacity Mapping Mission (HCMM) was launched to observe thermal inertia of the Earth surface components. Its HCM Radiometer was designed with a ground resolution of 600 m. and a thermal band, and placed in a near polar orbit 620 Km above the Earth; the revisiting schedule had regular intervals of 12 hours, matching high and low heat peak levels.

Since 1984, the TM instrument on board Landsat 4 and 5 satellites, carries a thermal band, with a 120m spatial resolution, placed in a sun-synchronous early morning orbit with a 16 day repeating cycle. Such spatial resolution appears very convenient, but its swath is limited to 185 km and thermal measurements from a single thermal channel are not sufficient for land applications, which normally require observation values from several bands in the thermal IR for atmospheric corrections (Duguay, 1990). Difficulty in obtaining night observations and high costs of the images are further limitations of a real operational use of Landsat TM thermal data for fire detection (Gregotsky et al, 1991).

Presently, the most widely known space sensor providing thermal IR data on a routinary basis is the Advanced Very High Resolution Radiometer (AVHRR), on board NOAA satellites, whose missions began in 1978. Subsequent launchings have followed as shown in the following chart:

| ***Satellite*** | ***Sensor*** | ***Launching*** |
|---|---|---|
| NOAA-6 | AVHRR/1 | Jun-79 |
| NOAA-7 | AVHRR/2 | Jun-81 |
| NOAA-8 | AVHRR/1 | Mar-83 |
| NOAA-9 | AVHRR/2 | Dic-84 |
| NOAA-10 | AVHRR/1 | Sep-86 |
| NOAA-11 | AVHRR/2 | Oct-88 |
| NOAA-12 | AVHRR/2 | May-91 |
| NOAA-14 | AVHRR/2 | Dic-94 |

NOAA satellites follow a sun synchronous orbit, 840Km above the Earth with an angle over the poles, which varies between 98.7º and 98.9º. The US

Commerce Department NOAA, is fulfilling its commitment of maintaining at least two operative satellites, complementing each other's orbit (i.e.: one of them should cross the equator at solar UTC 07.30 and 19.30.-approx- and the other, at about 02.30 and 14.30).

Even numbered satellites cover the "morning orbit" (07.30) while odd numbered ones cover the "afternoon orbit" (14.30) (*theoretical hours*). Since NOAA 9 and NOAA 11 are not operational any more, and NOAA 13 escaped control shortly after launch, the latest NOAA 14 has assumed the afternoon coverages, despite the fact of having an even number: This arrangement of orbits is rather significant for the application to forest fire detection, allowing a homogeneous and frequent enough **temporal** coverage. NOAA scanning swath is 2800 Km, allowing a maximum **spatial** resolution of 1.1Km at nadir.

**Spectral** resolution capabilities of the AVHRR 1 and 2 sensors are summarised below, for the purpose of completing this short review on the NOAA general characteristics and also because spectral data processing is crucial for the intended application.

| | SPECTRAL RESOLUTION (μm) | | | | | |
|---|---|---|---|---|---|---|
| Sensor | ***Channel*** | ***Channel*** | ***Channel*** | ***Channel*** | ***Channel*** | Satellite |
| AVHRR 1 | .55-.90 | .72-1.0 | 3.55-3.93 | 10.5-11.5 | n/a | NOAA 10 |
| AVHRR 2 | .58-.68 | .72-1.0 | 3.55-3.93 | 10.3-11.3 | 11.5-12.5 | other NOAA |

## 3. CONSIDERATIONS ABOUT THE AVHRR SENSOR

Within the Earth Observation devices for thermal detection, we can review some considerations about the AVHRR sensor.

Technical characteristics of the AVHRR sensor have been brought together into the MEGAFIReS project and, particularly within the tasks of forest fire detection, for the purpose of testing out the accuracy, benefits and chances of real time application of a new detection algorithm based on splitting the Channel 3 radiance of a given element in its emissive and reflective components.

Trials of algorithm verification have been carried out over well known areas that suffered a fire during the 1996 summer. 120 NOAA 12 and 14 images were captured by Infocarto's NOAA tracking station between June and September 1996.

Several NOAA images other than those matching the *theoretical hour* can certainly be registered during the day, but there are technical reasons to prevent their use in the verification stage of the fire detection algorithm. The reasons for this option are:

1. These images suffer greater geometric distortions than those closer to proper acquisition time; hence, spatial resolution is lower too.
2. Radiometric values are biased and, therefore, standard discrimination algorithms would most probably not work appropriately.

As explained by Kennedy et al. (1994), the temperature of a body above absolute zero determines the level of electromagnetic energy emitted at a particular wavelength. According to Stefan-Boltzmann and Wien's laws, radiant emittance increases as the object temperature increases: therefore, maximum radiant emittance values are found in shorter wavelength values (*Figure 1*).

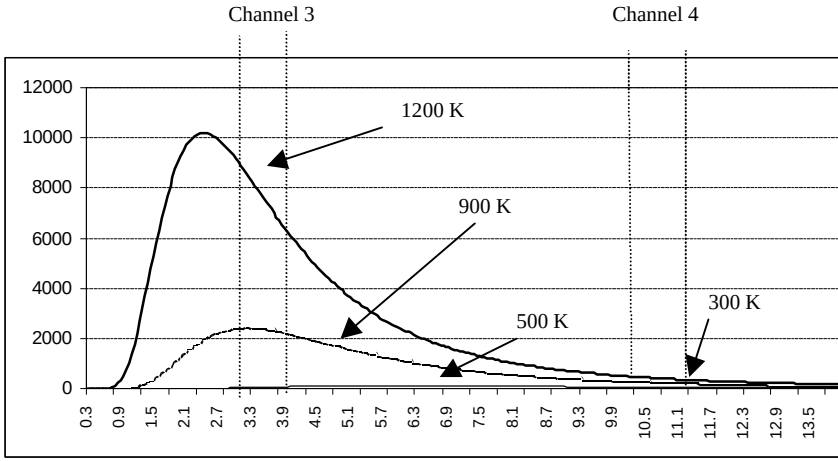


*Figure 1: Plank radiances for blackbody temperatures from 300 K to 800 K. Temperature increases are greater under channel 3 than under channel 4*

Assuming that the Earth's average daytime temperature is 300 K (Langaas, 1993; Kennedy, 1994) the highest emitted electromagnetic flux occurs between 9.7 and 11μm. This means that, from a spectral perspective, the most suitable channels for Earth temperature measurements would be channels 4 and 5 (the latter one, if available).

There are different figures in relation to temperatures forest fires can reach: in a single wildfire event at Lamto Station (Ivory Coast), Belward et al (1993) measured temperatures ranging from 526.12ºK to 594.2ºK; Robinson (1991) reports the highest temperature ever recorded in a forest fire, 1000. Fire temperatures will depend on various factors such as fuel type, time of the day or night, moisture contents, weather conditions, accumulated heat, etc.

Bearing in mind Wien's law, a hot spot radiating temperatures between 800-1000ºK has a maximum spectral radioactive emission between 3.33μm and 5.08μm. Hence, to measure bodies reaching those temperatures, channel 3

(3.55µm - 3.93µm) is most suitable. Figures 2 and 3 show channel 3 spectral response of the AVHRR sensor, for NOAA 12 and NOAA 14.

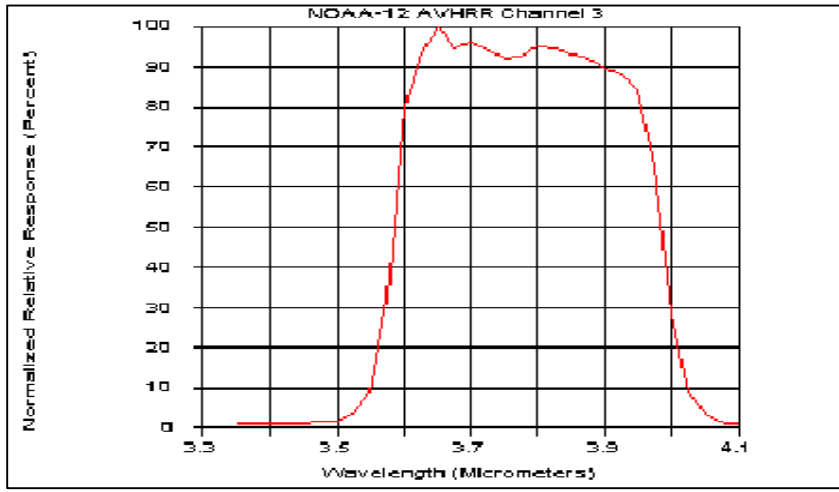


*Figure 2: Normalised spectral response of Channel 3, AVHRR-NOAA 12*

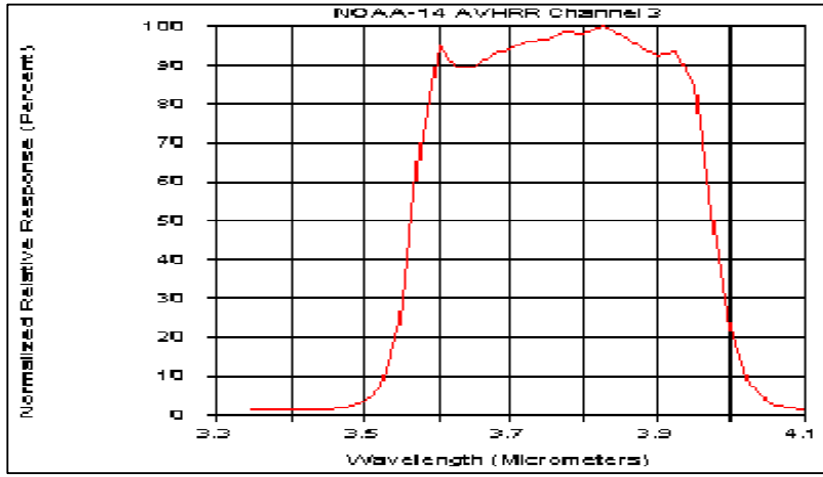


*Figure 3: Normalised spectral response of Channel 3, AVHRR, NOAA 14.*

Having determined channel 3 as the most suitable source of observed data for the project, it is necessary to determine whether this channel is operating in shape in all NOAA satellites currently orbiting. Data from NOAA 10 has been set aside due to inner technical deficiencies: AVHRR has a northern latitude ascending spacelook apparent sunlight intrusion that affects the channel 3 spacelook and calibration for brief periods (Kidwell, 1995). In practical terms this implies that NOAA 10 channel 3 data is altered by intruding noise, making data not reliable.

NOAA 12 and 14 channel 3 data need an initial split into two components before further analysis: reflective and emissive components should be singled out. In other words, this means that the digital number (DN) of a channel 3 is due to the **reflected** energy on one hand and, on the other, to the **emitted** temperature. The search of hot pixels denouncing possible forest fires will hence be based on the search of "hot pixels". A high DN due to reflected energy should be identified as such and disregarded in this application, so as not to present as burning pixels those that are not.

## 4. LITERATURE REVIEW ON THE USE OF NOAA-AVHRR FOR FOREST FIRE DETECTION.

Earliest attempts to detect forest fires from satellites did not use thorough data analysis but visual analysis; that was the case of Jijia's study (1989), carried out at Beijing's Meteorological Satellite Centre, over a massive wildland forest fire occurred in the Ling region. A channels 3, 2, 1 pseudocolor composition was arranged and viewed in such way that, channel 3 saturated pixels did appear in bright red colour. No further analysis was carried out with the AVHRR data, but support to this evidence was seek from TOVS channels 8 and 19, which are particularly sensitive to cool temperature sources; in case

of fires, these channels yield high negative values. This procedure can be adequate enough in the case of huge fire events, but it needed a sharp refinement, which is being achieved in time

There are numerous sample case studies mentioned in the literature that have tested out refined techniques for forest fire detection with NOAA. Some have been quoted above. This section will focus on a few studies particularly relevant to MEGAFIReS on account of the use they made of channel 3 and 4 data.

Casanova (1991), applied channel 3 and 4 data to three interrelated items: fire detection, fire temperature estimation and calculus of burnt area at subpixel level. The study was developed using a multispectral technique based on the difference of brightness temperature between both channels in pixels partially burnt. The algorithm used in this case study relates, for each channel, the emitted radiances according to brightness temperature (Plank's function) for two areas within the same pixel having diverse temperatures, i.e.: a cool and a hot area. Both equations allowed to determine the brightness temperature of the burning site as well as its area.

The study of Illera et al (1995) develops an automatic algorithm for detection and analysis of both large fires and those smaller than a pixel. Infrared AVHRR images are used together with Dozier's multispectral analysis technique. To decide whether a pixel corresponds to a fire or not, difference values between channels 3 and 4 temperatures are used as a threshold, which should be greater than 8º K; the threshold value needs to be carefully modified in the case of burning spots smaller than a pixel. In these later cases, the factor *p* (pixel) in the equations is not considered as *1* (whole pixel burning) but variations of *p* are introduced, ranging between 0 and 1. Authors state that results of the method are far better in the case of large fires

and that atmospheric correction of thermal images is advisable. The procedure of finding a threshold value from channel 3 and 4 temperatures has also been used by other authors such as Flannigan and Vondeer Haar (1986), Kauffman *et al* (1990) and Lee and Tag (1990).

## 5. METHODS THAT WILL BE USED IN THE MEGAFiReS PROJECT

The main objective addressed in the MEGAFiReS project, in relation to forest fire detection, is to obtain an algorithm able to search automatically for fire saturated pixels. Basic data used in the process are constituted by NOAA-AVHRR Channel 3, calibrated to brightness temperature. Daily mid-day NOAA 14 images will be gathered with INFOCARTO´s in house NOAA-HRPT tracking station.

To focus image analysis on areas susceptible to forest fires, the process will initially disregard those coverages (e.g.: water bodies) or land uses (e.g.: urban) unable to bear a forest fire. Spectral behaviours similar to those of forest fires, such as over-heated bare soils, will also be filtered out of the image data to be analysed, by means of land-use masks. Further, pixels containing radiometric values not characteristic of active forest fires or burnt down surfaces will be set aside.

The analysis will proceed establishing a comparative relation of pixels against the background (according to Ceccato et al., 1995), in order to discriminate hot pixels saturating channel 3 and those that are not burning.

The automatic algorithm that Infocarto will develop, will include a series of filters that shiver those pixels not meeting certain given conditions. The final outcome of the process must be constituted by an image including those burning pixels, if any.

The specific activities to be developed for fire detection will be the following :

### *5.1 Image recording*

Software governing the NOAA Tracking Station will be used for programming and capturing needed images. Besides the mid-day NOAA 14 pass, NOAA 12 daytime passes will also be recorded, so as to avoid information gaps, in case NOAA 14 does not provide the full coverage required.

Image gathering period runs from June to September (included), corresponding with the forest fire season in the Mediterranean countries of Europe. The original HRP formats will be converted to ERDAS Imagine® format, so that the Earth Resources and Data Analysis System® can drive the analysis further to its expected end. Digital Numbers (DN) are immediately converted into absolute geophysical parameters.

The next data will be used as information source to feed the fire detection algorithm:

- Channels 1 and 2: reflected energy (albedo values).
- Channels 1, 2, 3, 4 and 5: radiance values.
- Channel 3: brightness temperature

### *5.2 Geometric correction of images*

The orbital model SGP4, provided by the NOAA Agency itself, will be applied to derive the ground control points (GCP) needed for image geometrical correction and later projection.

For the correction of images used in MEGAFIReS, the time correction data will be provided by a GPS installed in the tracking station, instead of the "time-mark" contained in the images, due to the fact that time measuring devices carried on board NOAA satellites are less accurate than adjustments provided by GPS. As a consequence, greater precision will be obtained in the image correction process.

Images interpolation will be carried out applying the nearest neighbour method. This procedure prevents the possibility of saturated pixels being lost when averaged with the values of surrounding pixels in the process of generating a new image. Images will finally be adjusted to vector information.

### *5.3 Development of fire detection algorithm*

The fire detection algorithm will be built as a processing model and automated with the model maker module of ERDAS IMAGINE. The output image *H* will be obtained after a series of processing nodes, as an image of "pixels in fire" shown against a background of non burning pixels with a value of 0.

### *5.4. Testing of the algorithm and verification*

The benefits and accuracy of the algorithm will be tested out on actual or past wildfire events (1994-1995) prior to its application to the MEGAFIReS imagery (1996-1997). For this purpose the next will be necessary:

1. To have a fully up-graded data base of fire records. Wrong data relative to the time of the forest fire or to the burnt area will lead to sound mistakes in the design of the algorithm.

2. The use of the NDVI will be essential to:

- Establish the NDVI as a primary filter. Candidate fire pixels would have to occur in areas of forest NDVI values.
- The sharp lowering of NDVI values caused by a forest fire could be introduced in the algorithm as a threshold or evidencing factor for fire candidate pixels previously chosen.
- Some authors have proposed methods to measure the area in fire within a pixel, as well as its temperature (Casanova, 1991). The use of sub-pixel techniques could help to ascertain these detailed measurements.

3. Channel 3 data decomposition process will be further improved for the automatic withdrawal of reflective and emissive components. This goal will also improve the application of the algorithm by decreasing the processing time needed. This will be a high priority action so that the detection algorithm may end up being truly dynamic.

**REFERENCES**

BELWARD, A.S., GREGOIRE, J.M. D'SOUZA, G., TRIGG, S., HAWKES, M., BRUSTET, J.M., SERÇA, D., TIREFORD, J.L., CHARLOT, J.M. and VUATTOUX, R. (1993). In situ, real time fire detection using NOAA / AVHRR data. 6th AVHRR data users' meeting. Belgirate, Italy. Proceedings. EUM P 12. ISSN 1015 9576. 333-339.

BUSSIERES, N. (1995). Preliminary analysis of AVHRR brightness temperature for evapotranspiration estimation over the Mackenzie basin, summer 1994, in Proceedings of the 17th Canadian Symposium on Remote Sensing, June 13-15, Saskatoon, Sakatchewan, Canada, pp.15-20.

CASANOVA, J.L., ILLERA, P., DELGADO, J.A., and RODRIGUEZ, P. (1991). Análisis de incendios mediante imágenes NOAA. Teledetección y medio ambiente. Junta de Andalucia. pp 40-45.

CASELLES, V., 1994. Mapping actual evapotranspiration by combining Landsat-TM and NOAA-AVHRR images. Proceedings of the Workshop on Thermal Remote Sensing, La Londe Les Maures, France, 20-23 September 1993, (Cemagref ed.), 309-312.

CECCATO, P., FLASSE, S.P. and DOWNEY, I. D. (1995). Fire detection with AVHRR: a useful contextual algorithm. Proceedings: The 1995 meteorological satellite data users' conference. Winchester, UK. 4-8 Sept. pp 101-108.

CHUVIECO, E. and MARTÍN, M. P. (1994). Global fire mapping and fire danger estimation using AVHRR images. PEandRS. Vol 60. No. 5. 563-570.

CRACKNELL, A. and XUE, Y. (1996). Estimation of heat flux using AVHRR data and an advanced thermal inertia model (SoA-Ti Model). Int. Jour. of Remote Sensing. 17 637-641.

DOWNEY, I. D., FLASSE, S.P., CECCATO, P. and TRIGG, S.N. (1995). Real time monitoring of active vegetation fires for better natural resource management. Proceedings 21st Annual conference of the Remote Sensing Society. Southampton, UK. 11-14 Sept., pp 275-282.

DUGUAY, C.R. (1990). Net radiation mapping of mountainous terrain using Landsat-5 TM imagery and DTM data. University of Waterloo, Ontario, Canada. Ph.D. Thesis.

EUROPEAN COMMISSION (1980). HCMM satellite flow-on investigation no. 25. Soil moisture and heat budget evaluation in selected European zones of agricultural and environmental interest (TELLUS Project). Progress Report 31 Apr - 31 Aug 1980. Washington DC. E81 - 10057; NASA-CR-163765, 48 p., 31.

FLANNIGAN, M., and VONDEER HAAR, T. (1986). Forest fire monitoring using NOAA satellites AVHRR. Canadian Journal of Forest Research, 16: 975-982.

GREGOTSKY, M. and WANG, J. (1991). The mapping of net surface radiation using Landsat-TM imagery. University of Waterloo, Ontario, Canada. Earth Observation Laboratory. *Institute for Space and Terrestrial Science,* report # *ISTS-EOL-TR91-004.*

HARRIS, A. and ROTHERY, D. (1995). Thermal monitoring of volcanoes using data from the AVHRR. Proceedings 21st Annual conference of the Remote sensing Society. Southampton, UK. 11-14 Setp., pp 558-535.

ILLERA, P., FERNANDEZ, A and CASANOVA, J.L. (1995). Automatic algorithm for the detection and analysis of fires by means of NOAA AVHRR images. Earsel advances in remote sensing. Vol. 4 No. 3-XII.

JIJIA, Z., and QINGSHAN, Z. (1989). Detection of forest fire in the Hinggan Ling region by meteorological satellite. Acta Meteorologica Sinica. VOL. 3 Nº 4. 563-568.

KAUFMAN, M., TUCKER, C., and FUNG, I. (1990). Remote sensing of biomass burning in the tropics. Journal of Geophysical Research, 95: 9927-9939.

KENNEDY, P.J., BELWARD, A.S., and GREGOIRE, J.M. (1994). An improved approach to fire monitoring in West Africa using AVHRR data. Int. Jour. of Remote Sensing, vol 15. No. 11, 2235-2255.

KIDWELL, K. (1993). NOAA polar orbiter data users guide. National Environmental Satellite Data and Information Service, National Climate Data Center, Satellite Data Services Division, p 3-19.

LANGAAS, S. (1993). A parametrised bispectral model for savanna fire detection using AVHRR night images. Int. Jour. of Remote Sensing. Vol 14, No. 12. 2245-2262.

LEE, F., and TAG, P. (1990). Improved detection of hot spots using the AVHRR 3.7 μm channel. American Meteorological Society. 71 (12): 1722-1730.

LUXLEY, P. PARSON, L. M. and MURTON, J.B. (1995). Magmatic and tectonic interaction in the Iceland region. Proceedings 21st Annual conference of the Remote Sensing Society. Southampton, UK. 11-14 Setp., pp 503-511.

MARTÍN, M. P., and CHUVIECO, E. (1995). Cartografía y evaluación superficial de grandes incendios forestales a partir de imágenes de satélite. Ecología. Nº 9. 9-21.

RAO, C.R.N., SULLIVAN , J.T., WALTON, C.C. BROWN, J.W., and EVANS, R.H. (1993). Nonlinearity corrections for the thermal infrared channels of the AVHRR: assessment and recommendations, NOAA Technical Report NESDIS 69, USDoC, NOAA, Washington DC.

RIDLEY, I.K. and VAUHAM, R.A.. (1995). Use of AVHRR to detect and monitor volcanic eruptions of mount Etna in 1981 and 1984. Proceedings

21st Annual conference of the Remote sensing Society. Southampton, UK. 11-14 Setp., pp 536-543.

ROBINSON, J.M. (1991). Fire from space: global fire evaluation using infrared remote sensing. Int. Jour. of Remote sensing 12. 3-24.

TRONIN, A. (1996). Satellite thermal survey: a new tool for the study of seismoactive regions. Int. Jour. of Remote Sensing. 17 (5). 1143-1161

VIDAL, A., and PERIER, A. (1990). Control of irrigation following the water balance from NOAA-AVHRR thermal IR data. IEEE Transactions on Geoscience and Remote Sensing, 28, 5, 949-954.

# REMOTE SENSING OF BURNED AREAS: A REVIEW

*José M.C. Pereira[(a)], Emilio Chuvieco[(b)], André Beaudoin[(c)] and Nathalie Desbois[(c)]*

[(a)] Departamento de Engenharia Florestal, Instituto Superior de Agronomia, Portugal

[(b)] Departamento de Geografía, Universidad de Alcalá, Spain

[(c)] Laboratoire Commun de Télédétection Cemagref-ENGREF, France

## 1. INTRODUCTION

Vegetation fires are common in tropical, temperate, and boreal biomes. In the tropics fire is often used as a land management tool, employed in shifting agriculture, hunting practices, to prevent the invasion of grasslands by shrubs, and in the conversion of primary forest to other uses. In temperate regions fire is also extensively used for slash burning, but is most often considered a hazard, when it burns in ecosystems that are prized for their economic and/or ecological value. In both tropical and temperate biomes, a great majority of fires, whether desired or not, occur as a result of human activities. However, in boreal regions natural causes (i.e. lightning) still account for a significant proportion of the total area burned, and fire is a very important ecological factor influencing plant community dynamics.

These various kinds of fire activity generate a range of economic, ecological, atmospheric and climatic impacts, with magnitudes that are strongly dependent on the areal extent of the burns. Detailed and current

information concerning the location and extent of the burned areas is important for assessing economic losses and ecological effects, monitor land use and land cover changes, and model atmospheric and climatic impacts of biomass burning. Given the extremely broad spatial expansion and often limited accessibility of the areas affected by fire, satellite remote sensing is an essential technology for gathering the required information.

However, the spectral properties of burned surfaces are prone to confusion with various land cover types, affecting the accuracy of burned area estimates derived from remotely sensed data. The development of methodologies capable of producing more accurate burned area estimates from remotely sensed data is, therefore, an active topic of research at geographic scales ranging from local to global (Justice et al., 1993).

## 2. SPECTRAL PROPERTIES OF BURNED AREAS

Spectral characterisation of the post-fire signals was considered by Chuvieco and Congalton (1988) as the starting point for research on remote sensing of burned areas. An essential aspect of the problem is the recognition that there are two quite different post-fire signals (Robinson, 1991): the deposition of charcoal (char), and the alteration of vegetation structure and abundance, commonly designated by fire scar. The first type of signal is a quite unique consequence of vegetation combustion, but has relatively short duration and tends to be almost completely erased by wind and rainfall in a few weeks or months after the fire. The second signal is more stable, although its persistence may vary from 2-3 weeks in tropical grasslands to several years in boreal forest ecosystems. However, this signal is less significant to discriminate fire effects, since partial or complete removal of plant canopies may also be due to other factors such as cutting, grazing, wind throw, water stress, or the action of insects and pathogens.

This fundamental distinction seldom is explicitly recognized, leading to apparent inconsistencies in the literature concerning the spectral properties of burned areas. Most authors, however, indicate the length of time between fire occurrence and spectral data acquisition, from which the type of signal (char or scar) may be inferred approximately, by taking into account biome-specific differences in post-fire spectral dynamics.

It is also important to make a clear distinction between ash and char or, using the terminology of Chandler et al. (1983) "white ash" and "black ash". Ash is a light colored, predominantly mineral residue, produced by complete combustion of plant materials in the presence of unrestricted oxygen supply, and as a result of high fire intensity (Cope and Chaloner, 1985; Riggan et al., 1994). Charred fuels are essentially composed of black C, indicate inefficient combustion of biomass, under more restricted oxygen supply conditions (Cope and Chaloner, 1985) and are the typical product of less severe wildfire behaviour (Chandler et al., 1983; Ambrosia and Brass, 1988). Unfortunately, both of these solid products of biomass burning are often designated by "ash", thus confusing interpretation of the spectral properties of burned surfaces.

### *2.1. Visible spectral range (0.4 - 0.7 mm).*

The reflectance of pure charcoal in the visible range was studied by Jones et al. (1991), who experimentally produced charcoal from the wood of Norway spruce (*Picea abies*), silver birch (*Betula pendula*), and Scots pine (*Pinus sylvestris*), and correlated the reflectance of charcoal at 0.546 μm with the temperature of charcoal formation. Reflectance values varied from ca. 0.00 for charcoal formed at 200°C, up to 0.06 for charcoal produced at 1000°C.

A few authors provided field data on the reflectance of recently burned surfaces in the visible spectral range. Fuller and Rouse (1979) performed spectroradiometric measurements over burned surfaces with an age range of 0

to 80 years old. In the visible range they found a significant degree of overlap between the spectral signatures of burns with 0 and 1 years of age, and that of mature boreal forest which is, however, slightly darker. The reflectance values of the burned surfaces varied from ca. 0.025 at 0.4 μm, up to 0.05 at 0.7 μm.

Tanaka et al. (1983) burned a stack of pine branches, and immediately measured the reflectance of the partially combusted stack, which varied from ca. 0.09 at 0.4 μm, up to 0.14 at 0.7 μm, representing a 0.05-0.08 increase in reflectance in the visible range, by comparison with the unburned vegetation. However, they also mention the occurrence of spectral overlap between the signatures of intact pine forest and of burned areas in the Landsat MSS channels 4 (0.5-0.6 μm) and 5 (0.6-0.7 μm).

Frederiksen et al. (1990) measured reflectance values of savanna burns in Africa, using a two-band portable radiometer. One day after a late dry season fire the reflectance of the charred surfaces in the red spectral range was 0.054, compared to 0.121 for the dry, senesced herbaceous vegetation, and 0.104 for green vegetation. But only 11 days after the fire, the red reflectance of the burned surface had risen to approximately 75% of the pre-fire reflectance of dry grass. Langaas and Kane (1991) provided complementary data on the same experiment, and also reported results for an early season burn. In this case, the pre-fire red reflectance of dry grass was lower (ca. 0.085), but the surface reflectance on the first day after the fire was also approximately 0.05. However, only seven days after the fire, the red reflectance of the burned surface had risen back to the pre-fire level, now mostly due to the contribution of the soil signal. The laboratory data of Jones et al. (1991), and the field data of Fuller and Rouse (1979), Tanaka et al. (1983), and Frederiksen et al. (1990) are measurements of surface reflectance, an intrinsic property of the targets, unaffected by atmospheric effects, and also immune from topographically-induced variations in illumination geometry. In principle, these data ought to

be the most reliable characterisations of the spectral properties of burned natural surfaces.

Three other studies (López and Caselles, 1991; Siljeström and Moreno, 1995; Silva, 1996) reported results in apparent, or top-of-the-atmosphere reflectance units, which are influenced by atmospheric effects. In the visible spectral range scattering is the dominant atmospheric process, and its impact is an increase in apparent reflectance, relatively to the true surface reflectance. López and Caselles (1991) used the Landsat5 TM and reported a slightly higher apparent reflectance of a burned area in channels 1-3, five weeks after a fire in a forest of evergreen oaks, pines and Mediterranean shrublands, in Spain. Reflectance values over the burned area were of approximately 0.10 in TM1 and TM2, and 0.12 in TM3, the latter channel recording the largest increase in visible reflectance (ca. 0.04) relatively to the pre-fire condition. Siljeström and Moreno (1995) used the Landsat-5 TM to study two fires in xerophytic shrub formations growing on bright, sandy soils in Spain. A 1981 fire was observed with a 1984 image, and a 1985 fire with a 1986 image. An increase in channel 3 reflectance from a pre-fire value of 0.20 to a post-fire value of 0.35 is reported, although it remained unclear whether these data referred to the 1-year-old scar or to the 3 year old scar. Soil type and burn scar age possibly explain the large increase in reflectance from pre- to post-fire conditions. Silva (1996) calculated apparent reflectance values for six land cover types in central Portugal, namely water, bare soil, urban, bright vegetation (mostly irrigated agriculture), dark vegetation (mostly pine forests), and burned surfaces, under a very clear atmosphere according to the criteria of Chavez (1988). The burned areas, aged between three and six months, displayed reflectance values of 0.095, 0.073 and 0.066 in the channels TM1, TM2 and TM3, respectively. These values are very close to those of the bright vegetation class, and 0.01-0.02 brighter than dark vegetation.

Other authors have reported comparable spectral properties of burned areas and similar changes induced by fire, using radiance units and raw digital numbers (Ponzoni et al., 1986; Chuvieco and Congalton, 1988; Jakubauskas et al., 1990; Pereira and Setzer, 1993; Caetano et al., 1994; Koutsias and Karteris, 1996). These measurements do not separate intrinsic surface properties from atmospheric and illumination effects, and not even from sensor calibration effects in the case of digital numbers. Although the need to interpret these results more cautiously is acknowledged they are, nevertheless, in substantial agreement with those previously discussed.

Ponzoni et al. (1986) worked with Landsat TM images of the "cerrado" ecosystems of Brazil, ranging from savanna grasslands to sclerophyllous woodlands, and analysed two-week old burns. The digital numbers (DN) of the burned area in channel TM3 are similar to those of water, and six to eight DN levels lower than those of "cerrado" shrublands and gallery forest. A fire in a region dominated by pine forests and Mediterranean shrublands, in eastern Spain was analysed by Chuvieco and Congalton (1988) using a Landsat TM image acquired immediately after the fire. The burned area displayed higher radiance in channels TM1-TM3 than surrounding unburned vegetation. Jakubauskas et al. (1990) relied on Landsat MSS imagery to study a five-week old burn in a forest dominated by Jack pine (*Pinus banksiana*), mixed with red pine (*P. resinosa*), white pine (*P. strobus*), aspen (*Populus tremuloides*), paper birch (*Betula papirifera*), and oak species (*Quercus sp.*). The burned area was classified into three fire severity levels (light, moderate, and severe), all of which were found to have lower reflectance than the pine forest in the green spectral range (MSS4). The moderate and light burn classes were brighter than the pine forest in the red wavelength (MSS5), but the severely burned class had lower DNs.

Pereira and Setzer (1993) analysed part of a Landsat TM image from Brazil, containing burned areas, tropical forest, pastures, and an early regeneration stage of secondary forest, designated by "capoeiras". The exact dates of the burns are not mentioned, but they are probably no more than a few weeks old, since the image dates from August of 1985, that is during the peak of the dry season. In the blue channel (TM1), the burns are the brightest of all land cover types considered, just barely brighter than the pastures, and they also display higher DNs than tropical forests and "capoeiras" in channels TM2 and TM3, but lower DNs than the pastures. The dynamic range in the TM visible channels for this subscene is quite low, varying from about 10 DNs in TM2, up to ca. 25 DNs in TM3. In the blue and green channels, pastures and burns are almost indistinguishable.

A single large fire in an area dominated by maritime pine forest (*Pinus pinaster*) and shrublands was analysed by Caetano et al. (1994) with two Landsat TM images, one acquired ten days after the fire, and the other acquired four months later. The authors used spectral mixture analysis, and analysed the data in terms of the DNs of each pure endmember, namely green vegetation (from a mature pine stand), soil, charcoal, and shade. Soil was the brightest surface in all TM channels, the radiance of the charcoal endmember was slightly higher than that of green vegetation in all visible channels, and the shade endmember was the darkest at all wavelengths. However, in channels TM1 and TM2 there was almost no distinction between green vegetation, charcoal, and shade, while in TM3, charcoal and vegetation had very similar brightness levels, a few DNs higher than the shade endmember. The major change between the two dates was a decrease of the charcoal endmember fraction, and an increase in the soil fraction within the burned area perimeter, due to logging of the burned trunks, and removal of charcoal by wind and rainfall. Another very recent fire (ca. one week old) was also analysed with

Landsat TM by Koutsias and Karteris (1996), in Greece. They compared pre-fire and post-fire DNs, both in the burned area, and in an unburned control area, and found a small increase in radiance levels, due to the burning, in all three visible channels.

This large set of results is considerably consistent. The reflectance values of experimentally obtained pure charcoal of 0.00 to 0.06 of Jones et al. (1991), overlap the field measurements of Fuller and Rouse (1979), and those of Frederiksen et al. (1990), and Langaas and Kane (1991) for the first day after the fire. The measurements of Tanaka et al. (1983) are somewhat higher, but it is possible that an increase in burn efficiency due to the artificial vegetation structure produced by stacking of branches, may have increased the abundance of light-coloured mineral ashes as a product of combustion. López and Caselles (1991) and Silva (1996) obtained quite similar apparent reflectance values from Landsat TM imagery of recent burns, and in the same range of those reported by Tanaka et al. (1983). The significantly higher values of Siljeström and Moreno (1995) refer to clearly older burns, and represent the fire scar signal on a bright soil, rather than the char spectral signature. Satellite-derived apparent reflectances are likely to produce higher values than those obtained at the surface, due to the additive effect of atmospheric radiance in the visible spectral range.

A comparative analysis of the spectral signatures of burned areas with those of unburned vegetation and other land cover types also reveals significant agreement, when framed in the proper ecological context. Burned area signatures from boreal and temperate biomes show an increase in visible reflectance or radiance levels, relatively to pre-fire or surrounding vegetation in conifer forest ecosystems (Fuller and Rouse, 1979; Tanaka et al., 1983), mixed conifer forest and shrubland ecosystems (Chuvieco and Congalton, 1988; Caetano et al., 1994; Koutsias and Karteris, 1996; Silva, 1996), mixed

evergreen oak and shrublands (López and Caselles, 1991), shrublands (Siljeström and Moreno, 1995) and mixed conifer and hardwood forests (Jakubauskas et al., 1990), for light and moderate burn severity, although not for high severity, in this case.

In tropical biomes, most observations reporting a decrease in visible reflectance of the burned areas, from one day to a few weeks after the fire, refer to savanna grasslands (Frederiksen et al., 1990; Langaas and Kane, 1991), or pastures (Pereira and Setzer, 1993). These herbaceous ecosystems have a canopy structure that absorbs less visible radiation than conifer forests or dense shrublands, and therefore appear brighter, especially in the case of the African savannas, where the burns consume dry grass, which has a relatively higher visible reflectance. The ecosystems analysed by Ponzoni et al. (1986), where a fire-induced darkening of the surface in the visible was also observed, were dominated by broadleaf gallery forests, which tend to have higher visible reflectance than conifer forests, and by relatively open shrublands, where the brighter soil background signal, typical of many semi-arid tropical ecosystems is likely to have a significant contribution to the mixed spectral signature.

### *2.2. Near infrared range (0.7 mm - 1.3 mm).*

Fire-induced changes in the spectral properties of vegetated surfaces are more evident in the near infrared (NIR) than in the visible, especially when pre-fire fuel loadings are high, and the combustion process produces large quantities of charcoal residue. In areas of sparse vegetation cover, typical of semi-arid ecosystems where soils tend to be brighter, charcoal production is less abundant, the reduction in plant biomass is lower, and both char and scar signals contrast less with pre-fire spectral signatures.

The field spectroradiometric measurements of Fuller and Rouse (1979) showed that during the fire year the burned area was the darkest of all surfaces

analysed, and had not changed much after one year. Reflectance values increased from about 0.06 at 0.7 μm, to ca. 0.15 at 1.3 μm. Two years after the fire NIR reflectance of the scar had increased, but was still below that of the mature forest, up to 1.1 μm, although the fire scar was brighter at longer wavelengths. After 25 years, the burned area was the brightest of all surfaces, with an almost monotonical increase in reflectance from about 0.09 at 0.7 μm, to approximately 0.4 at 1.3 μm. Tanaka et al. (1983) reported a decrease of 0.05 to 0.1 reflectance units for their stacks of burned pine branches, relatively to the pre-fire reflectance, yielding values of 0.09-0.1 at 0.7 μm, up to values of 0.17 to 0.22 at 1.1 μm. In channels MSS6 and MSS7 the burned area is brighter than water, and clearly darker than the pine forest, contrary to what had been observed in the visible bands MSS4 and MSS5, where the signatures of the three cover types overlapped considerably.

Frederiksen et al. (1990) measured field reflectances in the NIR of 0.059 one day after the fire, much darker than the 0.189 of the dry savanna. Langaas and Kane (1991) reported post-fire reflectances of 0.065 on the same day as a late dry season fire and of 0.075 one day after and early dry season fire. These values compare with dry savanna reflectances of 0.22 and 0.19, at the late and early dry season dates, respectively. Razafimpanilo et al. (1995) performed various simulations using the data from Frederiksen et al. (1990) for a study on detectability of sub-pixel fires with the AVHRR, and report an interesting conclusion concerning the NIR reflectance of African savanna burns. They found that, for the reflectance values measured in the field, there was compensation between scattering and absorption, resulting in the almost complete absence of a net atmospheric effect, and consequently a nearly exact correspondence between top-of-the -atmosphere and surface reflectance values.

The range of NIR reflectances obtained by the authors who performed field measurements is well matched by the apparent reflectances calculated from Landsat TM imagery by some authors. López and Caselles (1991) observed a strong drop in NIR reflectance (0.18 to 0.12) nine days after a shrubland fire, and mentioned that TM4 was the only channel where the fire had caused reflectance to decrease. Silva (1996) reported a mean NIR reflectance value for several burns of 0.067, which is lower than that of all other land cover types except water, in contrast to what he had observed with the visible channels, where the burns were as bright, or even brighter than agricultural and forest vegetation types. Siljeström and Moreno (1995) analysed older burns than the two previous authors, and found one to three year old fire scars to be brighter than shrublands in the NIR (0.30 and 0.42 reflectance, respectively), which is certainly also due to the contribution of a bright soil background, as previously mentioned. High NIR reflectance due to an exposed soil background, and rising as vegetation recovers, was equally mentioned by Milne (1986).

Chuvieco and Congalton (1988) also detected a strong decrease in NIR radiance due to fire in a pine forest, and TM4 was the only channel where radiance decreased, a result very similar to those of Koutsias and Karteris (1996), who observed a sharp reflectance drop due to fire in TM4, and a very minor, probably insignificant decrease in TM5. Jakubauskas et al. (1990) mention that fire effects reduce NIR brightness proportionally to fire intensity, and considered this relationship reliable enough to assist in the delineation of fire severity classes with Landsat TM imagery. In TM4 all three burn severity classes were darker than the intact pine forest, while in the visible range the moderate and lightly burned areas had been brighter.

The burns observed in the study of Ponzoni et al. (1986) were darker than all land cover types (shrubby grassland, shrubby woodland, and gallery

forest) and brighter only than water, in close agreement with the results of Caetano et al. (1994), who also found that the charcoal endmember of their spectral unmixing study was darker than soil and vegetation, but not as dark as the water/shade endmember. Pereira and Setzer (1993) noted that the lowest DNs observed in their study area in Landsat TM4 occurred over recent burns, and remained so during at least four years, although their radiance levels increase during this period. Finally, the dark char signal of burned savannas in analog products of the Landsat MSS NIR channel was mentioned by Deshler (1974), and later by Parnot (1988), who studied savanna and woody savanna ecosystems in Burkina Faso during the 1986-87 dry season. Both authors refer that the char signal is rapidly attenuated due to vegetation regeneration, and removal of charcoal by wind and rainfall.

If the reflectance values at the longer NIR wavelengths of Fuller and Rouse (1979) and Tanaka et al. (1983) are excluded, as well as those of Siljeström and Moreno (1995), that clearly refer to fire scars, we obtain a relatively narrow range of NIR reflectance values (0.06-0.15) for burned surfaces, which is remarkable given the great diversity of ecological settings, atmospheric conditions, and instrumentation differences considered. Concerning qualitative findings, the char signal was always found to be the darkest of all cover types, except when water was present. The possible differences between biomes in relative brightness changes induced by fire discussed in the previous section do not seem to be present in the NIR range. However, persistence of the scar signal appears to vary from over one year in boreal and temperate ecosystems, to less than two weeks in tropical grasslands. Such variability is probably due to differences in charcoal particle size, reflecting the typical dimensions of fuels. While in forests and shrublands the fuel complex is composed of a range of particle sizes, including large tree trunks and branches which get charred by the fire, in grassland ecosystems, or

other ecosystems where the fires essentially burn through a grassy layer, the fuels are fine herbaceous leaves and the resulting charcoal particles are small and light, and thus easily dispersed by wind and rainfall.

### *2.3. Mid-infrared (1.3 mm to 8.0 mm).*

Observations of the Earth surface in the mid-infrared (MIR) only became widely available after the launch of the Landsat-4, carrying the Thematic Mapper sensor with two channels in this spectral range, TM5 (1.55 - 1.75 μm) and TM7 (2.08 - 2.35 μm). We could not find in the literature any field radiometric or spectroradiometric data concerning burned areas in the MIR. Most of the work relied on the Landsat TM, with the exceptions of the studies by Eva et al. (1995) with the ATSR-1, and Pereira (1996) with the AVHRR.

The only published reflectance data for burned areas refer to apparent reflectances, and were calculated with Landsat TM (López and Caselles, 1991; Siljeström and Moreno, 1995; Silva, 1996) and AVHRR imagery (Pereira, 1996). López and Caselles found that the largest increase in reflectance due to fire occurred in TM7 (0.08 pre-fire, to 0.18 post-fire), followed by TM5 (0.17 pre-fire, to 0.22 post-fire). High reflectance in TM7 persisted for about one year after the fire, started decreasing after two years, and had dropped to the pre-fire levels typical of the Mediterranean-type mixed evergreen oak - shrublands after six years. In their analysis of one to three year old fire scars on a bright sandy soil, Siljeström and Moreno (1995) detected the largest increase in MIR reflectance induced by a shrubland fire in TM5, which rouse from 0.40 up to almost 0.90, followed by TM7, where there was an increase from 0.20 to ca. 0.55. The ecological context of this study ought to explain the very high reflectance values obtained.

Silva (1996) also found three to six month old burns to be quite bright in the MIR. Urban areas and burns were the brightest surfaces in TM5, with

reflectances of 0.154 and 0.153, respectively. Only bare soils were brighter in TM5 ($\rho$ = 0.187). In TM7 the burns were the brightest of all surfaces ($\rho$ = 0.141), but just barely brighter than bare soil ($\rho$ = 0.136). In the studies of López and Caselles (1991) and Silva (1996) burned areas displayed a sharp rise in reflectance between TM4 and TM5, comparable to the "red edge" of green vegetation between the red and NIR. Pereira (1996) split the AVHRR channel 3 radiance into reflected and emitted components, and calculated the apparent reflectance at 3.75 μm of recent burns (up to four months old) and other land cover types in central Portugal. He classified the landscape into burned and unburned classes, and found that the reflectance of burned surfaces was higher than that of the unburned class. This contrasts with what had been found for the AVHRR channel 1, where there was great overlap between the two classes, and for channel 2, where the burned surfaces were darker than the rest of the landscape. The results were tentatively explained on the basis of the spectral properties of the solid residues of combustion, and of surface drying caused by the fires.

The data of Ponzoni et al. (1986) showed that TM5 had the broadest scatter of brightness values in their study area, while TM7 had a dynamic range closer to that of TM4. In TM5 burned areas were darker than any vegetative land cover type, but clearly brighter than water, while in TM7 the burns and gallery forests had very similar DNs, and were darker than moderately to sparsely vegetated areas. Water remained the darkest surface type in TM7. Chuvieco and Congalton (1988) found also an increase in MIR radiance data for a recently burned pine forest for Landsat TM5 and TM7. Burned pine stands were brighter in both channels than unaffected stands, and the dynamic range of radiance values in the Landsat MIR channels, especially for TM7, was much lower than for the visible and NIR channels. This contrasts with the findings of other authors, who reported that the largest dynamic range

for burned areas was observed in TM5 (Pereira and Setzer, 1993; Koutsias and Karteris, 1996) and in TM7 (Silva, 1996).

The burns analysed by Pereira and Setzer (1993) had lower brightness values than those of regenerating secondary forest ("capoeira"), and higher than primary tropical forest, in TM5. In TM7, burns and pastures had very similar DNs, much lower than those of "capoeiras", but again higher than mature tropical forest. Burned areas displayed a very impressive dynamic range of 138 DN levels in TM5. In Koutsias and Karteris' (1996) analysis of a recent burn in Greece it was also found that TM5 was the channel with the largest standard deviation of DN values. However, there was almost no change in TM5 brightness due to the fire. TM7 had the second largest data scatter in the burned area, and registered a marked increase in brightness after the fire. The spectral endmember signatures of Caetano et al. (1994) showed that the charcoal endmember was brighter than the vegetation endmember in TM5 and especially in TM7, but the soil endmember was the brightest of all, in both channels. The marked rise in DN values from TM4 to TM5 over burned areas previously mentioned was also visible in the charcoal endmember spectral signature. Riggan et al. (1993) made similar mention to the fact that charred surfaces are very dark in the NIR, but bright in the MIR.

The only study available in the literature, dealing with remote sensing of burned areas using the ATSR-1 was performed by Eva et al. (1995), who developed a method to detect burned areas by analysing the joint temporal profiles of the 1.6μm channel and the 10.85μm channel, in a study area located in the eastern part of the Central African Republic, during the 1993-94 dry season. Pixels where a sudden drop in MIR digital counts was associated with a rise in brightness temperature were considered burned, recalling an earlier suggestion by Malingreau (1990) who had noted that the deposition of black C

due to fire caused a strong decrease in the NIR reflectance, and an increase in surface temperature of the areas affected.

MIR spectral changes induced by fire show again, like in the visible range, a contrasting pattern between temperate forests and shrublands, where recent burns are brighter in the MIR than pre-fire vegetation, and tropical grassland and shrubby savannahs, where they are darker. The possible explanations suggested for the visible range, involving differences in dominant soil colour, canopy structure, and vegetation phenology, probably are also valid for the MIR range.

### *2.4. Thermal infrared (8.0 - 14.0 mm).*

This section deals with the post-fire thermal signal generated by heating due to darkening of the surface, and/or reduction in latent heat transfer by evapotranspiration, as a consequence of a reduction in leaf area. It does not consider the thermal signal generated during the fire, by flaming or smouldering combustion.

The methodology proposed by Eva et al. (1995), already mentioned in the previous section partially relied on the pre-fire/post-fire thermal signal dynamics, but the single date increased heat signal from burned areas had been used before for detection and mapping (López and Caselles, 1991; Pereira and Setzer, 1993; Cahoon et al., 1994). López and Caselles converted Landsat TM6 data to brightness temperature, and found that, at the time of satellite overpass (9:30h GMT) mean temperature values over a one month old burn were 5-6°C higher than in unburned reference areas. They did not correct for emissivity values, but considered that such a correction could add up to 1°C to this difference. However, the differential thermal signal vanishes rapidly as soon as the vegetative cover starts to regenerate. Pereira and Setzer (1993) reported data on the spectral signatures of burns and other land cover types,

also in channel 6 of the Landsat TM. Both recently burned areas, dominated by the char signal, and older fire scars have higher DNs than the other three cover types considered. However, the temperature differences were considered too small to reliably detect burns. Cahoon et al. (1994) used thermal data from the AVHRR channel 4, by including it in a multispectral classification of areas burned by very large fires in northern China. Hope and McDowell (1992) carried out comparisons between surface temperature and vegetation indices data on burned and unburned grasslands.

### *2.5. Microwave (> 1mm).*

All studies of microwave remote sensing of burned areas reported in the literature used active sensor techniques, namely the Synthetic Aperture Radar (SAR). Active radar instruments transmit microwave pulses towards the Earth surface, at a given frequency, incidence angle, and polarisation, where they interact with natural targets. Part of the energy is scattered back to the sensor, allowing the measurement of the signal and creation of an image of the surface backscatter coefficient, a fundamental characteristic of target properties. The radar backscattering coefficient is sensitive to biomass density, and also to water content and surface roughness of plant canopies and soils. Changes in these surface parameters induced by fire ought to be detected on single-date or multitemporal SAR imagery.

Almost all of the work on SAR remote sensing of burned areas was performed using C-band (3.90 - 5.75 GHz) imagery, but different types of response have been found. A lower backscatter intensity from burned areas, relatively to pre-fire conditions, or surrounding unaffected vegetation, was reported by Kneppeck and Ahern (1989), and Landry et al. (1995). However, Kasischke et al. (1992, 1994), French et al. (1994), Bourgeau-Chavez et al. (1994, 1995), and Malingreau et al. (1995) found the opposite signal, while

Werle et al. (1991) and Landry et al. (1995) refered the low detectability of recently burned areas.

This variability in the active microwave signal of burned areas was certainly due to the diversity of ecological effects of fire. Kneppeck and Ahern (1989) analysed a fire on a pine and spruce forest on hilly terrain, in Canada. They observed that detectability of the burn was higher with HV polarisation than with VV polarisation, and considered that the reduced backscatter intensity was due to the fact that dead and burned tree trunks acted as microwave absorbers. Landry et al. (1995) studied a burned conifer forest using SAR C-band with HH polarisation. One year after the fire, the burned area had a clearly lower backscatter intensity than the unburned forest, a pattern the authors attributed to the disappearance of foliage from the canopies, a decrease in the dielectric constant caused by drying of the tree trunks and branches, and microwave attenuation by the charred tree bark.

The opposite effect, that is an increase in backscatter intensity was observed in burned Alaska boreal forests by Kasischke et al. (1992), and Kasischke et al. (1994). In this latter study it was found considerable spatial variability of the backscatter coefficient within fire scars, but also dominated by an enhanced return. The spatial pattern of the signal is attributed to differences in soil moisture content, ground layer roughness, level of canopy damage, and vegetation regrowth. French (1994) and Bourgeau-Chavez et al. (1994, 1995) reported stronger backscatter from burned areas, and explain it as the result of increased soil moisture due to fire induced permafrost melting. A study in a shrubby savanna region straddling the border between Gabon and the Congo Republic was performed by Malingreau et al. (1995). They detected changes in the backscatter signal during an acquisition in July and another one in August of 1994. Since this period coincides with the local dry season, fire is considered a possible explanation for the observation of a strong increase in

the backscatter signal, which seems to be corroborated by the shape and spatial pattern of the area affected. The authors hypothesise that the tall grass canopy operates as a microwave absorber, and when it is removed by fire the backscatter from the bare surface increases, and is possible reinforced by the burned tree trunks, which may act as individual reflectors. However, Malingreau et al. (1995) have not performed any ground-truthing of their data, and consider fire only as a possible explanation for the increased backscatter observation. Werle et al. (1991) used airborne C/X-SAR in HH and HV polarisation over a boreal forest and found very low detectability over a recent (less than one week old) burn. A similar result is mentioned by Landry et al. (1995) for an image acquired immediately after a fire, but this was considered a result of rainfall in the period between fire occurrence and image acquisition.

In summary, some uncertainties appear to remain, concerning the microwave backscatter pattern generated by burned forests, and the physical processes underlying the observed patterns. The use of SAR also seems problematic for mapping burns in mountainous terrain, due to incidence angle problems. This line of work is still at an immature stage outside boreal forest ecosystems, but its potential for observing the surface under cloudy conditions makes it very attractive for work in tropical and boreal environments.

### *2.6. Spectral discrimination of burned areas*

The identification of adequate unidimensional or multidimensional spectral spaces for detecting and mapping charred surfaces and fire scars depends on a clear characterisation of the spectral properties, not only of burned surfaces, but also of the vegetation unaffected by fire, and of other land cover types commonly present in areas where biomass burning occurs.

There appears to be a reasonable degree of agreement concerning some basic aspects of burned area detection and mapping. For example, the

NIR is considered the best spectral region for the detection of burned surfaces by a large number of authors working on a broad range of ecosystems (Hall et al., 1980; Tanaka et al., 1983; Richards, 1984; Ponzoni et al., 1986; Frederiksen et al., 1990; Langaas and Kane, 1991; López and Caselles, 1991; Pereira and Setzer, 1993; Caetano et al., 1994; Lombraña, 1995; Razafimpanilo et al., 1995; Koutsias and Karteris, 1996, Pereira, 1996; Silva, 1996). Since healthy vegetation tends to be very reflective in the NIR, while charred surfaces are strong absorbers of radiation in this spectral range, the contrast between the two cover types tends to be very clear. NIR detectability of the scar signal will be higher if the soil background of bare or sparsely vegetated patches is at least moderately dark.

On the contrary, most of the same studies have shown that the visible range is not very effective for discriminating burns (Tanaka et al., 1983; Ponzoni et al., 1986; López and Caselles, 1991; Pereira and Setzer, 1993; Razafimpanilo et al., 1995; Koutsias and Karteris, 1996, Pereira, 1996; Silva, 1996). Pereira (1996) suggested a few reasons for this: 1) like recent burns, several common land cover types, namely water bodies, wetlands, some forest types, especially dense coniferous forests, and many soil types are quite dark in the visible. These similarities reduce the possibility of using the visible range to discriminate burns; 2) Earth observation satellites were designed to image all types of surface features, ranging from the very bright, such as clouds, snow, and deserts, to very dark ones, such as water. Therefore, the dynamic range available for discriminating between different types of surfaces, all of which are dark in the visible, is narrow; 3) path radiance, an important component of the atmospheric effect, predominates in the visible range especially over dark surfaces, and causes a loss of contrast between different land cover types.

The often reported increase in visible reflectance as a consequence of fire in boreal and temperate ecosystems is, in general, too small to be used as a reliable detector of burns. In tropical biomes, especially when the fires burn on dry grassland savannas, or sparse shrublands growing on relatively bright soils, the darkening of the surface may provide a stronger spectral contrast.

The mid-infrared spectral region has been more recently identified by a few authors, mostly working on temperate ecosystems, as promising for detecting burns, since the fire-induced increase in brightness is larger than in the visible range (López and Caselles, 1991; Lombraña, 1995; Koutsias and Karteris, 1996; Pereira, 1996; Silva, 1996). Healthy vegetation has low MIR reflectance, due to water absorption, and therefore the scorching or combustion of vegetation, and the soil drying caused by fire, are likely causes for the observed increase in MIR brightness. Natural materials seem to display a broader range of reflectance values in the MIR than in the visible, facilitating the discrimination of different land cover types. Also, atmospheric scattering is very insignificant in this wavelength range, and therefore does not reduce spectral contrast at the surface. The Landsat TM MIR channels were identified by some authors as those where burned surfaces displayed a larger scatter of brightness values (Ponzoni et al., 1986; Pereira and Setzer, 1993; Koutsias and Karteris, 1996; Silva, 1996), and Pereira (1996) presented similar results for the reflective component of the AVHRR channel 3. This suggests the possibility of using the MIR for characterizing the internal variability of burned areas, which may be correlated with the severity of fire effects and the spatial pattern of fire intensity (Justice et al., 1993). On the other hand, this means that burned areas have a relatively noisy signal in the MIR, which may be detrimental for an effective separation from other cover types. Verstraete and Pinty (1996) argued convincingly that detection and characterisation of targets involve intrinsically conflicting objectives, and that the same spectral

information cannot be used for adequately performing both tasks. This may apply to the use of MIR data for burned area studies.

Nevertheless, the better discriminant ability of the MIR, in comparison with the visible region of the spectrum, appears to be confirmed by studies that identified the NIR-MIR bi-spectral space as more adequate for burned area detection and mapping, than the classical visible-NIR space. Ponzoni et al. (1986), and Pereira and Setzer (1993) considered the bi-spectral space defined by the Landsat channels TM4 and TM5 as the most adequate for detecting burns, while the TM4 vs. TM7 space performed best for López and Caselles (1991), Koutsias and Karteris (1996), and Silva (1996), while Pereira (1996) obtained good results combining the AVHRR NIR with the reflective component of the MIR channel. Chuvieco and Congalton (1988) also mentioned the superior performance of a 4-5-7 red-green-blue color composite of Landsat TM channels for visual identification of recently burned surfaces, and a composite using these same bands has been successfully used for mapping savanna burns in Africa (Paulo Barbosa, personal communication).

In a few cases, thermal infrared imagery of burned surfaces was combined with shorter wavelengths (López and Caselles, 1991; Cahoon et al., 1994), while in other cases the combination of thermal with NIR or MIR data has also relied, at least to some extent, on the heat signal of active fires (Malingreau et al., 1990; Barbosa and Grégoire, 1995; Eva et al., 1995). Microwave imaging of burned surfaces is usually performed on a single spectral region and, as already mentioned, the C-band has been the most widely used for this purpose.

## 3. DISCRIMINATION OF BURNED AREAS WITH REMOTELY SENSED IMAGERY.

Analysis of the spectral properties of burned surfaces and associated land cover types, within the constraints imposed by the use of specific sensors, has led to the application of a large number of different methodologies for burned area detection and mapping. Spectral resolution of the instruments seems to exert a stronger influence on the types of methods used than spatial or temporal resolution. Rarely is a given method or closely related family of methods exclusively associated with a given type of instrument, but some generalisations are possible, namely that visual analysis and simple density slicing techniques are typically associated with monospectral SAR imagery, vegetation indices are very commonly used with the AVHRR, and a more diverse set of methods has been applied to Landsat data, especially to those obtained with the TM sensor. For our overview of image classification of the post-fire signals, we considered a grouping of methods that may not be exhaustive, and is certainly not mutually exclusive, but that was considered to represent reasonably well the range of applications available in the literature.

### *3.1. Visual analysis*

These are the simplest of all classification methods that have been applied to burned area mapping, but they may be quite effective, especially visual classification using an adequate color composition of digital imagery (Chuvieco and Congalton, 1988). They are often applied together, with the slicing thresholds being iteratively re-adjusted, based on visual interpretation of results. The main advantage of this method is that a well-trained human image interpreter has the ability not only to perceive very subtle color gradations apparent in the imagery, but also of integrating textural and contextual information in a very effective manner. The problem is, of course

that it is a very labour intensive approach, and prone to inter-personal subjectivity. The same comments apply to the visual analysis of single-channel monocromatic data performed, for example, by Wightman (1973), Deshler (1974), Parnot (1988), and Defourny and Totle (1991) who found good results from visual analysis of quick-looks of Landsat-MSS images. There are also some reliable experiences with space photography provided by manned missions such as the Skylab's and Space Shuttle's (Herfert and Lulla, 1990). Visual interpretation of greyscaled backscatter coefficient imagery is also the most common form of analysis of C-band SAR data, and has been performed at a local scale (Kasischke et al., 1992, 1994; Bourgeau-Chavez et al., 1994, 1995; Landry et al., 1995) and at a regional scale (French et al., 1994; Malingreau et al., 1995).

### *3.2. Single channel density slicing.*

In this section, we only considered single channel density slicing applied to individual channel data, and not to classifiers resulting from the mathematical combination of two or more channels, such as vegetation indices. Hall et al. (1980), after having identified the Landsat MSS channel 7 (NIR: 0.8 - 1.1μm) as the best discriminator for a two-week old, large tundra fire in Alaska, sliced the histogram in order to obtain a three-level classification of burn severity. Kasischke et al. (1994) visually identified the outline of a recent, large forest fire in Alaska, and then performed an eight-level density slicing of the backscatter image, within the fire perimeter.

Density slicing has also been the most common technique to discriminate fires in channel 3 data. Although fire detection algorithms will be covered in another position paper, we should emphasize here that hot spot detection from channel 3 has been the most frequent source of remotely sensed data for generating fire statistics, specially in tropical areas (Setzer and Pereira, 1991a;

Langaas, 1992). Forest fires with a flame temperature of 900 K have emittances 5,153 bigger than average land cover in the middle infrared band (3.75 μm). This radiative contrast is much less clear in the thermal band (11.9 μm), where forest fires of that temperature would have only 38 times more emittance than healthy vegetation (Milne and Hall, 1992).

Experiences in using middle infrared sensors for fire detection and mapping include airborne scanners (Hirsch et al., 1971; Matthews and Jessel, 1992), as well as satellite systems (Chuvieco and Martín, 1994). In these studies the burned area is estimated from active fires and the total burned area is obtained from extrapolation of that burning area over a period of time, considering average fire duration (Setzer and Pereira, 1991b).

This method assumes that fires are active at the time of satellite acquisition and that channel 3 is accurate enough to discriminate these burning spots. Both requirements are often not fulfilled. Firstly, the frequency of AVHRR acquisitions can be reduced by cloud coverage or gaps in reception, making daily coverage unreliable. Secondly, the thermal sensitivity of channel 3 is rather poor, as the sensor is saturated at 320 K, and includes a high level of noise (Robinson, 1991). In the case of Mediterranean forest, fire spots can be easily confused with agricultural burns or even with bare soils, which frequently reach the saturation temperature in the summer during the afternoon pass (Belward, 1991). Discrimination from agricultural fires could be partially achieved by choosing evening or night images, because this type of burning tends to be done during daylight periods (Malingreau, 1990). Fire active areas and bare soils are also discernible on night images, as a result of the lower soil temperatures at this time (Langaas, 1992).

On the other hand, low thermal sensitivity of AVHRR channel 3 data may also create problems of overestimation of the burned area. It should be noted that a pixel may be saturated even if only a small proportion is actually occupied by

fire. In fact, fires with a temperature above 500 K, even if they occupy less than 0.1 % of the pixel size, will most likely reach pixel saturation temperatures (Kaufman et al., 1990). For this reason, a consistent tendency of overestimation has been found when AVHRR channel 3 fire mapping estimations are compared with higher resolution data, such as Landsat-MSS or TM. According to several experiences in the Amazon basin, this overestimation is in the order of 43 % (Setzer and Pereira, 1991a), or 1.5 times the areal extent observed with Landsat-TM (Pereira et al., 1991).

In spite of these problems, the use of AVHRR channel 3 data for fire detection and mapping has been successfully tested in several studies. High accuracy for detecting large-scale forest fires was found in a pilot study conducted in Alberta (Flanningan and Vonder Haar, 1986). Overall, 46 percent of the total number of fires were located with data obtained from AVHRR channel 3. This accuracy increased to 80 % when only fires in cloud-free images were considered. Precision reached 95 %, when only medium to large fires (over 40 hectares) were taken into account. Accuracy for small fires was limited, 10 to 12 %, although better results were reported if only cloud-free areas were considered (up to 87 %). In the Brazilian Amazonia, analysis of AVHRR channel 3 images for the summer season of 1987 yielded a total estimation of 350,000 fires, covering as much as 200,000 sq km (Setzer and Pereira, 1991b). These results were obtained from the extrapolation of observed fires in 46 AVHRR images acquired from July to October. Pixels with high temperatures in channel 3 were labelled as fires and these calculations were extrapolated to cover the whole study period based on the average duration of fires and their average size.

In addition to the use of AVHRR imagery, other sensors have also been shown to be very useful for determination of active fires. These studies include the use of geostationary data (Prins and Menzel, 1992), space photography (Herfert and Lulla, 1990), and DMSP (*Defense Meteorological Satellite*

*Program*) night images (Cahoon et al., 1992). Smoke emissions have also been monitored from the MAPS (*Measurement of Air Pollution from Satellites*) experiment on board the Space Shuttle (Watson et al., 1990).

### *3.3. Multitemporal thresholding of vegetation indices*

Discrimination of areas affected by fires, either very recent (mainly charcoal) or more distant in time (fire scar), has been mostly based on multitemporal comparisons of images acquired from before and after the fire. As said before, the spectral characteristics of burned areas change sharply as a result of fire, especially in the Near Infrared. Therefore, multitemporal comparisons of vegetation indices (VI), which take into account the spectral contrast between NIR and visible bands, are very suitable for discrimination of burned areas. VI enhance the vegetation signal, while minimizing atmospheric, solar irradiance, and soil background effects (Jackson and Huete, 1989). As said before, most applications of AVHRR data to fire mapping have been based on channel 3 data. For discrimination of fire scar, NDVI has been the most common source of data, primarily because of the low - spectral resolution of this instrument in the visible and NIR part of the spectrum. Studies based on the Landsat MSS and TM sensors have also resorted to VI, but often using them together with other band combinations, and integrated into more elaborate classification procedures. One of the earliest uses of the NDVI to detect burned areas was reported by Malingreau et al. (1985), who analysed the 1982-83 Kalimantan and North Borneo fires. AVHRR Global Vegetation Index data, at 15 km resolution and tri-weekly composited showed burns as sharp drops in the NDVI time series. Chuvieco et al. (1993) also used multitemporal analysis of AVHRR-NDVI data to map a recent forest fire in the Mediterranean coast of Spain. Kasischke et al. (1993) and Kasischke and French (1995) applied similar AVHRR-based multitemporal approach to map

forest fires in Alaska, during the 1990 and 1991 fire seasons. Kasischke et al. (1993) created two sets of NDVI maximum value composites (MVC), corresponding to early summer and late summer dates, and differenced the two composites. Burned areas were identified as those exceeding a given NDVI decrease threshold. This procedure underestimated the area burned, but generated a large number of single pixel false alarms. However, a less restrictive threshold reduced the area underestimation, and resulted in the detection of 89.5% of all fires larger than 2000 ha.

This methodology was improved by Kasischke and French (1995), who compared an approach based on burned area estimation using imagery from the same season as the fires, with another which also relied on imagery from the following year. Thresholding of the NDVI MVC difference image of the same-year data produced various types of false alarms, requiring elimination of single pixel potential burns, of detections above the treeline, and of single or double pixel detections within 1km of major rivers. The burned area was underestimated, in spite of most fires being detected, and use of a less restrictive threshold produced an increase in the number of false alarms. In order to reduce the burned area underestimation, while minimising the number of false alarms, Kasischke and French (1995) imposed a spatial adjacency constraint on the burned pixels identified with the less restrictive threshold, and considered as correct only those new detections located within three pixels of the burns identified with the first threshold. The two-year data method was based on the detection of delayed green-up of burned areas during the first Spring season after the fires. Those pixels with an NDVI value lower than a given threshold below the mean NDVI of unburned forests, and located within a distance of four pixels from burns detected with the first threshold of the same-year dataset were considered as burns. This method led to 20-30%

improvements in burned area estimation, over the single-year method, at the expense of a delay in the availability of results.

Martín and Chuvieco (1994) employed a method similar to the single-year approach of Kasischke et al. (1993) and Kasischke and French (1995) to analyse wildfires in the Mediterranean coast of Spain, during the Summer of 1991. They also used pre-season/post-season image differencing of AVHRR NDVI imagery, and compared the performance of MVC with analysis of single-date images from the two periods, considering as burns all NDVI decrements larger than 0.2. Image differencing based on two single images was found to match better the available field estimates of fire sizes than MVC differencing, possibly due to residual misregistration between composited images. The area estimation accuracy for the largest fire (15400 ha) using non-composited image differencing was 97.4%. A similar study was performed by Pereira et al. (1994), also involving a comparison of image differencing based on NDVI MVC versus uncomposited imagery which had been corrected for atmospheric effects with a semi-empirical radiative transfer code. Both sets of difference images were thresholded at 0.2, 0.25, and 0.30 NDVI decrease levels, and although no cartographic validation data was available, the 0.25 threshold produced the most plausible spatial pattern of burns. Atmospherically corrected data appeared to be more sensitive to the presence of burned areas, possibly due to an expansion of the NDVI dynamic range.

Pereira (1996) performed the only AVHRR-based burned area study that employed other VI besides the NDVI, although the potential usefulness of such indices had been suggested by French et al. (1995). He compared four VI, namely the NDVI, the VI3, the GEMI (Pinty and Verstraete, 1992), a modified version of this index, called GEMI3, where the reflective component of channel 3 was used instead of channel 1, and finally channel 2 alone. The new GEMI3, which combines the atmospheric insensitivity of the MIR range with

the non-linear design of the GEMI, was found to be the best discriminator for burned areas, followed by GEMI and VI3, channel 2, and finally the NDVI. This study used a single image dated from the late Summer of 1991, and did not attempt to estimate areas burned, but concentrated on the comparative analysis of VI performance.

Use of VI in Landsat-based analyses of burned areas has been performed with unitemporal approaches, and the earlier studies resorted to the Simple Ratio (SR) VI (NIR/red), or the NDVI mostly to map fire severity levels. Milne (1986) used a Landsat MSS SR (MSS7 / MSS5) to map burn severity in a dry sclerophyll woodland fire, near Sidney, Australia. Chuvieco and Congalton (1988) used a similar approach to separate burning intensities in a pine forest fire in Spain. However, they only calculated the NDVI for an area previously classified as burned, to avoid confusion with other unvegetated or sparsely vegetated surfaces. Jakubauskas et al. (1990) also used this index to delineate a burn and assess levels of damage in a Michigan mixed forest. López and Caselles (1991) and Silva (1996) analysed different bispectral spaces in an attempt to develop a vegetation index especially adequate for burned area detection and mapping, based on the Landsat TM. Both independently proposed an NDVI-type index, but with TM7 replacing TM3, an index conceptually analogous to Kaufman and Remer's (1994) VI3, developed for the AVHRR.

### *3.4. Principal components analysis.*

Principal components analysis (PCA) is a dimensionality reduction technique that maps image data into a new and uncorrelated coordinate system. PCA produces a vector space in which most of the multispectral image data variance is aligned with its first axis or principal component (PC), while a large part of the unexplained variance lies along the second, mutually

orthogonal principal component axis, and so on (Richards, 1986). Principal components higher than about third order usually represent little original image variance, and are often ignored for classification purposes. However, when PCA is applied to multitemporal change detection studies, the first and second PCs tends to contain the variance associated with stable landscape features, while the regions of localised alterations are emphasised in lower order components, usually the third and fourth PCs (Milne, 1986; Richards, 1986).

Tanaka et al. (1983) applied PCA to classify a single Landsat MSS image into three degrees of burn severity and seven other land cover types, but most studies explored the technique in a multitemporal context (Richards, 1984, 1986; Milne, 1986; Pereira, 1992; Martín et al., 1994; Siljeström and Moreno, 1995). This approach entails combining in a single dataset imagery from before and after the fires of interest, and then performing the principal components transformation on this multitemporal dataset. All available data channels may be used in the analysis, as exemplified by the Landsat MSS 8-dimensional dataset of Richards (1984), and the 12-dimensional Landsat TM dataset of Pereira (1992), but Siljeström and Moreno (1995) started by identifying the four least correlated Landsat TM bands, and then performed an 8-dimensional multitemporal analysis. The order of the PCs which contain most of the relevant change information is somewhat variable, and affected by the relative proportions of stable and changed areas. Thus, while Richards (1984) and Milne (1986) found that burns were highlighted in PC3 and PC4, Pereira (1992) obtained a clear outline of the burn in PC2, possibly because the area burned occupied a larger proportion of the sub-scene than in Richard's study. The results of Siljestrom and Moreno (1995), who found burned area signals in the first, second, and sixth PCs may be a consequence of the fact that their study area contained not only a burn scar from a fire that occurred

between the two imagery dates, but also one older than both dates. The presence of a change-related signal in higher order PCs reported by Pereira (1992) and Siljeström and Moreno (1995) may also be related to the higher intrinsic dimensionality of Landsat TM data versus MSS data. A similar approach may be carried out with NDVI data from before and after the fire. The change component (usually the second one) provides a clear discrimination of burned area. Successful experiences have been obtained both with high and low resolution sensors (Martín et al., 1994).

A variation on the classical multitemporal PCA approach, designated by selective PCA (Chavez and Kwarteng, 1989) was also explored by Richards (1984) and Pereira (1992). Chavez and Kwarteng (1989) refer two problems with conventional PCA, namely the mapping of relevant information to higher order components, unusable in three-band color composites, and difficulties in interpretation of such images. The selective PCA approach to multitemporal burned area mapping is called spectral contrast mapping, and emphasizes the extraction of information that is unique to a single spectral region, which in this case was the near-infrared Thus PCA is performed using only the near-infrared bands from the two dates, forming a 2-dimensional dataset. Both PCs were extracted, and the change signal is enhanced in the second PC. This approach was considered effective and computationally very efficient (Richards, 1984; Pereira, 1992).

### *3.5. Regression analysis*

Multitemporal regression analysis, a well-known change detection technique has been rarely applied to burned land discrimination (Martín and Chuvieco, 1995). Following a well known statistical technique, the image after the fire (t2) is estimated from the one acquired before the fire (t1), based on a linear model (t2=a+b*t1). This model may be adjusted with original bands or

with NDVI values, which is more convenient for burned land discrimination. Stable areas between the two dates will show low residuals, while dynamic areas will offer higher residuals. Areas affected by the fire will appear with high negative residuals in NDVI images, because NDVI values for the image after the fire will be much lower that expected if changes would have not occurred. This technique was successfully applied for the determination of a recently burned area in the Mediterranean coast of Spain (Martín and Chuvieco, 1995).

A more elaborated application of regression analysis has been proposed by Koutsias and Karteris (1996). They constructed various multitemporal logistic multiple regression models, which imply a dichotomous dependent variable, i.e. burned versus unburned. Training sites were extracted from two successive Landsat TM passes, covering the period during which the fire occurred. Images form the two dates were radiometrically matched by haze removal, based on the histogram minimum technique. Koutsias and Karteris (1996) first assessed the discriminatory ability of each Landsat TM reflective band, by testing six pre-fire/post-fire models, and found that the model constructed with the two TM4 bands performed best, followed by those using TM7 and TM1. TM5 was shown to have the least discriminatory power of all six bands. Based on these results, they developed another three models (TM4+TM7, TM4+TM7+TM1, and an all-bands model), with respectively four, six, and 12 bands. No statistically significant differences were found between the three models, although the second one was considered slightly better, based on visual inspection. Overall classification accuracies for both burned and unburned pixels were very high (97.7%, 97.8%, and 98.0%, respectively), as a consequence of the burn having occurred just a few days prior to acquisition of the post-fire image data.

### *3.6.. Supervised and unsupervised classifications.*

Satellite image classification involves a set of procedures designed to automatically categorise all pixels in an image into distinct land cover classes (Lillesand and Kiefer, 1987). It is common to recognise two main types of approaches, namely supervised and unsupervised classification. In supervised classification, the analyst informs the pixel categorisation process by supplying the automatic classification algorithm with numerical prototypes of the various land cover types of interest. Then, each image pixel is numerically compared to these prototypes and assigned to the category it resembles the most, based on some kind of quantitative similarity metric. In unsupervised classification the image data are first aggregated into natural spectral clusters, and then these clusters are assigned land cover type labels, based on external information, usually in the form of ground reference data (Lillesand and Kiefer, 1987).

The goal of burned area mapping is not a complete partition of a region into distinct land cover types, but more of a single-feature extraction problem, conceptually similar to cloud-screening (Saunders and Kriebel, 1988), ice and snow mapping (Gesell, 1989), or active fire detection (Kennedy et al., 1994; Flasse and Ceccato, 1996), and therefore conventional image classification procedures have not been applied as extensively as in other research areas. Nevertheless, they remain relevant when there is also an interest in analysing spectral separability issues (Ponzoni et al., 1986; Pereira and Setzer, 1993), or fire-induced land cover changes (Isaacson et al., 1982; Reinhardt and Ringleb, 1990; Jakubauskas et al., 1990;). The first attempts to characterise burned areas were performed by digital classification of Landsat-MSS data, usually by comparing classifying images from before and after the fire (Hitchcock and Hoffer, 1974; Isaacson et al., 1982; Husson, 1982). Most recently, Landsat-TM data have been used instead, since its relatively high spectral resolution is

appropriate for application of multispectral classifiers, while its high spatial resolution facilitates the selection of truly prototypical training sites.

Supervised classification was employed by Ponzoni et al. (1986) with the Landsat TM channels 3, 4, 5, and 7, using maximum likelihood and k-means clustering algorithms. Training sites of varying sizes were chosen to characterise five distinct land cover types in Brazil: water, gallery forest, burns, "cerrado" shrublands, and "campo sujo" open savanna. The k-means classifier produced an outline of the burned areas most similar to that obtained by visual image interpretation, but generated significant levels of confusion between various land cover types. Chuvieco and Congalton (1988) reported unsatisfactory results from the first stage of a supervised classification of a forest area where a fire had recently occurred. Problems were due to spectral overlap of the burn with other land cover types. However, after refining the training statistics with a mixed unsupervised/supervised classification procedure, their results improved significantly (up to 89 %). Pereira and Setzer (1993) considered four land cover classes: primary tropical forest, secondary forest at an early stage of regeneration ("capoeiras"), pastures, and burned areas. They identified the Landsat TM4 as the best discriminator for these cover types. TM5 also performed well, but displayed some overlap between water and recent burns. Training sites were selected and a maximum likelihood classifier applied iteratively, with varying probability thresholds, to optimise the relative proportions of unclassified pixels and incorrectly classified pixels.

Unsupervised classification of burned areas was always employed in a unitemporal framework, even when more than one date was classified (Jakubauskas et al., 1990; Siljeström and Moreno, 1995). The minimum distance to means classifier was employed in two of the three studies analysed (Jakubauskas et al., 1990; Cahoon et al., 1994), and one of the studies relied on AVHRR imagery (Cahoon et al., 1994). Jakubauskas et al. (1990) used the

minimum distance to means algorithm to classify a pre-fire scene, and another scene acquired two years after the fire. The two individual classifications were then compared, to analyse fire-related land cover changes. However, image classification techniques were not used for mapping the burned area itself. Siljeström and Moreno (1995) also compared individual classifications of scenes acquired in 1984 and 1986, and showed evidence of fires that occurred in 1981 and 1985. Pixel clustering was performed with a maximum likelihood classifier, and the 12 clusters obtained were grouped into four land cover classes: burned areas, regrowing vegetation, unaffected vegetation, and water/other. The resulting map was smoothed with a 3x3 mode filter. These classifications were compared with another set based on PC transformed imagery and considered more satisfactory, in spite of some confusion between land cover types.

Cahoon et al. (1994) analysed the severe 1987 fires in northern China and southeastern Siberia with AVHRR Global Area Coverage (GAC) imagery. They created a clear-sky mosaic with images from multiple dates, and composited them using minimisation of channel 2 reflectance as the compositing criterion. The extent of the burned area was then assessed by classifying the mosaic with the minimum distance to means classifier, applied to AVHRR channels 1, 2 and 4.

### *3.7. Spectral mixture analysis.*

Spectral mixture analysis (SMA) is based on the assumption that the pixel spectra that form an image are made up of mixtures of the spectra of several dominant scene components, and SMA transforms the inter-pixel spectral variability of images into concentrations of reference endmembers (Ustin et al., 1993). These are the reflectance spectra of materials, such as live and dead plant parts, soils, rocks, etc., measured under clearly specified

conditions. Various methods are used to determine the number and type of endmembers, ranging from statistical analysis of the intrinsic dimensionality of the data set, to direct specification of surface materials of known interest (Ustin et al., 1993). A complete description of this technique is beyond the scope of the present review, but more details can be found in Adams et al., (1986, 1989), Smith et al. (1990), and Ustin et al. (1993).

Application of SMA to burned area studies was pioneered by Caetano et al. (1994, 1996). The earlier study focused on a single, large fire event that took place in central Portugal, in July 1990, and relied on Landsat TM imagery. The post-fire spectral dynamics of the burned area were assessed with two images, the first one acquired 10 days after the fire, and the second dated four months later. A digital terrain model was used to simulate illumination conditions at the time of scene acquisition, and areas in full shadow were excluded from the analysis. The July and November images were atmospherically corrected for the path radiance effect, and radiometrically matched. A linear mixture model was developed using the least squares method, constrained so that the sum of endmember fractions would equal one, and based on four image endmembers soil, green vegetation, charcoal, and shade.

A good model fit was obtained, with root mean square error (RMSE) values below the level of sensor noise, especially in pine stands and shrublands. The “tangible” endmember fractions (i.e., soil, vegetation, and charcoal) were normalised for the shade endmember fraction, and represented as a color composite, where charcoal, vegetation, and soil fraction images were assigned to the red, green, and blue colour display guns, respectively. This facilitated a visual analysis and interpretation of the changes in abundance of the various endmember fractions, as a result of wind and rainfall, vegetation recovery, and timber salvaging operations. The authors concluded that SMA

proved to be efficient in detecting the charcoal signal even in lightly burned areas that preserved a strong vegetation signal, a situation that is typically considered problematic.

Caetano et al. (1996) used a single NOAA/AVHRR 1.1 km image from mid-September of 1991 to detect and map fires occurred during that Summer season in central Portugal. The spectral unmixing process was again based on image endmembers, and used channel 1 (red), channel 2 (NIR), and NDVI spectral data. Use of a normalised band ratio was considered desirable since it tends to reduce the topographic effect, and this was important since no shade endmember was employed. The correlation between NDVI data and each of the original channels was lower than that observed between the two channels, reinforcing the adequacy of bringing the NDVI into the analysis. Green vegetation, soil, and burned were the three spectral endmembers used in the SMA. Underflows and overflows (i.e., endmember fractions lower than zero, and higher than one, respectively) were accepted, and used as model fitting diagnostics. Iterative analysis of endmember fraction and RMSE images served to optimise the selection of image endmembers. The resulting burned fraction image was density sliced to define three classes: burned, partially burned, and unburned, and partially burned pixels adjacent to burned ones were reclassified to burned. AVHRR-based areal estimates of burned areas were compared against a high spatial resolution fire perimeters map, developed from Landsat TM imagery. The SMA approach, complemented by the spatial adjacency criterion led to a correct classification of 91% of the burned area, but at the cost of a relatively large level of commission error, mostly due to areas where fires from the 1991 season were adjacent to 1990 burns that still maintained a strong charcoal signal. SMA was considered advantageous over VI-based methods, due to its improved capability to distinguish burns from other unvegetated or sparsely vegetated areas.

## 4. COMMON PROBLEMS IN BURNED AREA DETECTION AND MAPPING.

The spatial and temporal variability of the spectral signatures of burned areas shows diverse and complex patterns, and in spite of the large number of different classifiers used to detect and map them, it remains somewhat problematic to discriminate char and scar signals from those of other land cover types. The types of surfaces more commonly reported to generate spectral confusions with burned areas are water bodies (Tanaka, 1983; Ponzoni et al., 1986; Chuvieco and Congalton, 1988; Parnot, 1988; Pereira and Setzer, 1993; Lombraña, 1995; Silva, 1996), urban areas (Tanaka, 1983; Chuvieco and Congalton, 1988; Lombraña, 1995; Silva, 1996), and shadows (Milne, 1986; Chuvieco and Congalton, 1988; Parnot, 1988).

Different authors emphasize diverse aspects of each problem. Thus, with respect to water as a source of confusion with burned surfaces, Chuvieco and Congalton (1988) mentioned that it occurred mostly when the burns were in a topographically shadowed area. Parnot (1988) considered this specific problem more likely to occur in relation to recently burned surfaces, and Silva (1996) reported it when using the NDVI, but not its modified version, where TM7 takes the place of TM3. Tanaka (1983) reported problems with land-water boundaries, and Richards (1984) also noticed similarity in the spectral response of burns and mixed vegetation / water pixels observed with the MSS.

Confusion between burns and urban areas was also mentioned often (Tanaka, 1983; Chuvieco and Congalton, 1988; Lombraña, 1995; Silva, 1996), and results from spectral similarities between artificial surfaces such as asphalt and concrete, and the mixture of charcoal and exposed soil characteristic of burned surfaces. The problems posed by water bodies and urban areas for the detection and mapping of burns may be solved, or at least minimised by

mapping and masking out these land-use / land-cover categories, which tend to occupy relatively small, stable, and well defined areas. Caetano et al. (1996) found that endmember fraction images obtained through spectral mixture analysis provided more useful information than the NDVI for burned area mapping, namely because the burned fraction image reduced the amount of confusion between burned surfaces and urban areas, water bodies, and wetlands. Nevertheless, they still found the need to mask out urban areas and water bodies prior to segmenting the endmember fraction images.

Shadows, which occur as a result of the interaction between time-dependent illumination geometry and static terrain slope and aspect, in the case of topographic shadows, or are due to clouds, are not easily masked out. Obviously, topographic shadows predominate in mountainous terrain, and were reported as a surface of confusion in burned area mapping by Milne (1986), Chuvieco and Congalton (1988) and Lombraña (1995). Parnot (1988), working in the flat to undulating african savanna region had more problems with cloud shadows, and Pereira (1992) reported that multitemporal principal component analysis was an effective way to reduce the topographic effect on burned area mapping. Spectral mixture analysis with shade as an image endmember was effective at removing the topographic effect from the spectral signal of various land cover types including a recent burn, except for very large solar incidence angles, but areas in complete shadow had to be masked out with the help of a digital terrain model (Caetano et al., 1994).

Various other land cover types were identified as sources of confusion in the detection and mapping of burned areas, although they appear to be less common, and more ecosystem specific. Tanaka et al. (1983) had problems discriminating a burn from dense conifer forest, and Ponzoni et al. (1986) mentioned confusion between burns and gallery forest and “cerrado” shrublands of Brazil. Sparse shrublands were also considered problematic by

Chuvieco and Congalton (1988), who had difficulties with unburned vegetation being confused with lightly burned areas. Simpson (1990) reported problems with recent, low-intensity burns in arid woodlands, especially when only the understory burns, and the charred, shaded understory is spectrally similar to the darker overstory vegetation. Confusion between burns and bare soils was mentioned by Parnot (1988), specifically in the case of tropical lateritic soils, and humid clay soils on floodplains, and also by Pereira and Setzer (1993), and Siljeström and Moreno (1995). Finally, Milne (1986) and Chuvieco and Congalton (1988) also experienced problems when trying to discriminate various burn severity classes.

Frederiksen et al. (1990) mentioned that the AVHRR channel 1 does not discriminate well between burned areas and actively growing vegetation in southern Senegal, due to the low reflectance in the red range of these surfaces, and similar findings were reported in the simulation study by Razafimpanilo et al. (1995). Both channels 1 and 2 tended to confuse recent burns with mangrove forests and unvegetated lateritic plateaus, and the charcoal signal in channel 4 overlapped that of unvegetated surfaces, especially in sandy and lateritic soils (Frederiksen et al., 1990). In the case of the NIR channel, the confusion with mangrove forests may be due to pixels including a mixture of vegetation and water, which has also been reported as problematic by Caetano et al. (1996) and Pereira (1996). The confusion related to channel 4 was certainly due to the fact that both the recent burns and other unvegetated surfaces become very hot during the dry season in Africa.

In the Alaska boreal forest, Kasischke and French (1995) had to mask out areas above the tree-line, and within a 1km buffer around major river systems, due to the high number of one- or two-pixel false alarms generated in these areas by NDVI MVC image differencing. They also had limited success in detecting tundra fires with the same thresholds used for the forested areas,

which indicates that the fire-induced NDVI decrease is smaller in this ecosystem. Pereira (1996) compared the different types and magnitudes of commission error generated by various vegetation indices used for burned area mapping, and found that different VI tend to be affected by different types of confusions. For example, confusion between burned areas and sparsely vegetated, moderately bright soils, or agricultural fields covered with wheat stubble, were much more likely with the NDVI than if channel 2 alone, the GEMI, or GEMI3 are used. Also, the confusion between burned areas and wetlands mentioned above was very effectively eliminated by the VI3.

The difficulties reported in the literature clearly show that the problem depends to a large extent on the classifier used, but also on burn age and eco-climatic conditions. Therefore, it may prove hard to develop a generic, optimal, context-independent methodology for detecting and mapping burned areas, and spectral data obtained from satellite-based sensors will have to be complemented by region-specific ecological knowledge. An interesting challenge, especially for global applications will be to structure this knowledge in a sufficiently formal manner to still permit a large degree of automation in the procedure.

## 5. CONCLUSIONS.

Based on our review of the literature on detection and mapping of burned areas, using field radiometry data, and satellite imagery, it was possible to draw a series of conclusions. The degree to which these conclusions can be generalized, and the firmness with which they are established is, of course, variable. Scientist working in specific regions and dealing with concrete data sets should take them as tentative, and assess to what extent they are confirmed or denied by their own data and insights. Nevertheless, we propose the following list of conclusions:

1. In the visible spectral range, there appears to be a difference between the short-term post-fire response of boreal and temperate ecosystems, on the one side, and of tropical ecosystems, on the other side. In the former, recent burns tend to be brighter than pre-fire vegetation, while in the latter they generally appear darker.

2. This distinction does not occur in the NIR region, where the brightness of recently burned areas is systematically lower than that of the pre-existing land cover types.

3. Spectral response to fire in the MIR is similar to that observed in the visible region of the spectrum, but with a larger increase in brightness, in boreal and temperate ecosystems.

4. The thermal signal of burned areas has not been widely used, although higher temperatures have been observed for recently burned areas. It seems to be weaker than that of char, and less persistent than the fire scar.

5. Overall, persistence of the char signal varies as a function of climate and characteristic fuel particle size, while scar duration depends essentially on site primary productivity.

6. In the microwave range, control of the radiative response by plant canopy structure, and vegetation and soil water content results in diverse, apparently contradictory findings, which in some cases have not yet been thoroughly interpreted and confirmed.

7. The NIR provides the best (i.e. strongest and less equivocal) discriminant ability to identify burns in satellite imagery.

8. The visible range is not adequate for effective spectral discrimination of fire affected surfaces, due to confusion with several other land cover types that are also relatively dark in this spectral domain.

9. The MIR has, in general, higher capability to identify burns than the visible range. At least in boreal and temperate biomes, burns appear brighter

and, this spectral region is also much less sensitive to atmospheric disturbances.

10. As a consequence of the last three conclusions, the NIR vs. MIR bispectral space has a stronger discriminant ability for recently burned surfaces than the classical NIR vs. visible space.

11. Several kinds of image discrimination techniques have been used for mapping burns, ranging from older, very simple ones, such as single- channel density slicing, to the more modern and complex, like spectral mixture analysis.

12. Vegetation indices are very popular tools for burned area mapping, both in unitemporal and in multitemporal frameworks. They clearly are the dominant technique for low spectral (and spatial) resolution AVHRR imagery.

13. The NDVI has been used almost systematically, although there is evidence of its sub-optimality, derived not only form the formulation of the index, but also because of its reliance on information contained in the NIR vs. visible bispectral space.

14. Principal components analysis is more effective when used in multitemporal analysis mode. It has mostly been employed with high spatial resolution Landsat data, but it may be a promising technique for multitemporal AVHRR applications.

15. Conventional image classification methods, such as maximum likelihood, minimum distance, and various clustering procedures have been used predominantly with Landsat imagery, in unitemporal analyses. Application of these techniques to multitemporal studies may be difficult due to problems in comparing separate classifications from different dates, and genuinely multitemporal classifications have not been attempted. There is also no experience with more modern approaches, such as fuzzy and neural classifiers.

16. Application of spectral mixture analysis to burned area detection and mapping has also been very limited, so far, but with interesting results. The data were analysed with image endmembers, and burned areas extracted using a charcoal endmember. This approach appears to work effectively, an seems to minimise the effects of some of the more common sources of confusion.

17. Various land cover types are consistently prone to spectral confusion with burned areas, namely water, shadows, urban areas, bare soil, rock outcrops, and mixed land-water pixels. These different types of confusion vary with ecosystem, time since fire, and data classification method.

18. Multitemporal methods seem advantageous, since fire is an agent of land cover alteration, and therefore change detection methods reduce the likelihood of confusion with static land cover types, such as urban areas, water surfaces, and rock outcrops.

19. However, even in a multitemporal framework, data acquired shortly after the fire(s) is preferable, since the presence of charcoal is a more unequivocal diagnostic of fire occurrence than decrease of plant cover, which may be caused by a variety of other reasons.

**REFERENCES**

ADAMS, J.B., SMITH, M.O. and JOHNSON, P.E. (1986). Spectral mixture modelling: a new analysis of rock and soil types at the Viking Lander I site. *Journal of Geophysical Research* 91(B8): 8098-8112.

ADAMS, J.B., SMITH, M.O. and GILLESPIE, A.R. (1989). Simple models for complex natural surfaces: a strategy for the hyperspectral era of remote sensing. *Proceedings IGARSS'89*, vol. I, pp.16-21. IEEE, New York.

AMBROSIA, V.G. and BRASS, J.A. (1988). Thermal analysis of wildfires and effects on global ecosystem cycling. *Geocarto International* (1): 29-39.

BELWARD, A.S. (1991). Remote sensing for vegetation monitoring on regional and global scales. In: *Remote Sensing and Geographical Information Systems for Resource Management in Developing countries*, (A.S.Belward, and C.R.Valenzuela, editors), Kluwer Academic Publishers, Dordrecht: 169-187.

BOURGEAU-CHAVEZ, L.L., KASISCHKE, E.S. and FRENCH, N.H.F. (1994). Using ERS-1 SAR imagery to monitor variations in burn severity in an Alaskan fire-disturbed boreal forest ecosystem. *Proceedings IGARSS'94*, Pasadena, California, 8-12 August 1994.

BOURGEAU-CHAVEZ, L.L., HARREL, P.A., KASISCHKE, E.S. and FRENCH, N.H.F. (1995). The detection and interpretation of Alaskan fire-disturbed boreal forest ecosystems using ERS-1 SAR imagery. Pp. 1246-1248, *Proceeding IGARSS'95: Quantitative Remote Sensing for Science and Applications*. Firenze, Italy, 10-14 July 1995. IEEE Publications.

CAETANO, M.S., MERTES, L.A.K. and PEREIRA, J.M.C. (1994). Using spectral mixture analysis for fire severity mapping. Pp.667-677, *Proceedings, 2nd International Conference on Forest Fire Research*. Coimbra, Portugal, November 21-24, 1994.

CAETANO, M., MERTES, L., CADETE, L. and PEREIRA, J.M.C. (1996). Assessment of AVHRR data for characterising burned areas and post-fire vegetation recovery. *EARSeL Advances in Remote Sensing*, 4(4): 124-134.

CAHOON, D.R., STOCKS, B.J., LEVINE, J.S., COFER, W.R. and O'NEILL, K.P. 1992. Seasonal distribution of African savanna fires: *Nature*, 359:812-815.

CAHOON, JR, D.R., LEVINE, J.S., COFER III, W.R., MILLER, J.E., MINNIS, P., TENNILLE, G.M., YIP, T.W., STOCKS, B.J. and HECK, P.W. (1991). The great chinese fire of 1987: a view from space. Pp. 62-66, *Global Biomass Burning: Atmospheric, Climatic, and Biospheric Implications* (J.S. Levine, ed.). The MIT Press, Cambridge, MA, USA.

CAHOON JR, D.R., STOCKS, B.J., LEVINE, J.S., COFER III, W.R. and PIERSON, J.M. (1994). Satellite analysis of the severe 1987 forest fires in northern China and southeastern Siberia. *Journal of Geophysical Research* 99 (D9): 18627-18638.

CHANDLER, C., CHENEY, P., THOMAS, P., TRABAUD, L. and WILLIAMS, D. (1983). Fire in Forestry, Volume 1: Forest Fire Behavior and Effects. John Wiley and Sons, New York.

CHAVEZ Jr., P.S. (1988). An improved dark-object subtraction technique for atmospheric scattering correction of multispectral data. *Remote Sensing of Environment* 24: 459-479.

CHAVEZ Jr., P.S., and KWARTENG, A.Y. (1989). Extracting spectral contrast in Landsat Thematic Mapper image data using selective principal components analysis. *Photogrammetric Engineering and Remote Sensing*, 55: 339-348.

CHUVIECO, E. and CONGALTON, R.G. (1988). Mapping and inventory of forest fires from digital processing of TM data. *Geocarto International* (4): 41-53.

CHUVIECO, E., MARTIN, M.P. and DOMÍNGUEZ, L. (1993).: "Using AVHRR-NOAA images for forest fire detection and mapping in Mediterranean countries", Pecora 12 Symposium, Sioux Falls, South Dakota, pp. 433-440

CHUVIECO, E. and MARTÍN, M.P. (1994). Global fire mapping and fire danger estimation using AVHRR images. *Photogrammetric Engineering and Remote Sensing* 60 (5): 563-570.

COLLINS, J.B. and WOODCOCK, C.E. (1994). Change detection using the Gramm-Schmidt transformation applied to mapping forest mortality. *Remote Sensing of Environment* 50:267-279.

COLLINS, J.B. and WOODCOCK, C.E. (1996). An assessment of several linear change detection techniques for mapping forest mortality using multitemporal Landsat TM data. *Remote Sensing of Environment* 56:66-77.

COPE, M.J. and CHALONER, W.G. (1985). Wildfire: an interaction of biological and physical processes. In Tiffney, B.H. (Ed.) *Geological Factors and the Evolution of Plants*, pp.257-277. Yale University Press, New Haven, CT.

COPPIN, P.R. and BAUER, M.E. (1994). Processing of multitemporal Landsat TM imagery to optimize extraction of forest cover change features. *IEEE Transactions on Geoscience and Remote Sensing* 32 (4): 918-927.

COPPIN, P.R. and BAUER, M.E. (1996). Digital change detection in forest ecosystems with remote sensing imagery. *Remote Sensing Reviews* 13: 207-234.

DESHLER, U. (1974). An examination of the extent of fire in the grassland and savanna of Africa along the Southern side of the Sahara. Pp. 23-30, *Ninth International Symposium on Remote Sensing of the Environment*, ERIM, Ann Arbor, MI.

DUGUAY, C.R. and LeDREW, E.F. (1992). Estimating surface reflectance and albedo from Landsat-5 Thematic Mapper over rugged terrain. *Photogrammetric Engineering and Remote Sensing* 58 (5): 551-558.

EVA, H.D., BELWARD, A.S., GRÉGOIRE, J.M., MOULA, M., BRUSTET, J.M., JANODET, E. and VIOVY, N. (1995). The application of Along Track Scanning Radiometer to burnt area mapping in different savannah ecosystems in central Africa. Pp. 201-208, *Proceedings of the 1995 Meteorological Satellite Data User's Conference.* Winchester, U.K., 4-8 September 1995. EUMETSAT EUM P17.

FLANNIGAN, M.D., and VONDER HAAR, T.H. (1986). Forest fire monitoring using NOAA satellite AVHRR: *Canadian Journal of Forest Research*, 16: 975-982.

FLASSE, S.P. and CECCATO, P. (1996). A contextual algorithm for AVHRR fire detection. *International Journal of Remote Sensing* 17 (2): 419-424.

FRENCH, N.H.F., KASISCHKE, E.S., BOURGEAU-CHAVEZ, L.L., HARRELL, P.A. and CHRISTENSEN, N.L. (1994). Relating soil water measurements at fire disturbed sites in Alaska to ERS-1 SAR image signature. *Proceedings IGARSS'94*, Pasadena, California, 8-12 August 1994.

FRENCH, N.H.F., KASISCHKE, E.S., BOURGEAU-CHAVEZ, L.L. and BERRY, D. (1995). Mapping the location of wildfires in Alaskan boreal forests using AVHRR imagery. *International Journal of Wildland Fire* 5: 55-61.

FULLER, S.P. and ROUSE, W.R. (1979). Spectral reflectance changes accompanying a post-fire recovery sequence in a subarctic spruce-lichen woodland. *Remote Sensing of Environment* 8: 11-23.

FUNG, T. (1990). An assessment of TM imagery for land-cover change detection. *IEEE Transactions on Geoscience and Remote Sensing* 28 (4): 681-684.

GESELL, G. (1989). An algorithm for snow and ice detection using AVHRR data: an extension to the APOLLO software package. *International Journal of Remote Sensing* 10: 897-905.

GONG, P. (1993). Change detection using principal component analysis and fuzzy set theory. *Canadian Journal of Remote Sensing* 19 (1): 22-29

HALL, D.K., ORMSBY, J.P., JOHNSON, L. and BROWN, J. (1980). Landsat digital analysis of the initial recovery of burned tundra at Kokolik River, Alaska. *Remote Sensing of Environment* 10: 263-272.

HERFERT, M.R. and LULLA, K.P. 1990. Mapping continental-scale biomass burning and smoke palls over the Amazon basin as observed from the Space Shuttle: *Photogrammetric Engineering and Remote Sensing*, 56:1367-1373.

HIRSCH, S.N., KRUCKEBERG, R.F. and MADDEN, F.H. 1971. The bi-spectral forest detection system. In: *Proc. 7th Inter. Symp. on Remote Sensing of Environment*, Ann Arbor: 2253-2259.

HITCHCOCK, H.C. and HOFFER, R.M. (1974). *Mapping a Recent Forest Fire with ERTS-1 MSS Data*, LARS Information Note 032674, West Lafayette.

HLAVKA, C.A., AMBROSIA, V.G., BRASS, J.A., REZENDEZ, A.R. and GUILD, L.S. (in press). Mapping fire scars in the Brazilian cerrado using AVHRR imagery. In J.S: Levine (Ed.) *Biomass Burning and Global Change*, MIT Press.

HOPE, A.S. and McDOWELL, T.P. (1992). The relationship between surface temperature and a spectral vegetation index of a tallgrass prairie: effects of a burning and other landscape controls, *International Journal of Remote Sensing*, vol. 13, pp. 2849-2863.

ISAACSON, D.L., SMITH, H.G. and ALEXANDER, C.J. (1982). Erosion hazard reduction in a wildfire damaged area, en *Remote Sensing for Resource Management*, Johannsen, y Sanders, Eds., Soil Conservation Society of America, Ankeny, pp. 179-190.

JAKUBAUSKAS, M.E., LULLA, K.P. and MAUSEL, P.W. (1990). Assessment of vegetation change in a fire-altered forest landscape. *Photogrammetric Engineering and Remote Sensing* 56 (3): 371-377.

JUSTICE, C.O., MALINGREAU, J.P. and SETZER, A.W. (1993). Satellite remote sensing of fires: potential and limitations. Pp. 77-88, *Fire in the Environment: The ecological, atmospheric, and climatic importance of*

*vegetation fires*. P.J. Crutzen and J.G. Goldammer (Eds.) John Wiley and Sons, New York.

KASISCHKE, E.S., BOURGEAU-CHAVEZ, L.L., FRENCH, N.H.F., HARREL, P. and CHRISTENSEN Jr., N.L. (1992). Initial observations on using SAR to monitor wildfire scars in boreal forests. *International Journal of Remote Sensing* 13 (18): 3495-3501.

KASISCHKE, E.S., FRENCH, N.H.F., HARREL, P., CHRISTENSEN Jr, N.L., USTIN, S.L. and BARRY, D. (1993). Monitoring wildfires in boreal forests using large area AVHRR NDVI composite image data (1993) *Remote Sensing of Environment* 45: 61-71.

KASISCHKE, E.S., BOURGEAU-CHAVEZ, L.L. and FRENCH, N.H.F. (1994). Observations of variations in ERS-1 SAR image intensity associated with forest fires in Alaska. *IEEE Transactions on Geoscience and Remote Sensing* 32 (1): 206-210.

KASISCHKE, E.S. and FRENCH, N.H.F. (1995). Locating and estimating the areal extent of wildfires in Alaskan boreal forests using multiple-season AVHRR NDVI composite data. *Remote Sensing of Environment* 51: 263-275.

KAUFMAN, Y.J., TUCKER, C.J. and FUNG, I. (1990). Remote sensing of biomass burning in the Tropics: *Journal of Geophysical Research*, 95:9927-9939.

KENNEDY, P.J., BELWARD, A.S. and GRÉGOIRE, J.M. (1994). An improved approach to fire monitoring in West Africa using AVHRR data. *International Journal of Remote Sensing* 15 (11): 2235-2255.

KNEPPECK, I.D. and AHERN, F.J. (1989). Stratification of a regenerating burned forest in Alberta using Thematic Mapper and C-SAR images. Proceeding, IGARSS'89 Symposium, pp.1391-1396.

KOUTSIAS, N. and KARTERIS, M. (1996). Logistic regression modelling of Thematic Mapper data for burnt area mapping. Unpublished

manuscript, Aristotelian University of Thessaloniki, Dept. of Forestry and Natural Environment, Lab. of Forest Management and Remote Sensing.

LANDRY, R., AHERN, F.J. and O'NEIL, R. (1995). Forest burn visibility on C-HH radar images. *Canadian Journal of Remote Sensing* 21 (2): 204-206.

LANGAAS, S. and KANE, R. (1991). Temporal spectral signatures of fire scars in savanna woodland. Pp. 1157-1160, *Proceedings IGARSS'91 Remote Sensing: Global Monitoring for Earth Management.* Helsinki University of Technology, Espoo, Finland, June 3-6 1991. IEEE Publications.

LANGAAS, S. (1992). Temporal and spatial distribution of savanna fires in Senegal and the Gambia, West Africa, 1989-90, derived from multi-temporal AVHRR night images: *International Journal of Wildland Fire*, 2:21-36.

LILLESAND, T.M. and KIEFER, R.W. (1987). *Remote Sensing and Image Interpretation*, 2nd Ed. John Wiley and Sons, New York.

LOMBRAÑA, M.J. (1995). Monitoring of burnt forest areas with remote sensing data. A study in North-East Spain using Landsat TM and Spot XS data. Institute For Remote Sensing Applications, Joint Research Centre. Technical Note Nº I.95.80.

LÓPEZ, M.J. and CASELLES, V. (1991). Mapping burns and natural reforestation using Thematic Mapper data. *Geocarto International* (1): 31-37.

MALINGREAU, J.P. (1990). The contribution of remote sensing to the global monitoring of fires in tropical and subtropical ecosystems. In: *Fire in Tropical Biota*, (J.G.Goldammer, editor), Springer Verlag, Berlin: 337-370.

MALINGREAU, J.P., STEPHENS, G. and FELLOWS, L. (1985). Remote sensing of forest fires: Kalimantan and North Borneo in 1982-83. *Ambio* 14(6): 314-321.

MALINGREAU, J.P., LEYSEN, M. and DEGRANDI, F. (1995). Detecting and measuring burn scars in tropical vegetation using ERS-1 SAR

data. Paper presented at the *IGBP-DIS Workshop on Global Fire Monitoring*. Joint Research Centre, Ispra, Italy, October 17-19 1995.

MARTÍN, M.P. and CHUVIECO, E. (1994). Mapping and evaluation of burned land from multitemporal analysis of AVHRR NDVI images. Pp. 71-83, *Proceedings of the International Workshop on Satellite Technology and GIS for Mediterranean Forest Mapping and Fire Management*. Thessaloniki, Greece, 4-6 November 1993. JRC/AUTH/EARSeL.

MARTÍN, M.P, VIEDMA, O. and CHUVIECO, E**.** (1994). High versus low resolution satellite images to estimate burned areas in large forest fires, *Second International Conference on Forest Fire Research*, Coimbra, , vol. II, pp. 653-663.

MARTÍN, M.P. and CHUVIECO, E. (1995). Cartografía y evaluación superficial de grandes incendios forestales a partir de imágenes de satélite", Ecología, vol. 9, pp. 9-21.

MATTHEWS, A. and JESSELL, M. (1992). Firescan: a semiautomated system for mapping of bush fires: *6th Australasian Remote Sensing Conference*, Wellington, New Zealand, 2:166-173.

MILNE, A.K. (1986). The use of remote sensing in mapping and monitoring vegetational change associated with bushfire events in Eastern Australia. *Geocarto International* (1): 25-35.

MILNE, A.K. and HALL, A.M. (1992). Towards the operational detection and mapping of bushfires: *6th Australasian Remote Sensing Conference*, Wellington, New Zealand, 2:156-165.

PARNOT, J. (1988). Inventaire des feux de brousse au Burkina Faso saison sèche 1986-1987. Pp. 563-573, *Proceedings of the Twenty-Second International Symposium on Remote Sensing of the Environment.* 20-26 October 1988, Abidjan, Côte d'Ivoire. ERIM, Ann Arbor, MI.

PEREIRA, A., SETZER, A.W. and DOS SANTOS, J.R. (1991). Fire estimates in savannas of central Brasil with thermal AVHRR/NOAA calibrated by TM/Landsat: *Proc. 24th International Symp. on Remote Sensing of Environment*, Rio de Janeiro: 825-836.

PEREIRA, J.M.C. (1992). Burned area mapping with conventional and selective principal component analysis. *Finisterra*, XXVII, nº53-54, pp.61-76.

PEREIRA, J.M.C., CADETE, L. and VASCONCELOS, M.J.P. (1994). An assessment of the potential of NOAA/AVHRR HRPT imagery for burned area mapping in Portugal. Pp.C15, *Proceedings, 2nd International Conference on Forest Fire Research*. Coimbra, Portugal, November 21-24, 1994.

PEREIRA, J.M.C. (1996). A comparative evaluation of NOAA/AVHRR vegetation indices for burned surface detection and mapping. Submitted to *IEEE Transaction on Geosciences and Remote Sensing*.

PEREIRA, M.C. and SETZER, A.W. (1993). Spectral characteristics of fire scars in Landsat-5 TM images of Amazonia. *International Journal of Remote Sensing* 14 (11): 2061-2078.

PONZONI, F.J., LEE, D.C.L. and FILHO, P.H. (1986). Avaliação da área queimada e da regeneração da vegetação afetada pelo fogo no Parque Nacional de Brasília através de dados do TM/Landsat. Pp. 615-621, *Simpósio Latino-Americano de Sensoriamento Remoto / IV Simpósio Brasileiro de Sensoriamento Remoto, Vol.1*. Gramada, R.S., 10-15 August 1986. INPE, São José dos Campos.

PRINS, E.M. and MENZEL, W.P. 1992. Geostationary satellite detection of biomass burning in South America: *International Journal of Remote Sensing*, 13: 2783-2799.

RAZAFIMPANILO, H., FROUIN, R., IACOBELLIS, S.F. and SOMERVILLE, R.C. (1995). Methodology for estimating burned area from AVHRR reflectance data. *Remote Sensing of Environment* 54: 273-289.

REINHARDT, E.D. and RINGLEB, R.V. (1990). Analysis of changes in patterns of a forested landscape following wildfire using Landsat data and landscape ecology methodology, *Proc. Resource Technology 90*, Washington, D.C., 83-93.

RICHARDS, J.A. (1984). Thematic mapping from multitemporal image data using the principal components transformation. *Remote Sensing of Environment*, 16: 35-46.

RICHARDS, J.A. (1986). *Remote Sensing Digital Image Analysis: an Introduction*. Springer-Verlag, Berlin.

RIGGAN, P.J., BRASS, J.A. and LOCKWOOD, R.N. (1993). Assessing fire emissions from tropical savanna and forests of central Brazil. *Photogrammetric Engineering and Remote Sensing*, 59 (6): 1009-1015.

RIGGAN, P.J., FRANKLIN, S.E., BRASS, J.A. and BROOKS, F.E. (1994). Perspectives on fire management in Mediterranean ecosystems of southern California. Pp. 140-162, *The Role of Fire in Mediterranean-Type Ecosystems* (J.M. Moreno and W.C. Oechel, eds.) Springer-Verlag, New York.

ROBINSON, J.M. (1991). Fire from space: global fire evaluation using infrared remote sensing: *International Journal of Remote Sensing*, 12: 3-24.

ROBINSON, J.M. (1991). Problems in global fire evaluation: is remote sensing the solution? Pp. 67-73, *Global Biomass Burning: Atmospheric, Climatic, and Biospheric Implications* (J.S. Levine, ed.). The MIT Press, Cambridge, MA, USA.

SAUNDERS, R.W. and KRIEBEL, K.T. (1988). An improved method for detecting clear sky and cloudy radiances from AVHRR data. *International Journal of Remote Sensing* 9 (1): 123-150.

SETZER, A. and PEREIRA, M.C. (1991a). Operational detection of fires in Brazil with NOAA-AVHRR. In: *Proc. 24th. International Symp. on Remote Sensing of Environment*, Rio de Janeiro: 469-482.

SETZER, A.W. and PEREIRA, M.C. (1991b). Amazonia biomass burnings in 1987 and an estimate of their tropospheric emissions: *Ambio*, 20: 19-23.

SILJESTRÖM, P. and MORENO, A. (1995). Monitoring burnt areas by principal components analysis of multitemporal TM data. *International Journal of Remote Sensing* 16 (9): 1577-1587.

SILVA, J.M.N. (1996). Comparação entre os índices de vegetação NDVI e IV7 para cartografia de áreas ardidas com imagens Landsat5 TM. Unpublished final report. Instituto Superior de Agronomia, Universidade Técnica de Lisboa.

SIMPSON, C.J. (1990). Deep weathering, vegetation and fireburn. Significant obstacles for geoscience remote sensing in Australia. *International Journal of Remote Sensing* 11 (11): 2019-2034.

SMITH, M.O., USTIN, S.L., ADAMS, J.B. and GILLESPIE, A.R. (1990). Vegetation in deserts: I. a regional measure of abundance from multispectral images. *Remote Sensing of Environment* 31: 1-26.

SOUSA, A., SILVA, J.M.N., ZIEBELL, M.E.C. and PEREIRA, J.M.C. (1996). Cartografia das áreas ardidas em Portugal para os anos de 1993 e 1994, com imagens do satélite Landsat 5 TM. Laboratório de Detecção Remota e Análise Geográfica, DEF/ISA.

TANAKA, S., KIMURA, H. and SUGA, Y. (1983). Preparation of a 1:25000 Landsat map for assessment of burnt area on Etajima Island. *International Journal of Remote Sensing* 4 (1): 17-31.

USTIN, S.L., SMITH, M.O. and ADAMS, J.B. (1993). Remote sensing of ecological processes: a strategy for developing and testing ecological models using spectral mixture analysis. In J. Ehleringer and C.B. Fields (Eds.) *Scaling Physiological Processes: Leaf to Globe*. Academic Press, New York, USA.

VERSTRAETE, M.M. and PINTY, B. (1996). Designig optimal spectral indices for remote sensing applications. *IEEE Transactions on Geoscience and Remote Sensing* 34(5): 1254-1265.

VIOVY, N., ARINO, O. and BELWARD, A.S. (1992). The best index slope extraction (BISE): a method for reducing noise in NDVI time series. *International Journal of Remote Sensing* 13 (8): 1585-1590.

WATSON, C.E., FISHMAN, J. and REITCHLE, H.G. (1990). The significance of biomass burning as a source of carbon monoxide and ozone in the Southern tropics: a satellite analysis: *Journal of Geophysical Research*, 95:16443-16450.

WERLE, D., DRIEMAN, J.A., AHERN, F.J. and O'NEIL, R. (1991). Synthetic Aperture Radar (SAR): A promising tool for assessing recently burned forest in Canada? Proceeding of the 14th Canadian Symposium on Remote Sensing. Canadian Remote Sensing Society, Calgary, Alberta, pp.470-475.

WIGHTMAN, J.M. (1973). Detection, mapping and estimation of rate of spread of grass fires from southern african ERTS-1 imagery. Pp. 593-601, Proceedings *from the Symposium on Significant Results Obtained From ERTS-1*. NASA, 1973.

# EVALUATION OF FOREST FIRE DAMAGE WITH LANDSAT-TM IMAGES AND ANCILLARY INFORMATION

*Francisco Rodríguez y Silva[(a)], Rafael Mª Navarro Cerrillo[(b)], Carmen Navarro Mezquita[(a)], and Maria P. Gonzales Dugo[(a)]*

[(a)] Consejería de Medio Ambiente, Junta de Andalucía, Spain.

[(b)] E.T.S.I.A.M.-University of Córdoba, Spain.

## 1. INTRODUCTION

Since 1991, annual reports on major forest fires in Andalusia, that is, forest fires over 200 hectares have been produced to provide easy location and evaluation of these forest fires. Evaluation of forest effects, in terms of fire intensity, has been possible with the help of Landsat-TM images acquired after the fire together with ancillary data of the SinambA (landuse, fuel models, topography) and derived statistics (Consejería de Medio Ambiente, 1995).

For three 1991 and 1995 forest fires, validation of satellite-derived information on forest fire damage by field survey has been done in a pilot study carried out between the Andalusian Ministry of Environment and the School of Forestry of the University of Córdoba (Spain). Though regeneration monitoring with Landsat-TM has also been attempted, only the main goals established in relation to evaluation of forest damage will be mentioned:

-Characterization of Mediterranean vegetation in terms of its response to fire,

-Improvement of the previous methodology on forest fire intensity by the evaluation of the performance of different Vegetation Indexes (NDVI, SAVI, ARVI) by field survey,

-Evaluation of the economic costs of these new technologies (satellite imagery and G.I.S.) versus other traditional methods of information gathering (field survey and photointerpretation),

-Applicability of this new methodology to quick and cheap evaluation of forest fire damage as a basic help for decision making in recently-burned forests.

## 2. METHODOLOGY

### *2.1. Vegetation characterization*

Vegetation plays an important role in the regeneration process after the fire so that the regeneration process can be forecasted to a certain extent depending on the type of vegetation before the fire. According to vegetation response after the fire, defined by both species composition and vegetation structure, vegetation types were identified in the three forest fires by the help of panchromatic aerial photography acquired before the fire so that pre-fire vegetation conditions could be modeled.

For each vegetation type some parameters related to regeneration were registered: main species, secondary species, presence of this vegetation type in Andalusia, expected post-fire vegetation type, expected restoration period and regeneration index.

### *2.2. Evaluation of fire effects*

Different annual reports compiled by the Environmental Agency of Andalucia since 1991 had used the NDVI images to describe vegetation status

after the fire. Techniques were based on either a single date or a combination of both prefire and postfire dates, which on its turn allowed masking out certain zones within the area with bare soil, rock or sparse vegetation before the fire.

Afterwards, evaluation of the performance of different Vegetation Indexes (NDVI, SAVI, ARVI) (Huete, 1988; Kaufman and Tanré, 1992) by field survey was attempted so as to minimize the different atmospheric and soil effects on the vegetation response after the fire. Also an atmospheric correction procedure (Pons, 1994) was applied, but it is still on research.

In order to assess the performance of the different Vegetation Indexes so as to describe the levels of damage, field data had to be collected in the three sites by the use of control parcels, which also would be used in the supervised classification stage. These control parcels were visually assigned a damage level during the field survey according to a damage index developped specifically for this study.

This damage index consisted of five damage levels regarding fire intensity and proportion of damaged and non-damaged trees:

0. No damage

1. Light damage: soil fire. Shrub partially scorched. Trees affected only at the bottom.

2. Moderate damage: crown fire. Partially affected trees (<1/3).

3. Hight damage: crown fire. Partially affected trees (>1/3).

4. Extreme damage: all the vegetation is scorched.

5. Extreme damage: total combustion

Each control parcel had a circular shape with a 15 m. radius (707 $m^2$) and was located every 25 up to 40 hectares within the scorched area by a previous 250x250 m. cell size mesh overlaid. These different ranges of location, between 25 and 40 hectares, were subject to the distribution of damage levels on the zone

and site characteristics, determined by the vegetation map and a Digital Terrain Model, so that a good stratification of the zone in representative and homogeneous units could be done.

Nevertheless, a minimum of 20 control parcels were selected for each unit spatially representative, with a maximum of control parcels in the middle units (moderate to very intense damage level), which were regarded as the most problematic from a point of view of their spatial characterisation.

In order to avoid misregistration errors, the average of a 2x2 pixel window as Vegetation Index estimation in the supervised classification stage.

Also, for damage evaluation and regeneration monitoring, five 60x60m parcels were established. A complete study related to vegetation conditions before the fire, different damages and regeneration process was made for each one.

Data gathering in the 60x60m. parcels has been done according to damage and regeneration parameters collected by field work. Damage parameters such as the spatial pattern of vegetation, species frequency, density, percentage of tree cover and damage assignation were registered in the damage inventory during field work.

## 3. RESULTS

Application of a maximum likelihood classification by the help of the control parcels with a damage level assigned in the field allowed comparison of the different Vegetation Indexes by error matrices. For SAVI a coefficient of 0.5 was used, and for ARVI three different coefficients were used to evaluate their influence over the Vegetation Index (0.5, 1, 2). From the outcoming results, some considerations could be made:

-according to Vegetation Index sensitivity to describe damage level, the different Vegetation Indexes can be grouped in two categories: NDVI and SAVI, and ARVI with its three different coefficients. NDVI and SAVI had similar

accuracy values, with 57% and 56% respectively, which are usual accuracy values obtained in vegetation classification (50-60%). SAVI performed better in the less affected categories and NDVI in the definition of the scorched area from the healthy vegetation.

-these values of accuracy are lower in comparison to other sources of information (photointerpretation and field inventories), where values over 70% are usually not reached.

-ARVI, for which the best results were expected, performed very poorly in the classification stage, thus indicating a low sensitivity in detecting damage levels. Nevertheless further reserach should be devoted to this Index in other to test its performance over other forest fires.

-Also in relation to classification accuracy, field work had also some difficulties at the beginning of the study, which should be mentioned: problems in assignation of visual damage in the field, and location of some parcels in places with no homogeneous illumination and vegetation conditions in wide extensions so as to avoid problems in parcel characterization resulting from misregistration errors.

-Only for totally burned and non-burned areas (extreme damage and no damage) it was possible to find a straight 'universal' relation between spectral values and the damage index defined in the field, which it was not possible for intermediate categories (moderate to very extreme damage), whose values fluctuated in the different parcels for each Vegetation Index. This is due partly to the different proportions of the damaged and non-damaged trees within the pixel and partly to the definition of these categories by the damage index, which should be more accurately established.

## 4. CONCLUSIONS

From an operational and management-focused policy point of view, some interesting conclusions from this study can be pointed out:

-Landsat pixel size is very suitable to forest management and plannig, as it is even smaller than the usual basic unit (in spanish 'rodal').

-The cost of Landsat images, together with the advantages of multitemporal information, makes them very useful for the evaluation of forest damage and regeneration monitoring at a reasonable price. Future sensors will, however, play an important role in forest fire evaluation in the next years.

-Further research has to be devoted to the evaluation of damaged areas with Landsat images in order to improve the relation between damaged areas and spectral values, specially in middle damaged categories, where different proportions of damaged and non-damaged trees within pixel can explain the differences found in pixel values as well as the proportion of bare soil. In relation to this, we would like to suggest some working lines for future studies:

-evaluation of individual bands, including the potential of band 6 in spite of its poorer spatial resolution, as well as other vegetation indexes, which can be empirically designed for the study.

-use of easy and simple atmospheric correction models, such as the mentioned model of Pons and Solé (1994).

-within-pixel research, where some initial approaches have been reported (Vine, 1995).

-a self-calibration procedure by the help of field work for each big forest fire, so as to establish the different categories of damage found in control parcels. Improvement of the mentioned damage index needs also to be done so that more precise categories can be defined. In relation to this a user manual will be elaborated in order to assure normalization of the criteria used to assign each category by the staff in charge of this work in the future. As a pilot experiment,

for the 1997 annual report all the big forest fires will be field surveyed with the damage index in order to test its applicability from an operational point of view.

-For a better management of the forest after the fire, a potential regeneration map seems more useful than a damage map. That is why a pilot study will attempt to formulate a potential regeneration index by the help of spectral information, a vegetation map, topography and soil data. As it was mentioned at the beggining of this paper in relation to the role of vegetation in the regeneration process, different vegetation maps, such as the Corine 1987 Landcover map, the Spain Forest Map and the 1991 and 1995 Landuse and Vegetation Maps of Andalusia will be tested versus vegetation maps done with aerial photography as a way to determine to which degree their level of detail meets the requirements of our potential regeneration index.

## REFERENCES

CONSEJERÍA DE MEDIO AMBIENTE (1991 to 1995). Evaluación de superficies y niveles de afectación ocasionados por los incendios forestales más importantes acaecidos en Andalucía. Junta de Andalucía, Sevilla.

HUETE, A.R. (1988). A soil-adjusted vegetation index (SAVI). Remote Sensing of Environment, 17: 37-53.

KAUFMAN, J. and TANRÉ, D. (1992). Atmospherically resistant vegetation index (ARVI) for EOS-MODIS. IEEE Transactions on Geoscience and Remote Sensing, Vol. 30, Nº2: 261-270.

PONS, X. and SOLÉ SUGRAÑÉS, L. (1994). A simple radiometric correction model to improve automatic mapping of vegetation from multispectral satellite data. Rem. Sensing of Env., 48: 191-204.

RUIZ DE LA TORRE, J. (1990). Mapa Forestal de España. Memoria General. Ministerio de Agricultura, Pesca y Alimentación. ICONA.

VINÉ, P., PUECH, C., CLÉMENT, B. and BOUGERZAZ, F. (1996). Remote sensing and vegetation recovery mapping after a forest fire. EARSeL Advances in Remote Sensing, Vol. 4, No. 4-XI: 155-158.